ANTERIOR SEGMENT ALTERATIONS AND COMPARATIVE AQUEOUS HUMOR PROTEOMICS IN THE BUPHTHALMIC RABBIT (AN AMERICAN OPHTHALMOLOGICAL SOCIETY THESIS)

BY Deepak P. Edward MD AND Rachida Bouhenni PhD

ABSTRACT

Purpose: To use an integrated proteohistologic approach to gain insight into the anterior segment alterations in the buphthalmic rabbit.

Methods: Eyes from 2- and 5-year-old buphthalmic and normal rabbits (n=20) were studied histologically. Liquid chromatography–tandem mass spectrometry (LC-MS/MS) of aqueous humor (AH) was used to determine differential protein expression between animal groups. Western blot and immunohistochemistry were performed on selected differentially expressed proteins identified by LC-MS/MS.

Results: The buphthalmic rabbits manifested a mild clinical phenotype with typical angle anomalies that appeared progressive by histology. Significantly thickened Descemet's membrane (DM) and anterior lens capsule in all buphthalmic rabbits showed increased fibronectin and collagen-IV immunolabeling. LC-MS/MS applying stringent filtering criteria revealed significant differential expression of several AH proteins in these rabbits. The protein of interest in the 2-year-old group was histidine-rich glycoprotein, and those in the 5-year-old group included alpha-2-HS-glycoprotein, clusterin, apolipoprotein E, interphotoreceptor retinoid-binding protein, transthyretin, cochlin, gelsolin, haptoglobin, hemopexin, and beta-2 microglobulin. The proteomic data for selected proteins was validated by Western blot and immunohistochemistry. A wide range of functional groups were affected by the altered AH proteins. These included extracellular matrix modulation, regulation of apoptosis, oxidative stress, and protein transport.

Conclusions: Multiple anterior segment alterations were histologically identified in the buphthalmic rabbits that showed progressive changes with age. The differentially expressed AH proteins in these rabbits suggest a multifunctional role for AH in modulating pathologic changes in DM, anterior lens capsule, and the angular meshwork in these animals.

Trans Am Ophthalmol Soc 2011;109:66-114

INTRODUCTION

Developmental glaucomas are a group of disorders that result in abnormal development of the trabecular meshwork (TM) and the anterior segment of the eye.[1] They manifest during infancy or in childhood and are characterized by an increase in intraocular pressure (IOP) due to obstruction of aqueous outflow, resulting from functional and anatomic defects in the TM and the anterior chamber angle. This phenotype may be associated with other anterior segment and systemic anomalies. Among this group of glaucomas, primary congenital glaucoma (PCG), which is an uncommon autosomal recessive disease, is characterized by an abnormal anterior chamber angle and a typical clinical phenotype.[1,2]

Although studies have confirmed that mutations in *CYP1B1* are the predominant cause of PCG in humans in certain communities,[2] the pathway by which *CYP1B1* causes pathologic alterations in the TM remains elusive. It has been suggested that CYP1B1 may regulate proteins downstream in the pathway causing aberrant development of the anterior segment tissues. Previous studies localized CYP1B1 in human fetal and adult eyes mainly to the nonpigmented ciliary epithelium[3] and not the TM. This suggests that CYP1B1 may play a crucial role in metabolizing a yet-to-be-identified substrate that could play an important role in TM and anterior segment development. This substrate may be secreted into the aqueous humor (AH) and transported to target tissues such as TM, cornea, and lens. Therefore, studying the composition of AH becomes an important issue in investigating downstream events in this disease. Recent studies have suggested that the AH in human PCG may be altered and may involve differential expression of proteins, some of which are responsible for vitamin A transport.[4] Animal models that mimic human PCG are lacking, and although several species have been described, none of these are ideal models for studying the disease. For example, the C*yp1b1-/-* or the *Foxc1* mutant mouse does not exhibit glaucoma unless the tyrosinase gene is modified.[5] The complexity in genetic changes in these mutant mice, along with the challenge of working with a small animal eye, makes it difficult to study downstream alterations of this disease in the mouse. These factors prompted a search for other animal models with developmental defects that resemble the developmental phenotype in humans. These models could provide a better understanding of some of the anterior segment anomalies observed in developmental glaucoma.

The buphthalmic rabbit, as described in the review of literature in the following sections, is a reasonable model to test some aspects of pathways that might be involved in developmental glaucoma. This rabbit possesses an autosomal recessive genotype and shares clinical and histologic features with those described in human PCG. However, the genetic defect that causes glaucoma in the rabbit remains unknown. Prior to testing some aspects of the hypothesis, we investigated whether mutations in *CYP1B1* could be identified in the rabbit. The genetic testing in the rabbit has been restricted because of the limited rabbit genomic resources that were available at the time of testing (http://www.broadinstitute.org/science/projects/mammals-models/rabbit/rabbit-genome-sequencing-project). In unpublished observations, we were unable to identify a *CYP1B1* mutation in the buphthalmic rabbit. The outcome of this experiment suggested that there are likely other gene(s) that may cause the defects in the buphthalmic rabbit and yet undiscovered pathways that lead to anterior segment changes and glaucoma. The absence or altered level of the proteins encoded by aberrant gene(s) could result in altered AH proteins that may play important roles in anterior segment development or tissue damage to the

From the Wilmer Eye Institute, Johns Hopkins University School of Medicine, Baltimore, Maryland (Dr Edward) and the Department of Ophthalmology, Summa Health System/Northeastern Ohio Universities College of Medicine and Pharmacy, Akron, Ohio (Dr Edward and Dr Bouhenni).

anterior segment. Such aberrations in AH content may result in altered development of the TM and other anterior segment structures through complex and yet-to-be-determined pathways**.**

We therefore hypothesize that the buphthalmic rabbit demonstrates some histologic features in the outflow pathway similar to those seen in human developmental glaucoma. These histologic features are a result of alterations in the AH proteome (up-regulation, down-regulation, or absence of proteins). Changes in the AH proteome will result in aberrant development or damage to anterior segment tissues.

We tested this hypothesis by examining the histopathologic changes in the anterior segment of 2- and 5-year-old buphthalmic rabbits and their normal littermates using light and electron microscopy as well as immunohistochemistry. In addition, we studied alterations in the AH proteomic profile of buphthalmic rabbits compared to normal age-matched littermates using liquid chromatography–tandem mass spectrometry (nanospray LC-MS/MS). The findings were validated using Western blot when possible. In addition, we utilized immunohistochemistry to localize the key differentially expressed proteins to the anterior segment as an additional validation step.

The following paragraphs describe in detail the background information regarding congenital glaucoma in buphthalmic rabbits and highlight additional aspects of the rationale for the current study.

ANIMAL MODELS FOR CONGENITAL GLAUCOMA

Congenital glaucoma occurs spontaneously in rats,[6] dogs,[7] rabbits,[8] birds, and other species[9] but has been most extensively studied in the rabbit. The animal models for glaucoma have been reviewed in detail recently.[10] However; none of these models is perfect for studying PCG. Developmental glaucoma in genetically altered mice has not been well characterized or defined but may serve as a good model once these mice become available.[5]

THE BUPHTHALMIC RABBIT: HISTORICAL PERSPECTIVE

Schloesser,[11] in 1886, was the first to report buphthalmia in the rabbit that occurred following trauma, resulting in glaucoma and cataract formation. In 1910, Pichler[12] described spontaneous glaucoma in the right eye of a young, healthy albino rabbit. In 1919, Vogt[13] described severe bilateral buphthalmos that appeared at the age of 3 months in three rabbits and also in several progeny; however, no pathologic changes were described in these reports. In 1921, Rochon-Duvigneaud[14] described a single pigmented rabbit with buphthalmos and an IOP ranging from the 30s to the 40s mm Hg. In addition to the clinical description, he described histopathologic findings, including the presence of angle anomalies that were compared to a normal rabbit. In 1935, Beckh[15] reported uveitic glaucoma secondary to possible yaws infection, which caused buphthalmia in the rabbit. Greaves and Perkins[16] later described a delayed appearance of Evans blue dye into the episcleral vessels after it was injected into the chamber and suggested that there was an abnormality in the outflow facility of these animals.

In their studies of buphthalmic rabbits, Franceschetti[17] and Nachtsheim[18] in the 1930s, and Geri[19,20] in the 1950s, suggested that the inheritance of the disease may be autosomal recessive. In the 1960s, interest in the buphthalmic rabbit was rekindled by Hanna,[8] Fox,[21] and Kolker,[22] who characterized the clinical and histopathologic features of congenital glaucoma in these rabbits. Further studies then described the genetic nature of the disease and the biochemical anomalies of the AH. Furthermore, the ophthalmic findings in some of these rabbits were noted to be associated with the systemic features described in the next paragraphs. Following sporadic biochemical reports in the 1970s, few studies appeared in the 1980s and 1990s that described the ultrastructural findings of the angle in the buphthalmic rabbit.[23] The interest in studying this model decreased in the 1990s, when other genetic models of glaucoma became available. Since then, sporadic reports have appeared in the literature, further characterizing the histology and biochemical nature of the AH in this animal model.[24]

CLINICAL FINDINGS IN THE BUPHTHALMIC RABBIT

The New Zealand white buphthalmic rabbit model has been well characterized clinically since the 1960s.[25-27] Buphthalmia is also reported in pigmented rabbits but with lower frequency. Mortality rate was higher in pigmented *bu/bu* offspring from stillbirths and also from pneumonia of unspecified causes resulting in death prior to the time that they would have developed glaucoma.[9]

The disease typically manifests in the first 6 months of life and is associated with variable IOP elevation, enlarged cloudy corneas, and elongated globes. The outflow facility is decreased, suggesting a defect in the outflow pathway, which correlates with histologic findings. The phenotypic similarities between buphthalmic rabbits and human patients, such as inherited nature of disease, age at onset, IOP elevation, angle anomalies, and alterations in outflow make this animal a good model for studying developmental glaucoma. One limitation of using the rabbit model is that the rabbit genome was incomplete when this study was performed.

Hanna, Kolker, and others have described clinical findings and demographic features of the buphthalmic rabbit in detail.[8,22,26] Typically, the disorder is not present at birth but more commonly clinically manifests between 3 weeks and 6 months of age in many affected animals with elevated IOP. Hanna[22] and Kolker[8] found that bilateral buphthalmos with elevated IOP may be observed in 50% to 68% of animals. No gender differences were noted.

Aqueous humor dynamics has been studied in detail in the buphthalmic rabbit. An early study showed that the time taken for aqueous fluorescein to enter the anterior chamber after an intravenous injection was slow, suggesting that either aqueous production was decreased or its output was impaired.[28] However, tonography studies by Becker and Constant[29-31] clearly demonstrated a decreased outflow facility early in the disease. Kolker and associates[22] also noted that in some animals, IOP was not as high as one would expect with a low value of "C" (coefficient for AH outflow), assuming that the rate of AH production was normal. This

suggested that there might be a compensatory mechanism by which the rate of aqueous production was reduced. McMaster and Macri[28] calculated the rate of aqueous formation in buphthalmic rabbits and suggested that the rate was only 46% of that seen in normal rabbits of the same strain. The explanations offered for this phenomenon included pathologic changes secondary to high IOP causing ciliary body atrophy or, alternatively, some regulatory mechanisms that would decrease AH production when the IOP was high. Histologic studies, however, have not described whether ciliary body or epithelial atrophy occurs in buphthalmic animals. The episcleral venous pressure measured in these animals is within the normal range, confirming that the site of obstruction of AH outflow is between the angular meshwork and the episcleral veins.

The appearance of the buphthalmic rabbit cornea can be variable. An increase in corneal diameter is seen in most rabbits, when compared to age-matched controls; this stabilizes at the age of 1 year. Corneal cloudiness is also variable. In the milder forms of buphthalmia and early in the disease, the cornea may demonstrate a mild haze. However, as IOP levels increase, the cornea may become more opacified, giving the eye a bluish-velvety color. Later in the disease, the corneal opacity becomes more diffuse, followed by enlargement of the globe with staphyloma formation. The buphthalmos may be so severe that it prevents eyelid closure and results in secondary corneal changes and globe perforation. The anterior chambers of these animals are deep, whereas the iris and crystalline lens are reportedly normal. Gonioscopy in glaucomatous animals shows absence of pectinate ligaments and open iridocorneal angles. The angles appeared incompletely cleaved with solid sheets of uveal tissue that spanned the anterior chamber angle. Irregular round holes were noted in this tissue in some areas.[32,33]

Glaucomatous optic atrophy has been noticed late in the disease progression among some animals with severe cases. However, others have noted that the optic atrophy and axonal loss may not be seen because of the lack of a well-defined lamina cribrosa that may protect the nerve from pressure-related damage.[34]

Buphthalmic rabbits may demonstrate systemic manifestations. Hanna[8] noted that congenital anomalies were three times higher in buphthalmic animals (8.1% in normal vs 22% in buphthalmic). These anomalies included hydrocephalus, prognathism, microphthalmia, and skeletal anomalies. Fox and colleagues[21] suggested that buphthalmic animals may have a decrease in semen concentration and reduced spermatogenesis. Increased cornification of the corneal epithelium was noted in these animals, and its similarity to that seen in vitamin A deficiency gave rise to the hypothesis that vitamin A deficiency may play a role in the development of buphthalmia. Later studies, however, failed to show any association between vitamin A metabolism and the development of buphthalmia.[35] The condition may be lethal, as 10% to 25% of albino rabbits die at birth. Later in life, the rabbits appear to suffer from loss of general health, appetite, and libido.[8]

GENETICS OF THE BUPHTHALMIC RABBIT

Many studies have indicated that this disease is most likely autosomal recessive with incomplete penetrance. The *bu/bu* gene responsible for the disease in buphthalmic rabbits has not been identified. As previously stated, progress in identifying the gene(s) has been hampered by the lack of the complete sequence of the rabbit genome. Recently, a 7.48X coverage of the genome of the European rabbit was made available by the Broad Institute; this will help in further detailed genetic analysis of the buphthalmic rabbit in the near future.

HISTOLOGIC STUDIES IN THE BUPHTHALMIC RABBIT

Anterior Chamber and Angle Anomalies

In 1920, Rochon-Duvigneaud[14] elegantly demonstrated the abnormal appearance of the anterior chamber angle in the buphthalmic rabbit. Since then, many investigators have described the anterior chamber angle anomalies in greater detail.

The anterior chamber angle of the normal rabbit reveals many distinct structures. These include the presence of the pectinate ligament/iris pillars arising from the iris root to join the collagen bundles of the angular meshwork or Descemet's membrane (DM). The pectinate ligament/iris pillars are lined by endothelial cells that are continuous with the corneal endothelial cells. Posterior to the iris pillars is a space called the ciliary cleft, which separates the anterior chamber from the angular meshwork. The pectinate ligament/iris pillars, which contain hyaluronic acid, may provide some of the resistance to the aqueous outflow. The rabbit eye does not have a Schlemm's canal but instead has an angular aqueous plexus/sinus, which functions similar to the canal of Schlemm. The angular meshwork is composed of several trabecular sheets that lie stacked upon each other. Ultrastructural examination of the trabecular sheets showed that they consist of three layers—a central collagen fibril layer that is covered by endothelial cells on both sides. The trabecular sheets have round openings that give it a Swiss-cheese appearance. The uveoscleral outflow pathway does exist in the rabbit but has not been examined in detail, and its role in the buphthalmic rabbit has not been studied.[36] Despite these differences in the anterior chamber angle anatomy when compared to humans, the rabbit eye responds well to antiglaucoma medication.[37]

The anterior chamber of the buphthalmic rabbit demonstrates a number of abnormalities. In the affected animals at 6 months of age, there is a notable loss or compression of the iris pillars (pectinate ligaments). There is posterior displacement or poor development of the aqueous plexus. The intertrabecular spaces may be dilated or compressed with disorganized trabecular lamellae, a decrease in the number of trabecular endothelial cells, and a loss of trabecular endothelial cell-to-cell associations. Furthermore, some investigators have noted a replacement of the angular meshwork with thick extracellular matrix (ECM) and round cells just beneath the aqueous plexus. A large amount of basilar lamina material has been noted in the thick tissue by electron microscopy. Most of these histologic studies have been done in younger animals up to the age of 4 months.[23,38] The anterior chamber angle dysgenesis in the rabbit appears to be secondary to an alteration in the differentiation and maintenance of the structural integrity of the angular

meshwork. However, whether similar changes persist or change in older buphthalmic animals has not been studied.

AQUEOUS HUMOR BIOCHEMISTRY IN THE BUPHTHALMIC RABBIT

There has been an interest in the biochemical composition of AH in the buphthalmic rabbit. The AH in the buphthalmic rabbit was found to be hypo-osmotic compared to that seen in normal animals.[39] A constant decrease in ascorbate and chloride content was noted, though the total protein content was found to be unchanged.[40] Many researchers have noted that ascorbate levels were threefold lower in the buphthalmic rabbit AH when compared to the control. The serum ascorbate levels were unchanged, suggesting that the decrease was due to a defect in the transport across the ciliary epithelium.[41] The degree of the decrease in ascorbate content appeared to be proportional to the severity of glaucoma, and it was suggested that ascorbate may be responsible for regulating the AH outflow. Other researchers have described a decrease in taurine levels in the AH, suggesting a hereditary defect in taurine transport.[42] No follow-up work was available. A review of recent literature failed to identify a specific genetic defect or a transport mechanism that was solely dedicated to taurine transport. In another study,[43] aqueous fibrinogen concentration was found to be increased in buphthalmic rabbits. Immunohistochemistry of the outflow pathways demonstrated fibrin deposition in a follow-up study.[44] The relationship of these deposits to the pathogenesis of this type of glaucoma is not known, but the findings suggested that such deposits may further compromise AH outflow. More recently, some investigators reported that the changes in the reducing power of AH may be a result of increased oxidative stress caused by the disease, which may further impair the function of the angular meshwork.[24]

In recent years, attention has focused on primary open-angle glaucoma (POAG) and protein alterations in the TM proteome and pathways that may lead to its pathogenesis.[45] However, alterations in the AH proteome in the buphthalmic rabbit have not been studied. Recently, the AH proteome of normal healthy New Zealand white rabbits was studied.[46]

AQUEOUS HUMOR AS A SUBSTRATE TO STUDY ANTERIOR SEGMENT ANOMALIES

Aqueous humor is secreted by the ciliary epithelium. The fluid supplies nutrients and removes metabolic waste from the avascular tissues of the eye, such as the lens and cornea.[47,48] It also maintains the IOP and serves as an antioxidant agent by transporting ascorbic acid into the anterior segment, and it plays a role in local immune and protective responses during inflammation and infections. Secretion of AH fluid is primarily the result of an energy-dependent active transport of ions and water via a complex transport system composed of ion-exchangers, cotransporters, and ion channels.[49]

Aqueous humor contains proteins common to blood plasma, as well as various ions and amino acids. However, the concentrations of these components differ significantly between AH and blood plasma. An additional source of proteins in AH is the ciliary epithelium itself after de novo synthesis, processing, and secretion.[47] It is possible that the TM endothelium, iris, lens, and cornea are sources of secretory proteins in AH because of the direct contact between AH and these tissues. Since a disease such as PCG and some other developmental glaucomas demonstrate anomalies mainly localized to the anterior segment, it is conceivable that aberrant genes expressed in the anterior segment tissues may have local effects on the differentiation and/or function of the anterior segment structures during development. It is also possible that the products of affected genes are secreted into the anterior chamber, altering the AH proteome in the affected animals, which could be detected using proteomic techniques. Such an approach has recently been used to study other anterior segment diseases, as described in the next section.

PROTEOMICS IN GLAUCOMA AND OTHER ANTERIOR SEGMENT EYE DISEASES

Protein levels in the AH are altered in various eye diseases.[50-52] Several studies have demonstrated that some protein changes in the AH correlate with the mechanisms or prognosis of eye disorders such as POAG,[53,54] myopia, and Fuchs' endothelial corneal dystrophy.[55,56] The application of proteomics in the investigation of the pathogenesis of glaucoma is not new. Using traditional proteomic techniques such as two-dimensional (2D) gel electrophoresis, studies have shown that several proteins were expressed at higher levels in the AH of POAG patients. These proteins included TGFβ-2,[45] CD44,[57] TIMP-1,[58] TIMP-2, and VIP.[59] Proteomic studies have also provided new evidence to propose the role of oxidative damage in neurodegeneration in the posterior segment in glaucoma.[60] Some of these studies, however, used traditional proteomic approaches and were able to identify only single protein alterations. Recently, a global approach—label-free LC-MS/MS—was used to study the AH of PCG in humans, and this approach identified several proteins that were differentially expressed in the AH of the PCG patients; these proteins included albumin, antithrombin III, apolipoprotein A-IV, transthyretin (TTR), the interphotoreceptor retinoid-binding protein (IRBP), prostaglandin-H2D-isomerase, and opticin.[4]

Liquid Chromatography/Tandem Mass Spectrometry

This emerging technology has been used for the global analysis of protein expression. In this approach, proteins are first digested with a protease, usually trypsin, into a peptide mixture and subsequently analyzed by MS/MS and identified by database searching. Relative protein abundance is determined by either spectral counting or chromatographic peak intensity measurements.

Recent studies with label-free LC-MS/MS shotgun proteomics have demonstrated that sampling statistics, such as sequence coverage, peptide count, and mass spectral peak intensities of peptide ions correlate well with protein abundances in complex samples.[61] LC-MS/MS has been used in many diseases, such as Alzheimer's disease, to identify novel highly significant disease biomarkers and has been found to provide a relative quantitation of protein expression.[62,63]

In this study, we used label-free LC-MS/MS to identify protein alterations in the AH of 2- and 5-year old buphthalmic rabbits compared to age-matched controls.

METHODS

All experimental procedures using laboratory animals were approved by the local Institutional Animal Care and Use Committee and adhered to the Statement for the Use of Animals in Ophthalmic and Visual Research set forth by the Association for Research in Vision and Ophthalmology (ARVO).

ANIMALS

Buphthalmic and normal rabbits that were littermates were purchased from the Brown Family Enterprises (Odenville, Alabama). A total of six buphthalmic and six normal 2-year-old rabbits and four buphthalmic and four normal 5-year-old rabbits were included in this study. Younger animals were not available at the time of this study.

CLINICAL EXAMINATION

Rabbits were examined using a slit lamp, and the anterior segments were photographed. The corneal diameter was measured using calipers. Intraocular pressure was measured using a Mentor 30 Classic pneumotonometer (Medtronics, Minneapolis, Minnesota) or Tonopen XL (Bio-Rad, Santa Ana, California). Prior to enucleation, AH was collected by paracentesis, as described next.

AQUEOUS HUMOR COLLECTION

Aqueous humor samples were collected from buphthalmic rabbits and their control littermates by anterior chamber paracentesis using a 30-gauge needle inserted through the peripheral cornea under a surgical microscope. A volume of 200 to 500 μL of AH from each eye was collected into a tuberculin syringe. Contact with other intraocular structures, such as the iris and the anterior lens capsule, was avoided to prevent possible subsequent release of noninvolved proteins. Samples were immediately transferred to a cryotube, placed on dry ice, and stored at –80°C until processing. Samples were examined using LC-MS/MS.

GROSS PATHOLOGY

Following euthanasia, eyes were enucleated and the globe anterior/posterior and the corneal diameters were measured using calipers.

HISTOLOGY

Sixteen enucleated eyes from buphthalmic and age-matched normal 2- and 5-year-old rabbits were fixed in neutral buffered 10% formalin, processed, and embedded in paraffin for light microscopy. Five-micrometer sections were stained with hematoxylin and eosin, periodic acid–Schiff (PAS) to delineate basement membranes, Alcian blue pH 2.5 for acid mucopolysaccharide staining, or Masson's trichrome for collagen staining. The sections were viewed and analyzed with an Olympus BX51 brightfield microscope (Olympus, Japan). Quantitative assessment of the corneal stromal thickness, thickness of DM, and the anterior lens capsule was performed on PAS-stained sections using *Image Pro 6.3* software (Media Cybernetics, Bethesda, Maryland). Thickness measurements were taken at three points of the central DM and at the polar anterior and posterior lens capsule. The readings were averaged for each specimen, and differences in DM and capsular thickness between buphthalmic and normal animals were determined statistically using the Mann-Whitney *U* test. To determine whether ciliary epithelial atrophy played a role in lowering IOP in the older buphthalmic animals, the nonpigmented ciliary epithelial cells around the ciliary processes were counted using *Image Pro 6.3* analysis software (Media Cybernetics, Bethesda, Maryland). Cells per unit area were counted in the 2- and 5-year-old buphthalmic rabbits and their appropriate control littermates.

ELECTRON MICROSCOPY

One eye from each 2-year-old buphthalmic rabbit and normal control was fixed in McDowell-Trump's fixative (4% formaldehyde, 1% glutaraldehyde). Fragments of central cornea and anterior lens capsule were processed for transmission electron microscopy and embedded in epoxy resin. The tissue was examined under a Zeiss electron microscope (Zeiss, Germany). Attention was focused toward observation of alterations in the structures of corneal stromal collagen, DM, and corneal endothelium, and the lens capsule and its epithelium in the buphthalmic rabbit compared with the controls. The remaining tissue from the other two eyes was dissected and frozen for future analysis.

LIQUID CHROMATOGRAPHY/TANDEM MASS SPECTROMETRY

Sample Preparation

Aqueous humor samples were processed individually as described previously[64] with some minor modifications to the gel-washing steps. Samples were prepared for in-gel digest by mixing 100 μL of AH with 100 μL acrylamide/bis (30%T/2.67%C), 10 μL of 10% NaOH, 10 μL of 10% ammonium persulfate, and 5 μL of TEMED in the lid of a microcentrifuge tube. Gel pieces were transferred into the tubes, fixed in 1 mL of 40% methanol, 7% acetic acid for 30 minutes, washed four times with water, once with 200 mM ammonium bicarbonate, twice with 100 mM ammonium bicarbonate in 50% acetonitrile, then dried under vacuum using a SpeedVac. Next, 200 μL of 100 mM ammonium bicarbonate (pH 8.0) containing 0.5 μg trypsin (Promega, Madison, Wisconsin) was added to each gel piece and incubated overnight at 37ºC. Peptides in each gel piece were extracted with three washes of 70% acitonitrile and 0.1% formic acid. The extracts were then pooled together and dried. Twenty microliters of 6M guanidine HCl in 5 mM potassium phosphate and 1 mM DTT (pH 6.5) was added to each dried sample and sonicated. Peptides were then extracted using a C18 ZipTip

(Millipore, Billerica, Massachusetts) and subjected to nanospray LC-MS/MS analysis. Each sample was run once on the mass spectrometer using an extended linear gradient as described next.

Nanospray LC-MS/MS Spectrometry

Automated nanospray LC-MS/MS was performed using an LTQ-LC/MS (Thermo Fisher Scientific, Waltham, Massachusetts). Peptide mixtures were separated using a C18 reverse phase column (0.75-Å internal diameter at a flow rate of 1 μL/min) in line with the mass spectrometer. The mobile phases consisted of 0.1% formic acid containing 5% acetonitrile (A) and 0.1% formic acid in 95% acetonitrile (B), respectively. A 180-minute linear gradient was used followed by 60 minutes of equilibration in solvent A. The ions eluted from the column were electrosprayed at a voltage of 1.75 kV. The LC-MS/MS cycle was 6 MS/MS scans per full MS scan. Dynamic exclusion enabled ±1.5 Da tolerance and 12-second exclusion duration.

Data Analysis

The MS data collected were analyzed using the SEQUEST algorithm (Thermo Fisher Scientific, Waltham, Massachusetts) searched against the vertebrates, including the rabbit subset of the UniProt database,[65] using a peptide mass tolerance of 2.5 Da, a fragment mass tolerance of "0," which is effectively 1 Da, and monoisotopic masses. Relative quantitative expression of proteins was determined using scan counts as previously described.[65,66] To determine the proteins with significantly different levels between the buphthalmic rabbit and control samples, data from each group were combined using "Visualize" (Medical College of Wisconsin, Milwaukee, Wisconsin). Normalized *P* values were determined using the *G*-test (log likelihood ratio test for goodness of fit) as previously described.[67] Post hoc adjustment of the *P* value was performed using the Holm-Sidak test to correct for multiple comparisons. Proteins that appeared in 100% of samples with an adjusted *P* value <.05 were sorted into up-regulated or down-regulated sets based on a log 2 ratio of greater than 1 or less than 1 as previously described.[68] The analysis also included proteins that were detected with a high scan count number and were present in all normal rabbits but not in any of the buphthalmic rabbits.

WESTERN BLOT ANALYSIS

Western blot analyses were performed on AH samples to validate the results obtained by LC-MS/MS for some of the proteins that showed significant differences between the buphthalmic and normal AH. The AH protein concentration was determined using the Bradford assay (Bio-Rad Laboratories, Hercules, California). Equal amounts of sample (10 μg) were resolved on a 10% sodium dodecyl sulfate polyacrylamide gel. The proteins were then transferred into a polyvinylidene fluoride (PVDF) membrane (Bio-Rad Laboratories, Hercules, California). After blocking with 2% bovine serum albumin, the membranes were probed with rabbit anti-bovine IRBP (1:500; a gift from Dr Todd Dunkin, National Institutes of Health, Bethesda, Maryland), mouse anti-human beta-2 microglobulin (B2M) (1:1000, MyBiosource, San Diego, California), or mouse anti-human clusterin (1;1000, Lifespan Biosciences, Seattle, Washington) followed by horseradish-peroxidase–conjugated secondary antibody (1:50;000; Jackson ImmunoResearch Laboratories, Inc, West Grove, Pennsylvania). The signal was detected by enhanced chemiluminescence using SuperSignal West Pico (Thermo Scientific, Rockford, Illinois).

IMMUNOFLUORESCENCE

Deparaffinized slides from eyes of buphthalmic rabbits and controls were rehydrated using graded ethanol. Immunohistochemistry was performed using antibodies against two groups of proteins. The first group included antibodies against fibronectin and collagen IV, which are major basement membrane components. The second group of antibodies were against a panel of proteins that were differentially expressed in the AH of the buphthalmic rabbit. Antigen retrieval was performed using 1X antigen retrieval solution (Dako, Carpinteria, California) per the manufacturer's instructions. The sections were blocked for 45 minutes using 10% normal goat or donkey serum followed by labeling by overnight incubation at 4°C with the primary antibody (Table 1) followed by Texas Red or Alexa Fluor 488 conjugated secondary antibody (Jackson ImmunoResearch Laboratories, Inc, West Grove, Pennsylvania). Blocking and washing steps were performed in a humid chamber at room temperature. All washes were performed three times for 5 minutes each in phosphate-buffered saline. Antibody binding was detected by immunofluorescence and visualized using an Olympus BX51 fluorescent microscope (Olympus, Japan). Fluorescence intensity for fibronectin and collagen IV was measured using *Image Pro 6.3* software (Media Cybernetics, Bethesda, Maryland) at three different equal areas along DM and the lens capsule, and the staining intensity was averaged over the different locations.

The staining intensity for the other antibodies used in this study was semiquantitatively assessed by two observers on a scale from 0 to 4+, 0 representing no staining and 4+ representing intense staining.

STATISTICAL ANALYSIS

For LC-MS/MS data, *G*-test followed by post hoc Holm-Sidak was used to determine the significant differences in protein levels in AH as described above. For other analyses, Mann-Whitney *U* test was used. A *P* value <.05 was considered statistically significant.

RESULTS

OCULAR EXAMINATION

When examined, the buphthalmic eyes appeared more prominent with larger corneas and thinning of the sclera. The globe size and corneal diameter were increased in the buphthalmic rabbits when compared to normal rabbits (Figure 1, Table 2). The IOP was

slightly higher in the 2-year-old buphthalmic animals compared with the controls, but the difference reached statistical significance only in the 5-year-old buphthalmic animals, where the average IOP was 22 mm Hg and higher than that noted in the 2-year-old buphthalmic animals (Figure 2). The corneas in both 2- and 5-year-old rabbits showed a mild corneal haze that was noted upon slit-lamp examination, suggesting a milder phenotype. The anterior chamber appeared unremarkable, and the lens was clear. Optic nerve cupping was not observed.

TABLE 1. ANTIBODIES USED IN IMMUNOHISTOCHEMISTRY*

ANTIBODY	COMPANY
Mouse anti-human histidine-rich glycoprotein (HRG)	Abcam, Cambridge, Massachusetts
Goat anti human alpha-2-HS-glycoprotein (A2GS)	Novus Biologicals, Littleton, Colorado
Goat anti-human cochlin	Santa Cruz Biotechnology, Inc, Santa Cruz, California
Clusterin (Clu)	MyBioSource, San Diego, California
Goat anti-human apolipoprotein E (ApoE)	GenWay Biotech, Inc, San Diego, California
Rabbit anti-bovine interphotoreceptor retinoid-binding protein (IRBP)	A generous gift from Dr Todd Duncan, National Institutes of Health, Bethesda, Maryland
Sheep anti-human transthyretin (TTR)	Abcam, Cambridge, Massachusetts
Mouse anti-human gelsolin (Gel)	Abcam, Cambridge, Massachusetts
Sheep anti-human haptoglobin (HPT)	Novus Biologicals, LLC, Littleton, Colorado
Mouse anti-human hemopexin (HPX)	Novus Biologicals, LLC; Littleton, Colorado

*All antibodies were used at 1:100 dilution.

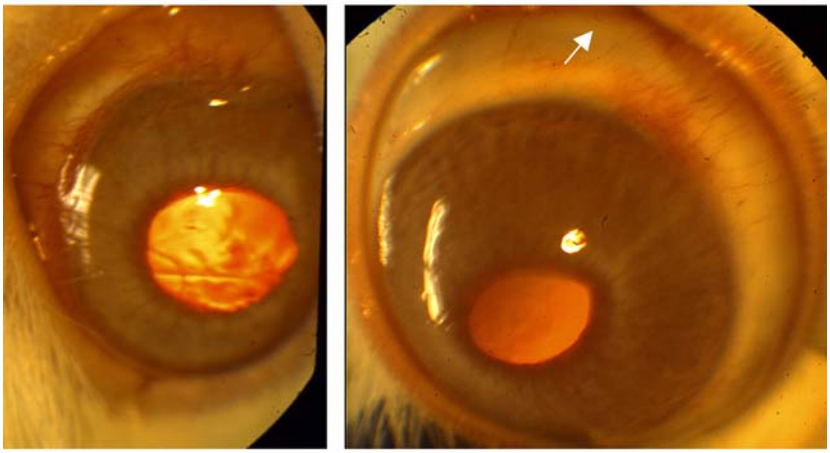

FIGURE 1

Slit-lamp photograph of 2-year-old normal rabbit eye (left) and 2-year-old buphthalmic rabbit eye (right). Note the clear corneas and normal size in normal rabbit and bulging enlarged globe with large cornea and scleral thinning (arrow) in buphthalmic rabbit.

TABLE 2. ANTERIOR/POSTERIOR (GLOBE) DIAMETER AND CORNEAL DIAMETER IN NORMAL AND BUPHTHALMIC RABBITS (MEAN ± SEM)

DIAMETER	TWO-YEAR-OLD RABBITS		FIVE-YEAR-OLD RABBITS		
	NORMAL	BUPHTHALMIC	NORMAL	BUPHTHALMIC	*P* VALUE
Anterior/posterior (mm)	14±0.5	19±0.8	Not done	Not done	.02
Corneal (mm)	13±0.57	17±0.5	Not done	Not done	.02

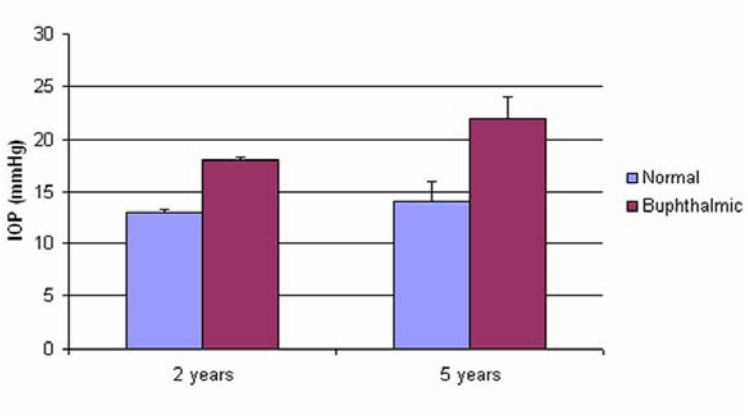

FIGURE 2

Intraocular pressure (IOP) in the 2-year-old normal and buphthalmic (*P*=.125) and 5-year-old normal and buphthalmic (*P*=.039) rabbits. (Values are mean ±SEM IOP of normal and buphthalmic rabbit right and left eyes).

HISTOPATHOLOGY

Cornea and Iris

In the control rabbits, the epithelium, stroma, DM, and corneal endothelial cells appeared unremarkable in both the 2- and 5-year-old animals. In the buphthalmic rabbits, the corneal epithelium appeared stratified, of normal thickness, and without keratinization. The 2-year-old rabbits showed variable degrees of corneal stromal edema in a few animals, but in the others the stroma appeared unremarkable. The buphthalmic corneal stroma in the 2-year-old animals was significantly thicker than the control stroma *(P*=.049). The 5-year-old buphthalmic rabbits showed variable corneal stromal thinning, likely due to stretching of the globe and significantly thinner than the controls *(P*=.049) (Figures 3 and 4). Ultrastructurally, the stromal collagen fibrils were regularly arranged in both the control and 2-year-old buphthalmic rabbits, and the collagen fibril size was comparable (Figure 5). There appeared to be a slight increase in the interfibrillar distance, but this observation was variable (Figure 5, inset).

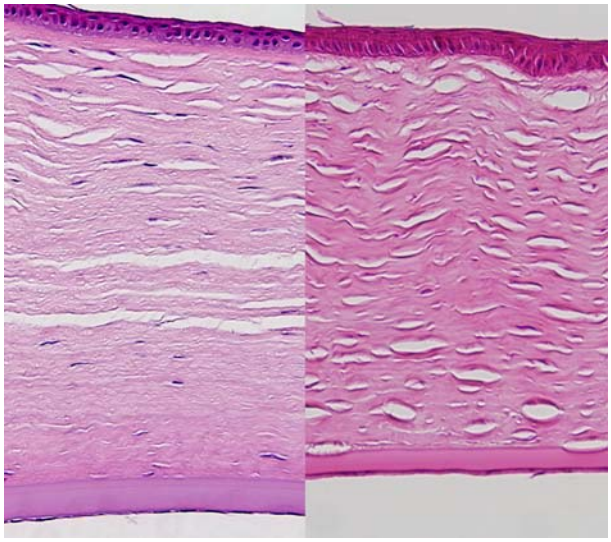

FIGURE 3

Photomicrograph of cornea from a 2-year-old buphthalmic eye showing posterior stromal edema and thickening of Descemet's membrane (left) and a 5-year-old buphthalmic eye showing central stromal thinning (right). Note that Descemet's membrane is normal in thickness in areas of stromal thinning, whereas in other areas there was moderate thickening (original magnification ×10; hematoxylin and eosin).

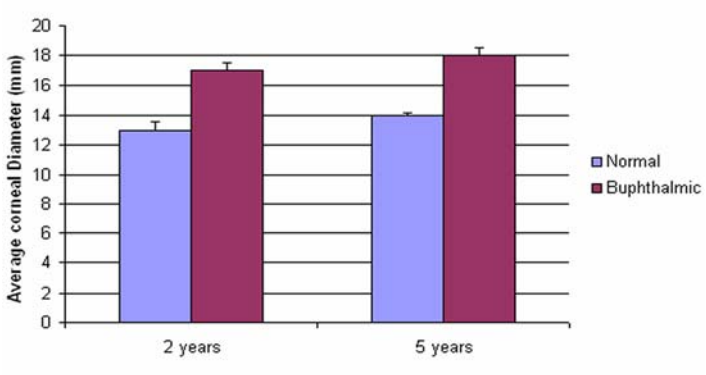

FIGURE 4

Corneal stromal thickness (mean ±SEM) in 2-year-old buphthalmic rabbits vs 5-year-old buphthalmic rabbits. (Measurements were taken from the central cornea.) The difference in thickness was significant at 2 and 5 years (*P*=.049).

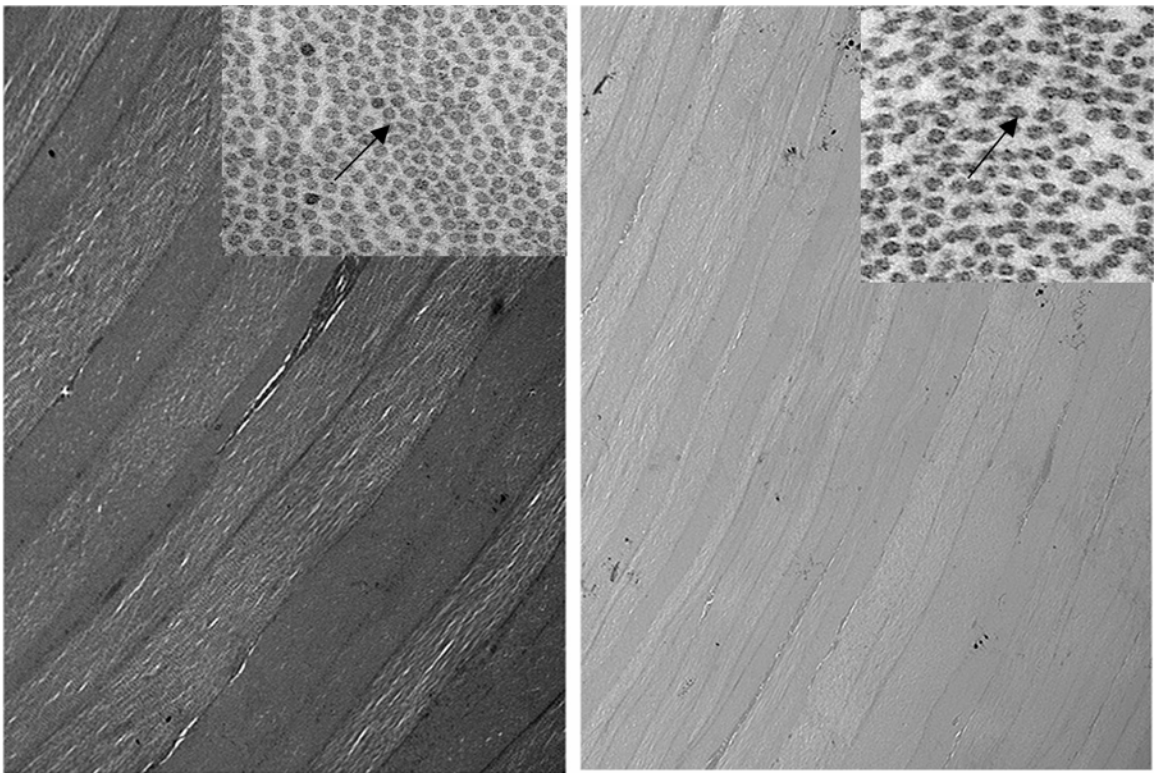

FIGURE 5

Electron micrograph showing arrangement of corneal stromal fibers at low magnification of a 2-year-old normal rabbit (left) and a buphthalmic rabbit (right). Note the regular arrangement of stromal collagen fibrils in both tissues (original magnification ×12,000, left, and ×8000, right). Inset, Stromal collagen fibrils at higher magnification. Note the normal-sized collagen fibrils that appear uniform in thickness. The interfibrillar distance (arrows) is somewhat widened in the buphthalmic animal, possibly as a result of stromal edema (original magnification ×30,000).

Both the 2- and 5-year-old buphthalmic rabbit groups showed significant thickening of DM when compared to their control littermates (Figures 6 and 7) (*P* value is available on Figure 7). The thickening of DM was more prominent centrally except in some 5-year-old animals, where DM was variable in thickness throughout its length due to globe stretching and corneal thinning. However, in some eyes, remarkable thickening was noted despite overlying stromal thinning. The endothelial cell density appeared attenuated subjectively based on endothelial cell nuclear spacing, but the cellular structure appeared intact. Vacuolization of the corneal endothelial cell cytoplasm was noted in some areas and was likely artifactitious (Figure 6). Ultrastructurally, DM showed a normal anterior banded zone in both the control and buphthalmic rabbits. Thickening of DM mainly resulted from increased thickness of the posterior nonbanded zone (Figure 8). In rare areas, a posterior collagenous layer was noted. Also, notably long-spacing collagen was observed consistently in the posterior parts of the posterior nonbanded zone in the normal control but was absent in multiple thin sections and grids from the 2-year-old buphthalmic rabbit (Figure 9). The corneal endothelial cells were present as a monolayer with prominent rough endoplasmic reticulum and dilated extracellular spaces in intercellular regions (Figure 9). No ultrastructural differences in the corneal endothelium were noted between the buphthalmic and control animals.

The iris structure appeared unremarkable in both the normal and buphthalmic animals, with normal stromal architecture, dilator muscle, and iris pigmented epithelium.

Anterior Chamber Angle

The normal 2- and 5-year-old animals demonstrated normal iris pillars and ciliary cleft with a well-defined spongy angular meshwork that demonstrated well-delineated trabecular beams. The aqueous plexus appeared to be located anteriorly in its normal position. DM was identified peripheral to the iris pillars. In this location, DM was thinner than that observed centrally (Figure 10).

In the 2-year-old buphthalmic rabbit anterior chamber angle, the trabecular beams appeared compressed and disorganized when compared to those seen in the control rabbit. The iris pillars were either more posterior or absent, and the ciliary cleft was not seen. Peripheral DM appeared to attach directly to the angular meshwork. Also, the trabecular beams were compressed and somewhat disorganized. The aqueous plexus was identified in buphthalmic rabbits and controls and appeared comparable under light microscopy. In the 5-year-old buphthalmic rabbits, thick cellular tissue replaced the trabecular beams and the pectinate ligament was not identified. The aqueous plexus was not well delineated (Figure 10).

Lens

The anterior lens capsule demonstrated marked thickening in the buphthalmic rabbits that was highlighted by PAS stain. It was significantly thicker in both the 2- and 5-year-old rabbits when compared to the controls (Figures 7, 11, and 12). The average thickening by morphometry was slightly less in the 5-year-old rabbits, likely due to globe stretching, but was still significantly thicker than in the controls (Figure 7). The lens capsule transitioned to normal thickness at the lens equator. The posterior capsule thickness in the buphthalmic and control animals was comparable (Figure 7) in both age groups (Figures 11 and 12). By electron microscopy, the anterior lens capsule demonstrated a fibrillar basement membrane that was comparable in appearance in both buphthalmic and control animals (Figure 13). The anterior lens epithelial cells did not show morphologic alterations by light or electron microscopy. The lens cortical fibers and nucleus appeared unremarkable.

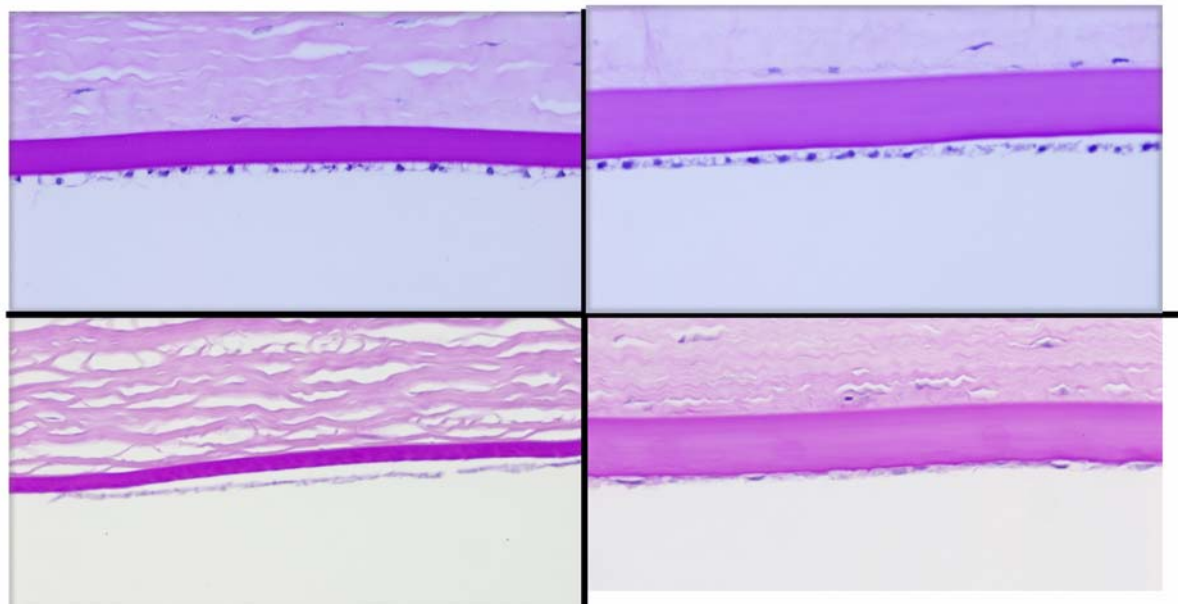

FIGURE 6

Photomicrograph showing central Descemet's membrane of a normal (left panel) and a buphthalmic (right panel) rabbit. Upper panel is from 2-year-old and lower panel from 5-year-old (lower panel) rabbit. Note that Descemet's membrane is thicker in the buphthalmic animal in both the 2- and 5-year-old rabbits. There is some variability in the thickness of Descemet's membrane, endothelial cell attenuation in the buphthalmic cornea, and some artifactitious changes in the corneal endothelium (periodic acid–Schiff stain; original magnification ×20).

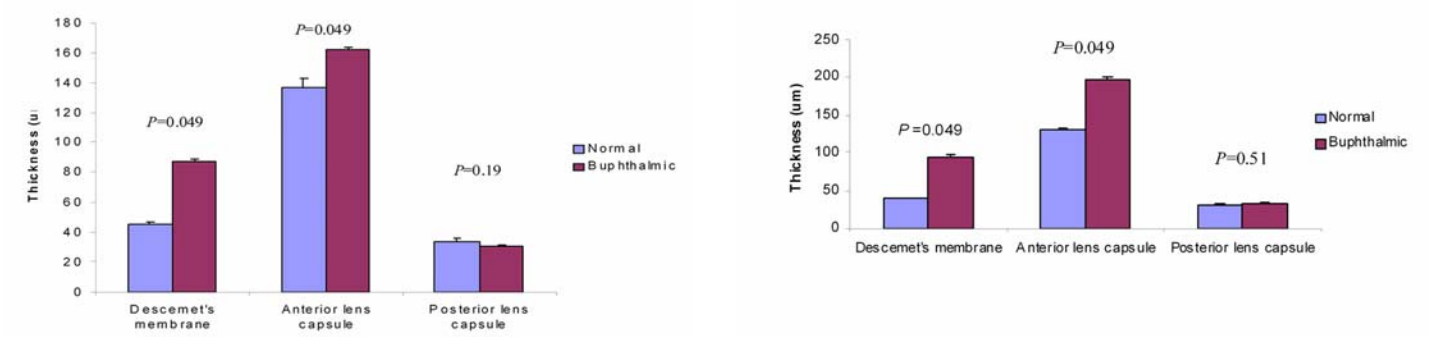

FIGURE 7

Bar graphs showing thickness of Descemet's membrane, anterior lens capsule, and posterior lens capsule in normal and buphthalmic rabbits at 2 years (left) and 5 years (right) of age (mean ±SEM). *P* values for differences in thickness are shown above each bar graph. Measurements were taken at ×10 magnification.

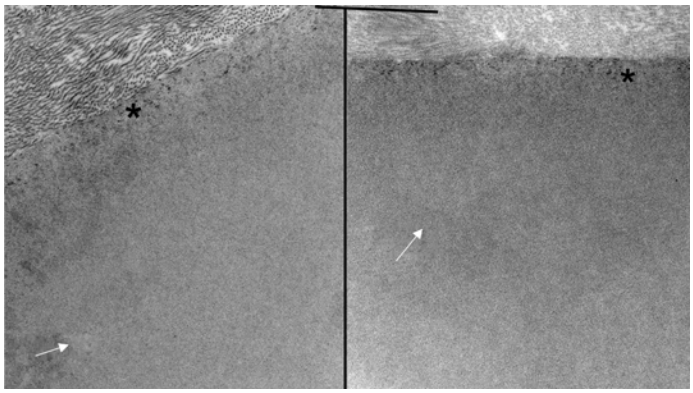

FIGURE 8

Electron micrograph of the interface between corneal stroma in Descemet's membrane in the normal control (left) and the buphthalmic (right) rabbit. Note the normal anterior banded zone (*) in both rabbits. The posterior nonbanded zone (arrows) in both animals appeared unremarkable (original magnification ×10,000).

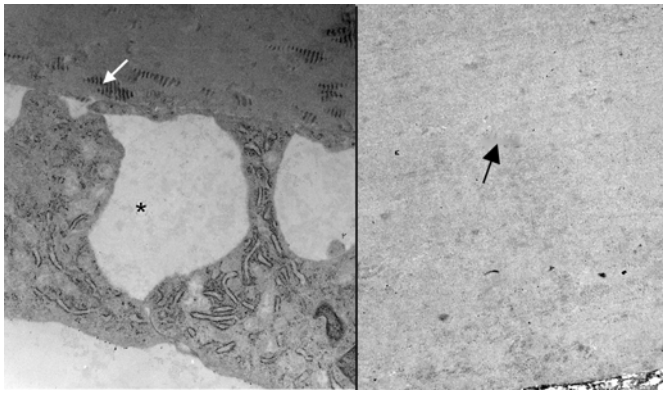

FIGURE 9

Electron micrograph showing the posterior Descemet's membrane and endothelium in the normal rabbit (left) and posterior part of thickened Descemet's membrane in a 2-year-old buphthalmic rabbit (right). Left, Note the presence of abundant long-spacing collagen (white arrow) in the posterior nonbanded zone of Descemet's membrane. The corneal endothelial cells show prominent rough endoplasmic reticulum and widened intercellular spaces (*). Right, Note the fibrillar collagenous basement membrane in the posterior nonbanded zone (black arrow) in the buphthalmic rabbit with absence of long-spacing collagen (original magnification ×12,000, and ×10,000, respectively).

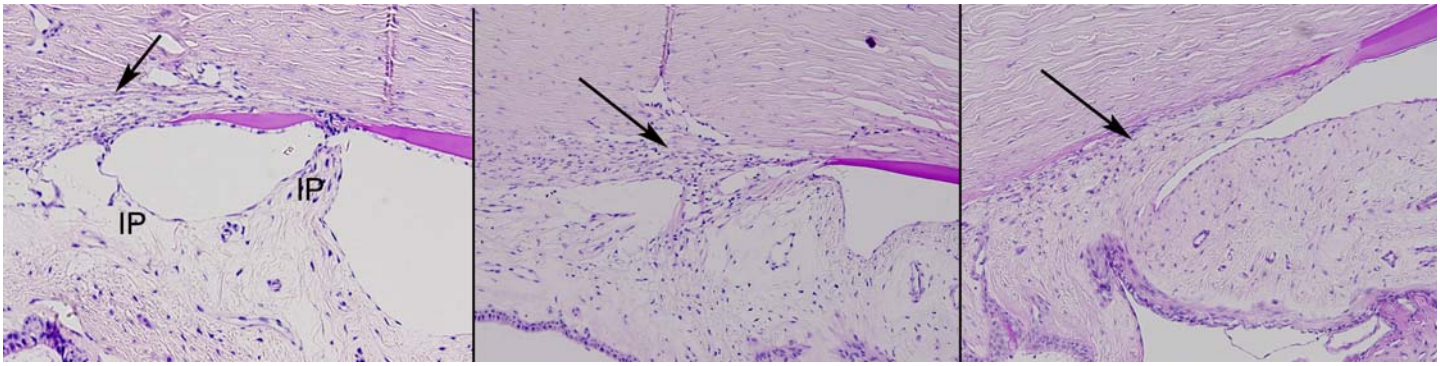

FIGURE 10

Photomicrograph of the anterior chamber angle in normal 2-year-old control (left), 2-year-old buphthalmic rabbit (middle), and 5-year-old buphthalmic rabbit (right). Left, The normal rabbit shows well-defined iris pillars (IP) that are attached to Descemet's membrane or the trabecular meshwork (TM) (arrow) to form a ciliary cleft posterior to the IPs. Descemet's membrane appears to extend beyond the IPs. The TM beams are well defined and separated (arrow) with the aqueous plexus seen superficial to the angular meshwork. Middle, In 2-year-old buphthalmic rabbit, IPs are absent; the TM appears to be located posteriorly with compressed beams that are fewer in number (arrow). The aqueous plexus is visible. Right, Five-year-old buphthalmic rabbit showing trabecular beams replaced by a thick collagenous matrix (arrow). The IPs are absent. The aqueous plexus is not well defined (original magnification ×10; periodic acid–Schiff stain).

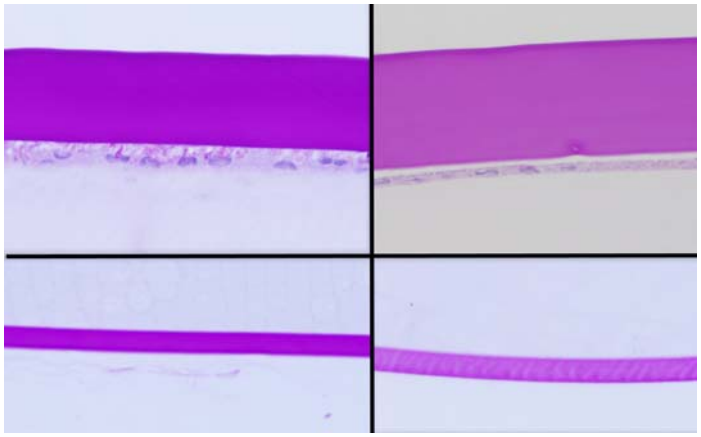

FIGURE 11

Panel showing the central anterior (upper panel) and posterior (lower panel) lens capsules in a normal (left panel) and 2-year-old (right panel) buphthalmic rabbit. Note the marked thickening of the anterior lens capsule in the buphthalmic rabbit when compared to the normal animal and to the 2-year-old buphthalmic animal. The posterior capsular thickness is comparable in the normal and buphthalmic animals (original magnification ×20; periodic acid–Schiff stain).

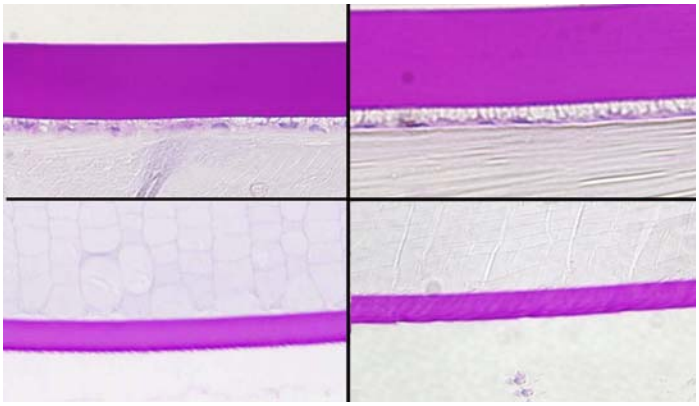

FIGURE 12

Panel showing the central anterior (upper panel) and posterior (lower panel) lens capsules in a normal (left panel) and 5-year-old (right panel) buphthalmic rabbit. Note the moderate thickening of the anterior lens capsule in the buphthalmic rabbit when compared to the normal. The posterior capsular thickness is comparable in the normal and buphthalmic animals (original magnification ×20; periodic acid–Schiff stain).

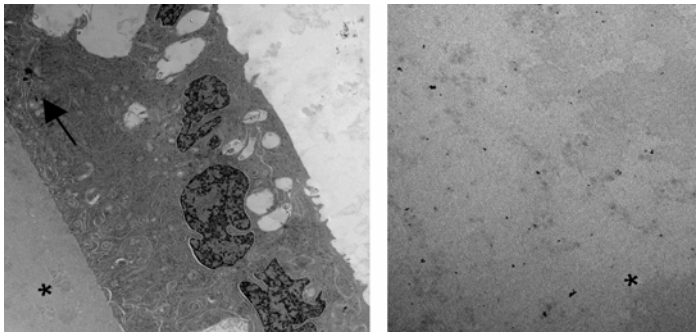

FIGURE 13

Electron micrograph of the anterior lens capsule from the 2-year-old buphthalmic rabbit. The basement membrane of the anterior lens capsule is amorphous and uniform in density and composed of fine, regularly arranged, parallel fibrillar collagen similar to that seen in normal control (not shown). Note the interdigitating cellular processes of the lens epithelial cells (arrow) with a smooth interface between the lens epithelium and lens capsule (*) (original magnification ×2000). Right panel demonstrated a homogenous appearance of the thickened anterior lens capsule at low magnification (original magnification ×2500).

Ciliary Body

The ciliary body in both animal groups appeared unremarkable. In the 5-year-old buphthalmic animals, the ciliary body may have been more slender owing to elongation of the globe. Morphometry of the nonpigmented ciliary epithelium in the normal and the 2- and 5-year-old buphthalmic rabbits revealed similar counts per unit area (P =.12), suggesting that the nonpigmented ciliary epithelium (inner layer) was not atrophic (Figure 14).

Retina

The retina in the buphthalmic rabbit showed scattered retinal ganglion cell attenuation when compared with the controls. No optic nerve cupping was noted. In addition, no other basement membranes in the eye were thickened other than DM and the anterior lens capsule.

HISTOCHEMICAL STAINING

Alcian blue (pH 2.5) staining for mucopolysaccharides showed mild to moderate staining of the corneal stroma, angular meshwork, and iris stroma in both normal and buphthalmic eyes. There were no differences noted in the Alcian blue staining intensity between the normal and buphthalmic angular meshwork. The degree of Alcian blue staining of the iris in the 5-year-old buphthalmic animals appeared slightly decreased compared to the 5-year-old normal controls and the 2-year-old buphthalmic rabbits. Also, dense collagen deposition was noted at the iridocorneal angle of the 5-year-old buphthalmic rabbit as demonstrated by Masson's trichrome staining (Figures not included).

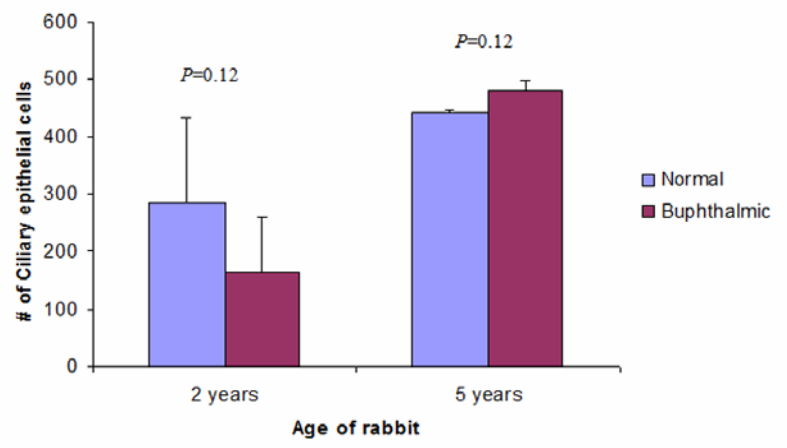

FIGURE 14

Ciliary epithelial cell count per unit area in the 2-year-old and 5-year-old normal and buphthalmic rabbits (mean ± SEM). The differences in cell counts were not statistically significant.

IMMUNOHISTOCHEMISTRY

To further define the alterations in DM and the lens capsule, immunofluorescence was performed to label major basement membrane components, fibronectin and collagen type IV. Anti-fibronectin and anti-collagen IV labeling intensity was significantly increased in the buphthalmic eyes when compared to normal eyes (P=.02) (Figures 15 and 16). Anti-fibronectin and anti-collagen type IV labeling was not detected in other anterior segment structures.

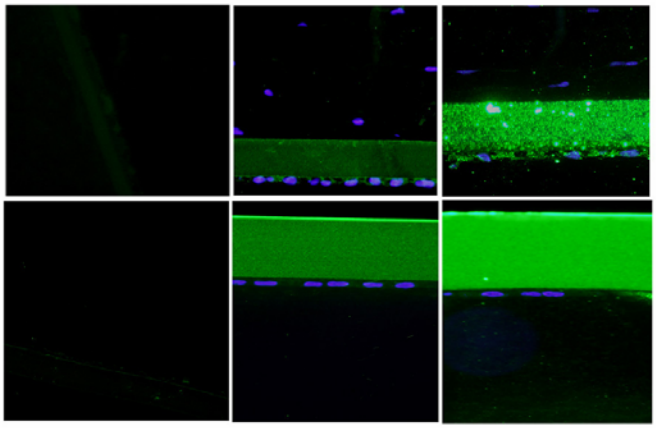

FIGURE 15

Immunoreactivity of Descemet's membrane (upper panel) and anterior lens capsule (lower panel) to anti-collagen type IV in negative control (left panel) and normal (middle panel) and 2-year-old (right panel) buphthalmic animal. Note the increased staining intensity in Descemet's membrane and the anterior lens capsule in the buphthalmic animal compared to normal control (original magnification ×20, Alexa Fluor; DAPI used as nuclear stain).

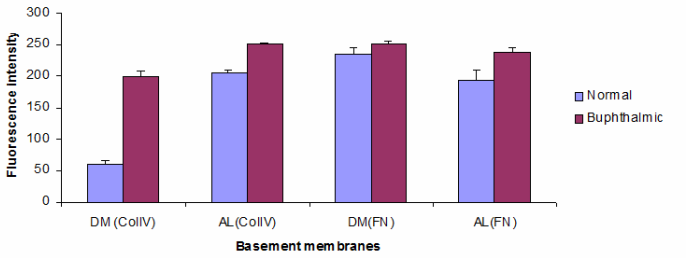

FIGURE 16

Fluorescent staining intensity with anti-collagen IV (CollV) and anti-fibronectin (FN) in Descemet's membrane (DM) and the anterior lens capsule (AL) for both normal and buphthalmic rabbits (mean ± SEM) (P=.02).

PROTEOMICS

LC-MS/MS

Tables 3 and 4 list all proteins identified in the 2- and 5-year-old normal and buphthalmic rabbits, respectively. Proteins are listed according to their UniProt protein accession number, number of unique peptides detected for each protein (proteins detected with only one peptide were excluded from the list and further analyses), scan count number, the number of samples in which the peptides were detected (frequency/total), normalized log ratio, and the adjusted P value. Differentially expressed proteins were selected according to the following criteria: detected with at least two unique matched peptides detected for each protein and two spectral counts or higher with a SEQUEST score of 2.5 or higher,[69] detected in 100% of the samples, and the adjusted P value is ≥.05.

TABLE 3. COMMON PROTEINS IDENTIFIED IN THE TWO-YEAR-OLD NORMAL (N) AND BUPHTHALMIC (B) RABBITS

ACCESSION	DESCRIPTION	N PEPTIDES	N SCANS	N FREQUENCY/ TOTAL*	B PEPTIDES	B SCANS	B FREQUENCY/ TOTAL*	NORMALIZED LOG RATIO†	ADJUSTED *P* VALUE
P12109	Collagen alpha-1(VI) chain precursor	5	76	2/6	6	312	3/6	1.863009	0.000000
P00004	Cytochrome c	2	288	1/6	0	0	0/6	Ns only	0.000000
P35527	Keratin, type I cytoskeletal 9	4	8	4/6	20	77	3/6	3.092321	0.000000
P79385	Lactadherin (MFG-E8) (MFGM)	4	19	2/6	6	103	3/6	2.264108	0.000000
P12110	Collagen alpha-2(VI) chain precursor	1	35	2/6	2	135	3/6	1.773067	0.000000
P35908	Keratin, type II cytoskeletal 2 epidermal	4	5	3/6	12	50	5/6	3.147463	0.000000
P04264	Keratin, type II cytoskeletal 1	7	31	5/6	20	97	5/6	1.471251	0.000005
P13645	Keratin, type I cytoskeletal 10	2	2	2/6	7	26	4/6	3.525974	0.000167
P12111	Collagen alpha-3(VI) chain precursor	7	8	3/6	8	37	3/6	2.034988	0.001948
Q28640	Histidine-rich glycoprotein precursor (HPRG) (Fragment)	21	216	6/6	20	160	6/6	-0.60742	0.002407
P01948	Hemoglobin alpha-1/2 subunit	0	0	0/6	2	8	1/6	Bs only	0.069580
Q9XSC5	Clusterin precursor (Apolipoprotein J) (Apo-J)	14	90	6/6	13	63	6/6	-0.68904	.153871
P49065	Serum albumin precursor	56	4651	6/6	57	5444	6/6	0.052661	0.188919
P04104	Keratin, type II cytoskeletal 1	0	0	0/6	3	6	4/6	Bs only	0.252042
P12387	Complement C3 precursor	6	49	6/6	5	30	6/6	-0.88228	0.306247
P12247	Complement C3 alpha chain (Fragment)	9	52	6/6	7	33	6/6	-0.83051	0.352699
Q28372	Gelsolin (Actin-depolymerizing factor) (Brevin)	17	184	6/6	12	158	6/6	-0.39425	0.441758
P01857	Ig gamma-1 chain C region	0	0	0/6	2	5	2/6	Bs only	0.446794
Q61703	Inter-alpha-trypsin inhibitor heavy chain H2 precursor (ITI heavy chain H2)	0	0	0/6	2	5	4/6	Bs only	0.446794
P07489	Transthyretin (Prealbumin)	15	222	6/6	15	198	6/6	-0.33952	0.552285
P01024	Complement C3 precursor	4	14	6/6	1	5	3/6	-1.65989	0.596636
P14943	Liver carboxylesterase 2 (EC 3.1.1.1)	7	25	5/6	7	13	4/6	-1.11788	0.628761
P0C0L4	Complement C4-A precursor (Acidic complement C4)	6	43	6/6	6	28	6/6	-0.79338	0.666810

TABLE 3 (continued). COMMON PROTEINS IDENTIFIED IN THE TWO-YEAR-OLD NORMAL (N) AND BUPHTHALMIC (B) RABBITS

ACCESSION	DESCRIPTION	N PEPTIDES	N SCANS	N FREQUENCY/ TOTAL*	B PEPTIDES	B SCANS	B FREQUENCY/ TOTAL*	NORMALIZED LOG RATIO†	ADJUSTED *P* VALUE
P09809	Apolipoprotein A-I precursor (Apo-AI) (ApoA-I)	36	486	6/6	34	474	6/6	-0.21053	0.700196
Q6ZQK0	Protein KIAA0056	2	3	3/6	0	0	0/6	Ns only	0.815664
P50757	72 kDa type IV collagenase precursor (Matrix metalloproteinase-2) (MMP-2)	2	3	3/6	0	0	0/6	Ns only	0.815664
O77588	Procollagen-lysine,2-oxoglutarate 5-dioxygenase 1 precursor	2	3	3/6	0	0	0/6	Ns only	.815664
P53601	Amyloid beta A4 protein precursor (APP) (ABPP)	3	3	2/6	0	0	0/6	Ns only	0.815664
O02833	Insulin-like growth factor-binding protein complex acid labile chain precursor (ALS)	2	3	2/6	0	0	0/6	Ns only	0.815664
P49822	Serum albumin precursor (Allergen Can f 3)	2	3	2/6	1	1	1/6	-1.75943	0.827185
P02770	Serum albumin precursor	1	4	2/6	2	3	3/6	-0.5895	0.832158
Q4AEH3	Glutathione peroxidase 3 precursor (GPx-3)	1	1	1/6	2	7	4/6	2.63289	0.845560
P04186	Complement factor B precursor (EC 3.4.21.47) (C3/C5 convertase)	2	2	1/6	3	9	5/6	1.99546	0.900907
Q5R4N8	Alpha-2-macroglobulin precursor (Alpha-2-M)	2	9	4/6	1	3	2/6	-1.75943	0.914661
P23775	Corticosteroid-binding globulin (CBG) (Transcortin)	2	12	6/6	2	5	4/6	-1.4375	0.918505
Q7YQD7	EGF-containing fibulin-like extracellular matrix protein 1 precursor	2	12	4/6	1	5	3/6	-1.4375	0.918505
P02057	Hemoglobin beta-1/2 subunit (Hemoglobin beta-1/2 chain)	0	0	0/6	2	3	1/6	Bs only	0.927145
Q13822	Ectonucleotide pyrophosphatase/phosphodiesterase 2 (E-NPP 2)	9	44	6/6	7	32	6/6	-0.6339	0.945972
Q9TTK6	Membrane copper amine oxidase (EC 1.4.3.6)	2	7	2/6	1	2	1/6	-1.98182	0.950901
P12337	Liver carboxylesterase 1 precursor (EC 3.1.1.1)	3	5	3/6	1	1	1/6	-2.49639	0.964417
Q9BX66	Sorbin and SH3 domain-containing protein 1 (Ponsin)	1	5	1/6	1	1	1/6	-2.49639	0.964417

TABLE 3 (continued). COMMON PROTEINS IDENTIFIED IN THE TWO-YEAR-OLD NORMAL (N) AND BUPHTHALMIC (B) RABBITS

ACCESSION	DESCRIPTION	N PEPTIDES	N SCANS	N FREQUENCY/ TOTAL*	B PEPTIDES	B SCANS	B FREQUENCY/ TOTAL*	NORMALIZED LOG RATIO†	ADJUSTED *P* VALUE
P41975	Extracellular superoxide dismutase [Cu-Zn] precursor	6	33	6/6	5	23	6/6	-0.6953	0.977677
P01026	Complement C3 precursor	2	27	6/6	2	18	6/6	-0.75943	0.984530
O94833	Bullous pemphigoid antigen 1, isoforms 6/9/10 (Trabeculin-beta)	2	2	2/6	0	0	0/6	Ns only	0.986244
Q61789	Laminin alpha-3 chain precursor (Nicein alpha subunit)	2	2	2/6	0	0	0/6	Ns only	0.986244
Q9NRN5	Olfactomedin-like protein 3 precursor (HNOEL-iso)	2	2	2/6	0	0	0/6	Ns only	0.986244
P01832	Polymeric-immunoglobulin receptor precursor	2	2	1/6	0	0	0/6	Ns only	.986244
O14709	Zinc finger protein 197 (ZnF20)	2	2	2/6	0	0	0/6	Ns only	0.986244
P08649	Complement C4 precursor	2	8	5/6	1	3	3/6	-1.5895	0.986938
Q15113	Procollagen C-endopeptidase	2	9	4/6	1	4	3/6	-1.34439	0.996131
O18759	Apolipoprotein A-I precursor (Apo-AI) (ApoA-I)	2	6	3/6	2	2	1/6	-1.75943	0.996406
Q02388	Collagen alpha-1(VII) chain precursor (Long-chain collagen)	0	0	0/6	2	2	2/6	Bs only	0.997234
Q9NP62	Chorion-specific transcription factor GCMa	0	0	0/6	2	2	2/6	Bs only	0.997234
Q8NEY8	Periphilin 1 (Gastric cancer antigen Ga50)	0	0	0/6	2	2	2/6	Bs only	0.997234
P01847	Ig lambda chain C region	1	2	2/6	2	7	2/6	1.63289	0.998641
P19879	Mimecan precursor (Osteoglycin)	3	7	4/6	2	3	2/6	-1.39686	0.999502
P31097	Osteopontin precursor (Bone sialoprotein-1)	2	11	5/6	1	6	3/6	-1.04893	0.999519
P04221	Ig mu chain C region membrane-bound form	2	17	6/6	3	29	6/6	0.596053	0.999910
P03988	Ig mu chain C region secreted form	2	17	6/6	3	29	6/6	0.596053	0.999910
P01870	Ig gamma chain C region	12	736	6/6	14	888	6/6	0.096389	0.999950
P01826	Ig heavy chain V-A1 region BS-5	2	40	5/6	1	33	4/6	-0.452	0.999955
Q8TEW8	Amyotrophic lateral sclerosis 2 chromosome region candidate gene 19 protein	1	14	6/6	2	9	5/6	-0.8119	0.999956
P02679	Fibrinogen gamma chain precursor	6	63	6/6	6	56	6/6	-0.34439	0.999978
P20305	Gelsolin precursor (Actin-depolymerizing factor)(Brevin) (Fragment)	3	28	6/6	3	22	6/6	-0.52239	0.999987

TABLE 3 (continued). COMMON PROTEINS IDENTIFIED IN THE TWO-YEAR-OLD NORMAL (N) AND BUPHTHALMIC (B) RABBITS

ACCESSION	DESCRIPTION	N PEPTIDES	N SCANS	N FREQUENCY/ TOTAL*	B PEPTIDES	B SCANS	B FREQUENCY/ TOTAL*	NORMALIZED LOG RATIO†	ADJUSTED *P* VALUE
Q95114	Lactadherin precursor (Milk fat globule-EGF factor 8) (MFG-E8)	1	1	1/6	2	4	2/6	1.825535	0.999992
Q28706	Keratin, type I cytoskeletal 12	1	4	2/6	3	9	5/6	0.99546	0.999998
O97862	Cystatin C precursor	2	12	6/6	3	8	3/6	-0.75943	0.999999
P19134	Serotransferrin precursor (Transferrin)	36	432	6/6	35	451	6/6	-0.11237	0.999999
P01608	Ig kappa chain V-I region Roy	1	3	2/6	1	1	1/6	-1.75943	1.000000
O46379	Lumican KSPG (lumican) (Fragment)	3	3	3/6	1	1	1/6	-1.75943	1.000000
P36233	SPARC precursor (Secreted protein acidic and rich in cysteine)	2	3	2/6	1	1	1/6	-1.75943	1.000000
P97278	Inter-alpha-trypsin inhibitor heavy chain H1 precursor (ITI heavy chain H1)	2	17	6/6	2	13	6/6	-0.56149	1.000000
Q91X72	Hemopexin precursor	1	2	2/6	2	5	4/6	1.147463	1.000000
P13635	Ceruloplasmin precursor (Ferroxidase)	1	10	5/6	2	7	6/6	-0.68904	1.000000
Q8K0E8	Fibrinogen beta chain precursor	2	10	5/6	2	7	4/6	-0.68904	1.000000
Q8CGM2	Retinitis pigmentosa 1–like 1 protein	2	4	3/6	1	2	2/6	-1.17447	1.000000
P48747	Complement component C9 precursor	3	11	5/6	2	8	4/6	-0.6339	1.000000
Q14515	SPARC-like protein 1 precursor (Hevin) (MAST 9)	2	11	6/6	1	8	6/6	-0.6339	1.000000
P69678	Protein CutA precursor (Brain acetylcholinesterase putative membrane anchor)	1	1	1/6	2	3	3/6	1.410497	1.000000
P12661	Interphotoreceptor retinoid-binding protein precursor (IRBP)	6	16	5/6	4	13	5/6	-0.47403	1.000000
P10745	Interphotoreceptor retinoid-binding protein precursor (IRBP)	3	39	6/6	3	36	6/6	-0.28994	1.000000
P01885	Beta-2-microglobulin	2	20	3/6	2	17	4/6	-0.40893	1.000000
P23035	Alpha-1-antiproteinase F precursor (Alpha-1-antitrypsin)	14	142	6/6	16	146	6/6	-0.13439	1.000000
P00761	Trypsin precursor (EC 3.4.21.4)	5	649	6/6	6	764	6/6	0.060889	1.000000
P37153	Apolipoprotein D precursor (Apo-D) (ApoD)	4	9	3/6	4	7	3/6	-0.53704	1.000000
P01696	Ig kappa chain V region K29-213	3	58	6/6	3	57	6/6	-0.19956	1.000000

TABLE 3 (continued). COMMON PROTEINS IDENTIFIED IN THE TWO-YEAR-OLD NORMAL (N) AND BUPHTHALMIC (B) RABBITS

ACCESSION	DESCRIPTION	N PEPTIDES	N SCANS	N FREQUENCY/ TOTAL*	B PEPTIDES	B SCANS	B FREQUENCY/ TOTAL*	NORMALIZED LOG RATIO†	ADJUSTED *P* VALUE
P02751	Fibronectin precursor (FN) (Cold-insoluble globulin) (CIG)	2	11	5/6	2	9	5/6	-0.46397	1.000000
P06396	Gelsolin precursor (Actin-depolymerizing factor) (Brevin)	3	24	5/6	2	22	6/6	-0.3	1.000000
Q8CJ27	Abnormal spindle-like microcephaly-associated protein homolog	2	2	2/6	1	1	1/6	-1.17447	1.000000
O18783	Plasminogen precursor	1	2	1/6	1	1	1/6	-1.17447	1.000000
O35600	Retinal-specific ATP-binding cassette transporter	1	1	1/6	1	1	1/6	-0.17447	1.000000
Q7YQM2	AF4/FMR2 family member 2 (Protein FMR-2)	1	1	1/6	1	1	1/6	-0.17447	1.000000
P41361	Antithrombin-III (ATIII)	4	20	3/6	4	21	6/6	-0.10408	1.000000
P18287	Apolipoprotein E precursor (Apo-E)	15	326	6/6	15	359	6/6	-0.03535	1.000000
Q9GLC0	Apolipoprotein E precursor (Apo-E)	2	20	6/6	2	22	6/6	-0.03696	1.000000
Q96Q27	Ankyrin repeat and SOCS box protein 2 (ASB-2)	1	5	4/6	2	7	3/6	0.310962	1.000000
Q95215	Transforming growth factor-beta-induced protein ig-h3 pre	5	16	5/6	3	16	6/6	-0.17447	1.000000
O60911	Cathepsin L2 precursor (EC 3.4.22.43) (Cathepsin V)	2	6	3/6	3	5	3/6	-0.4375	1.000000
P02458	Collagen alpha-1(II) chain precursor	3	4	1/6	3	6	5/6	0.410497	1.000000
Q28679	Complement component C8 gamma chain precursor	2	2	1/6	2	2	2/6	-0.17447	1.000000
O43405	Cochlin precursor (COCH-5B2)	8	32	6/6	7	36	6/6	-0.00454	1.000000
Q62507	Cochlin precursor (COCH-5B2)	3	41	6/6	2	41	6/6	-0.17447	1.000000
Q9NQ79	Cartilage acidic protein 1 precursor	8	39	6/6	6	39	6/6	-0.17447	1.000000
Q8R555	Cartilage acidic protein 1 precursor	1	7	4/6	2	7	6/6	-0.17447	1.000000
P11370	Retrovirus-related Env polyprotein from Fv-4 locus	1	1	1/6	1	1	1/6	-0.17447	1.000000
Q9UBX5	Fibulin-5 precursor (FIBL-5)	1	1	1/6	1	2	2/6	0.825535	1.000000
P80191	Alpha-2-HS-glycoprotein precursor (Fetuin-A)	6	38	6/6	8	42	6/6	-0.03008	1.000000
P02676	Fibrinogen beta chain precursor	3	24	6/6	2	31	6/6	0.194769	1.000000
P02675	Fibrinogen beta chain precursor	2	3	1/6	1	2	2/6	-0.75943	1.000000
P07589	Fibronectin (FN)	3	27	6/6	2	28	6/6	-0.122	1.000000
P20058	Hemopexin precursor	14	67	6/6	15	78	6/6	0.044848	1.000000

TABLE 3 (continued). COMMON PROTEINS IDENTIFIED IN THE TWO-YEAR-OLD NORMAL (N) AND BUPHTHALMIC (B) RABBITS

ACCESSION	DESCRIPTION	N PEPTIDES	N SCANS	N FREQUENCY/ TOTAL*	B PEPTIDES	B SCANS	B FREQUENCY/ TOTAL*	NORMALIZED LOG RATIO†	ADJUSTED *P* VALUE
P47776	Heparin cofactor II precursor (HC-II)	5	8	4/6	2	9	5/6	-0.00454	1.000000
P19007	Haptoglobin precursor	10	57	6/6	8	67	6/6	0.058734	1.000000
Q03164	Zinc finger protein HRX (ALL-1) (Trithorax-like protein)	1	1	1/6	1	1	1/6	-0.17447	1.000000
P49194	Interphotoreceptor retinoid-binding protein precursor	2	13	6/6	2	13	6/6	-0.17447	1.000000
Q29052	Inter-alpha-trypsin inhibitor heavy chain H1 precursor	2	5	4/6	1	8	6/6	0.503607	1.000000
P19823	Inter-alpha-trypsin inhibitor heavy chain H2 precursor	3	20	5/6	2	19	6/6	-0.24847	1.000000
O02668	Inter-alpha-trypsin inhibitor heavy chain H2 precursor	4	22	6/6	4	24	6/6	-0.04893	1.000000
Q06033	Inter-alpha-trypsin inhibitor heavy chain H3 precursor	2	5	3/6	1	4	2/6	-0.49639	1.000000
P46013	Antigen KI-67	1	1	1/6	1	1	1/6	-0.17447	1.000000
P01695	Ig kappa chain V region K16-167	2	33	6/6	2	34	6/6	-0.1314	1.000000
Q62000	Mimecan precursor (Osteoglycin)	3	7	3/6	3	6	3/6	-0.39686	1.000000
Q9Y4I1	Myosin-5A (Myosin Va) (Myoxin)	2	5	3/6	2	4	3/6	-0.49639	1.000000
O08976	Probasin precursor (PB)	1	1	1/6	1	1	1/6	-0.17447	1.000000
P27170	Serum paraoxonase/arylesterase 1 (PON 1)	10	113	6/6	13	119	6/6	-0.09983	1.000000
P98118	Vitamin K–dependent protein S precursor (Fragment)	2	4	4/6	1	4	3/6	-0.17447	1.000000
P06912	Plasma retinol-binding protein precursor (PRBP) (RBP)	3	13	5/6	4	14	6/6	-0.06755	1.000000
P59729	Ras and Rab interactor 3 (Ras interaction/interference protein 3)	1	1	1/6	1	1	1/6	-0.17447	1.000000
Q9GLX9	Spondin-1 precursor (F-spondin)	2	3	2/6	1	2	2/6	-0.75943	1.000000
P22105	Tenascin-X precursor (TN-X) (Hexabrachion-like protein)	1	1	1/6	1	1	1/6	-0.17447	1.000000
Q4KMQ2	Transmembrane protein 16F	2	4	2/6	2	4	3/6	-0.17447	1.000000
P51867	Tumor necrosis factor	1	1	1/6	1	1	1/6	-0.17447	1.000000
P53789	Vitamin D–binding protein precursor (DBP)	6	47	6/6	5	56	6/6	0.078301	1.000000
P22458	Vitronectin precursor (Serum spreading factor) (S-protein)	6	57	6/6	6	58	6/6	-0.14937	1.000000
Q9N0L8	Whey acidic protein precursor (tWAP)	1	1	1/6	1	1	1/6	-0.17447	1.000000

TABLE 3 (continued). COMMON PROTEINS IDENTIFIED IN THE TWO-YEAR-OLD NORMAL (N) AND BUPHTHALMIC (B) RABBITS

ACCESSION	DESCRIPTION	N PEPTIDES	N SCANS	N FREQUENCY/ TOTAL*	B PEPTIDES	B SCANS	B FREQUENCY/ TOTAL*	NORMALIZED LOG RATIO†	ADJUSTED *P* VALUE
P57999	Zonadhesin (Fragment)	1	2	2/6	2	3	2/6	0.410497	1.000000
O43167	Zinc finger and BTB domain-containing protein 24	1	1	1/6	1	1	1/6	-0.17447	1.000000

*****Number of animals in which protein was detected/Total number of animals used (N=6, B=6).
†Calculated from the ratio of the scans (B/N) adjusted to the ratio of the total scans for all proteins detected in the sample.

Based on these criteria, proteins that showed differential expression in the buphthalmic rabbit AH (detected at higher levels or detected at lower levels) were selected (Tables 5 and 6 for the 2- and 5-year-old animals, respectively). In addition, the analysis included proteins that were present in 100% of the control samples and absent in all buphthalmic samples.

In the 2-year-old buphthalmic rabbits, the only protein that was significantly differentially expressed was histidine-rich glycoprotein (HRG), which was expressed at lower levels in the buphthalmic rabbits compared to their control littermates (*P*=.043) (data not shown).

Figure 17 shows the normalized log ratio of the proteins that showed significant differential expression in the 5-year-old buphthalmic rabbits. The main functional groups altered in the 5-year-old group included those involved in ECM development/remodeling, oxidative stress, inflammation, and lipid transport. Proteins that showed significantly higher levels included albumin (Alb) (*P*=0), clusterin (Clu) (*P*=.001), and B2M (*P*=.007). Proteins that were significantly lower in this age group included apolipoprotein E (ApoE) (*P*=0), TTR (*P*=0), haptoglobin (HPT) (*P*=0), hemopexin (HPX) (*P*=0), gelsolin (Gel) (*P*=.002), and alpha-2-HS-glycoprotein (A2SG) (*P*=.006).

Two proteins—cochlin and IRBP—were absent in the 5-year-old buphthalmic rabbit AH and present in the AH of the controls.

Validation of Proteomic Data

Immunofluorescence. Immunohistochemistry was performed for the differentially expressed proteins identified by LC-MS/MS to localize these proteins in the anterior segment tissues and to determine whether there were differences in expression of these proteins between normal and buphthalmic rabbits. The intensity of fluorescence in the different anterior segment tissues is presented in Tables 7 and 8 for the 2- and 5-year-old rabbits, respectively. Immunolabeling of normal and buphthalmic tissues with specific antibodies that represent various processes affected in the buphthalmic tissues is presented in Figures 18 through 22. These illustrations include immunolabeling with Clu, APOE, cochlin, IRBP, and TTR.

For all the antibodies tested, no staining was noted in DM or the anterior lens capsule. Faint staining was noticed in the corneal stroma with some of the antibodies.

The immunolabeling was localized to the cytoplasm of ciliary epithelium, lens epithelium, and corneal and trabecular endothelium for most of the antibodies tested and appeared to mirror changes seen in LC-MS/MS or Western blot data with most antibodies.

Anticochlin labeling was absent in the normal angular meshwork and in the negative control. In the 2-year-old buphthalmic rabbit, intense labeling was localized along the trabecular beams, angular structures, superficial iris in the periphery, and the deep corneoscleral fibers adjacent to the aqueous plexus (Figure 20). Aqueous humor levels of cochlin were, however, comparable in the 2-year-old normal and buphthalmic rabbits. In the 5-year-old buphthalmic animals, immunolabeling in the degenerated angular meshwork was milder in intensity than that seen in the 2-year-old buphthalmic angle but greater than the control angular meshwork, whereas the protein was undetectable in the AH.

The IRBP was not detectable in the AH of the 5-year-old buphthalmic rabbit, but the anterior segment structures still showed IRBP immunolabeling, which was decreased in intensity or absent when compared to the control.

Transthyretin (Figure 22) and GSN (Figure not shown) showed a distinct staining pattern with labeling of the borders of the pectinate ligament of the angular meshwork and the anterior surface of the iris that was more prominent in the buphthalmic eyes.

Western blot. Because of difficulty in acquiring antibodies that cross-react with rabbit proteins as well as the limited volume of AH samples, Western blot was performed for only three of the differentially expressed proteins. Western blot analysis confirmed up-regulation of B2M and clusterin in the 5-year-old buphthalmic AH samples (Figure 23). It also confirmed the presence of IRBP in the 2-year-old AH buphthalmic samples (Figure 24) and its absence in the 5-year-old buphthalmic AH samples (Figure 25). The Western blot for the 5-year-old rabbit IRBP had a lot of background despite the multiple attempts at performing it.

TABLE 4. COMMON PROTEINS IDENTIFIED IN THE FIVE-YEAR-OLD NORMAL (N) AND BUPHTHALMIC (B) RABBITS

ACCESSION	DESCRIPTION	N PEPTIDES	N SCANS	N FREQUENCY /TOTAL*	B PEPTIDES	B SCANS	B FREQUENCY /TOTAL*	NORMALIZED LOG RATIO†	ADJUSTED *P* VALUE
P20305	Gelsolin precursor (Actin-depolymerizing factor) (Brevin)	1	20	4/4	2	7	3/4	-1.85406	0.059064
P01948	Hemoglobin alpha-1/2 subunit	8	168	4/4	7	626	2/4	1.558213	0.000000
P49065	Serum albumin precursor	38	4328	4/4	49	7068	4/4	0.368113	0.000000
P02057	Hemoglobin beta-1/2 subunit	14	234	4/4	15	524	2/4	0.82357	0.000000
O43405	Cochlin precursor (COCH-5B2)	5	29	4/4	0	0	0/4	Ns only	0.000000
Q62507	Cochlin precursor (COCH-5B2)	2	41	4/4	1	4	2/4	-3.69704	0.000000
P07489	Transthyretin (Prealbumin)	11	268	4/4	14	180	4/4	-0.91372	0.000000
P12661	Interphotoreceptor retinoid-binding protein precursor (IRBP)	4	26	4/4	0	0	0/4	Ns only	0.000000
Q13822	Ectonucleotide pyrophosphatase/phosphodiesterase 2 (E-NPP 2)	5	28	3/4	1	1	1/4	-5.14684	0.000000
P19007	Haptoglobin precursor	7	62	4/4	4	19	4/4	-2.04576	0.000000
Q9NQ79	Cartilage acidic protein 1 precursor	4	19	4/4	0	0	0/4	Ns only	0.000000
P00761	Trypsin precursor (EC 3.4.21.4)	4	60	4/4	2	21	4/4	-1.85406	0.000001
P12387	Complement C3 precursor	2	34	4/4	2	6	3/4	-2.84199	0.000001
P20058	Hemopexin precursor	10	80	4/4	6	38	4/4	-1.41349	0.000003
P01870	Ig gamma chain C region	7	346	4/4	12	313	4/4	-0.4841	0.000185
Q28372	Gelsolin (Actin-depolymerizing factor) (ADF) (Brevin)	9	91	4/4	8	62	4/4	-0.89309	0.000285
Q9XSC5	Clusterin precursor (Apolipoprotein J) (Apo-J)	7	47	4/4	13	115	4/4	0.951412	0.000150
P49194	Interphotoreceptor retinoid-binding protein precursor (IRBP)	2	10	3/4	0	0	0/4	Ns only	0.000105
P04264	Keratin, type II cytoskeletal 1 (Cytokeratin-1)	5	10	2/4	0	0	0/4	Ns only	0.000105
P36233	SPARC precursor (Secreted protein acidic and rich in cysteine)	2	10	3/4	0	0	0/4	Ns only	0.000105
P02458	Collagen alpha-1(II) chain precursor	3	9	3/4	0	0	0/4	Ns only	0.000499
P03988	Ig mu chain C region secreted form	3	36	4/4	3	18	4/4	-1.33949	-0.003465
P18287	Apolipoprotein E precursor (Apo-E)	8	442	4/4	9	165	4/4	-1.76107	0.000000
P14943	Liver carboxylesterase 2 (EC 3.1.1.1)	0	0	0/4	5	13	4/4	Bs only	0.004080
P04221	Ig mu chain C region membrane-bound form	3	36	4/4	3	18	4/4	-1.33949	0.034829
P01885	Beta-2-microglobulin	2	18	4/4	2	53	4/4	1.218507	0.041319
P80191	Alpha-2-HS-glycoprotein precursor (Fetuin-A)	4	39	4/4	5	21	4/4	-1.23257	0.046585
P10745	Interphotoreceptor retinoid-binding protein precursor (IRBP)	3	6	4/4	0	0	0/4	Ns only	0.068655
P0C0L4	Complement C4-A precursor (Acidic complement C4)	3	18	3/4	1	6	3/4	-1.92445	0.083700
P01026	Complement C3 precursor	2	27	4/4	2	13	4/4	-1.39394	0.113256
O97862	Cystatin C precursor	2	14	4/4	1	4	3/4	-2.14684	0.136729

TABLE 4 (continued). COMMON PROTEINS IDENTIFIED IN THE FIVE-YEAR-OLD NORMAL (N) AND BUPHTHALMIC (B) RABBITS

ACCESSION	DESCRIPTION	N PEPTIDES	N SCANS	N FREQUENCY /TOTAL*	B PEPTIDES	B SCANS	B FREQUENCY /TOTAL*	NORMALIZED LOG RATIO†	ADJUSTED *P* VALUE
P49822	Serum albumin precursor (Allergen Can f 3)	0	0	0/4	2	6	3/4	Bs only	0.286580
P19134	Serotransferrin precursor (Transferrin)	33	905	4/4	37	1017	4/4	-0.17116	0.324709
P35527	Keratin, type I cytoskeletal 9 (Cytokeratin-9))	4	4	1/4	0	0	0/4	Ns only	0.352303
P41975	Extracellular superoxide dismutase [Cu-Zn]	3	17	4/4	6	8	2/4	-1.42695	0.488897
P41361	Antithrombin-III (ATIII)	2	18	4/4	2	9	3/4	-1.33949	0.534790
Q9GLC0	Apolipoprotein E precursor (Apo-E)	2	8	4/4	2	2	2/4	-2.33949	0.564678
P37153	Apolipoprotein D precursor (Apo-D) (ApoD)	1	7	3/4	1	2	2/4	-2.14684	0.807719
P02031	Hemoglobin beta subunit (Hemoglobin beta chain)	1	19	4/4	2	41	2/4	0.770136	0.866974
Q8K0E8	Fibrinogen beta chain precursor	1	1	1/4	2	7	2/4	2.467866	0.890287
Q9BGI3	Peroxiredoxin-2 (EC 1.11.1.15)	0	0	0/4	2	3	1/4	Bs only	0.926154
P53789	Vitamin D–binding protein precursor (DBP)	4	12	4/4	5	28	4/4	0.882904	0.940194
Q86U86	Protein polybromo-1 (hPB1) (Polybromo-1D)	2	2	2/4	0	0	0/4	Ns only	0.950133
P69678	Protein CutA precursor	2	4	2/4	1	1	1/4	-2.33949	0.986814
P48747	Complement component C9 precursor	1	1	1/4	2	5	4/4	1.982439	0.998837
P02072	Hemoglobin beta subunit (Hemoglobin beta chain)	1	40	4/4	2	37	2/4	-0.45196	0.999510
P12247	Complement C3 alpha chain (Fragment)	3	22	4/4	6	19	4/4	-0.55099	0.999966
Q5R4N8	Alpha-2-macroglobulin precursor (Alpha-2-M)	2	4	2/4	1	2	1/4	-1.33949	0.999997
P01695	Ig kappa chain V region K16-167	2	44	4/4	1	68	4/4	0.288542	1.000000
P02679	Fibrinogen gamma chain precursor	2	4	1/4	1	9	2/4	0.830436	1.000000
P06396	Gelsolin precursor (Actin-depolymerizing factor)	1	13	3/4	3	11	2/4	-0.5805	1.000000
P01696	Ig kappa chain V region K29-213	3	128	4/4	2	145	4/4	-0.15958	1.000000
Q6NZC7	SEC23-interacting protein	2	9	3/4	2	16	4/4	0.490586	1.000000
P02058	Hemoglobin beta subunit	1	1	1/4	1	3	1/4	1.245474	1.000000
Q9NVH0	Protein C14orf114	2	2	1/4	1	1	1/4	-1.33949	1.000000
P02751	Fibronectin precursor (FN) (Cold-insoluble globulin)	1	2	1/4	1	1	1/4	-1.33949	1.000000
P23035	Alpha-1-antiproteinase F precursor (Alpha-1-antitrypsin)	9	96	4/4	9	110	4/4	-0.14309	1.000000
P97278	Inter-alpha-trypsin inhibitor heavy chain H1 precursor	1	4	3/4	2	7	3/4	0.467866	1.000000
P22458	Vitronectin precursor (Serum spreading factor)	3	33	4/4	4	37	4/4	-0.17443	1.000000
P02770	Serum albumin precursor	2	14	4/4	2	21	2/4	0.245474	1.000000
P09809	Apolipoprotein A-I precursor (Apo-AI) (ApoA-I)	25	375	4/4	25	490	4/4	0.046402	1.000000
P27170	Serum paraoxonase/arylesterase 1	6	41	4/4	4	57	4/4	0.135849	1.000000
P06912	Plasma retinol-binding protein precursor (PRBP) (RBP)	3	13	4/4	3	14	4/4	-0.23257	1.000000

TABLE 4 (continued). COMMON PROTEINS IDENTIFIED IN THE FIVE-YEAR-OLD NORMAL (N) AND BUPHTHALMIC (B) RABBITS

ACCESSION	DESCRIPTION	N PEPTIDES	N SCANS	N FREQUENCY /TOTAL*	B PEPTIDES	B SCANS	B FREQUENCY /TOTAL*	NORMALIZED LOG RATIO†	ADJUSTED *P* VALUE
Q28640	Histidine-rich glycoprotein precursor	11	131	4/4	13	158	4/4	-0.06913	1.000000
P47776	Heparin cofactor II precursor (HC-II)	1	1	1/4	2	2	1/4	0.660511	1.000000
P49064	Serum albumin precursor (Allergen Fel d 2)	2	3	2/4	1	5	2/4	0.397477	1.000000
P02676	Fibrinogen beta chain precursor	1	2	1/4	1	3	2/4	0.245474	1.000000
Q02224	Centromeric protein E (CENP-E protein)	1	1	1/4	1	1	1/4	-0.33949	1.000000
O75154	Rab11 family-interacting protein 3	1	1	1/4	1	1	1/4	-0.33949	1.000000
Q9JKF7	Mitochondrial 39S ribosomal protein L39 (L39mt)	1	1	1/4	1	1	1/4	-0.33949	1.000000
Q8IWV7	Ubiquitin-protein ligase E3 component N-recognin-1	1	1	1/4	1	1	1/4	-0.33949	1.000000
P02048	Hemoglobin beta subunit (Hemoglobin beta chain)	2	15	3/4	4	20	2/4	0.075549	1.000000
Q8BK62	Olfactomedin-like protein 3 precursor	1	5	3/4	1	4	2/4	-0.49639	1.000000
Q7YS99	Optineurin	0	0	0/4	1	1	1/4	Bs only	0.999996
P83286	Opticin precursor (Oculoglycan)	1	13	6/4	1	13	6/4	-0.17447	1.000000
Q8NGR4	Olfactory receptor 5C1 (Olfactory receptor 9-F) (OR9-F)	1	1	1/4	1	1	1/4	-0.17447	1.000000
Q8NGK9	Olfactory receptor 5D16	1	1	1/4	0	0	0/4	Ns only	0.999960
Q8NGN1	Olfactory receptor 6T1	0	0	0/4	1	1	1/4	Bs only	0.999996
Q9UBD5	Origin recognition complex subunit 3	0	0	0/4	1	1	1/4	Bs only	0.999996
Q9ER64	Oxysterol-binding protein-related protein 5	0	0	0/4	1	1	1/4	Bs only	0.999996
Q12889	Oviduct-specific glycoprotein precursor	0	0	0/4	1	3	1/4	Bs only	0.883260
P83859	Orexigenic neuropeptide QRFP	0	0	0/4	1	1	1/4	Bs only	0.999996
P51578	P2X purinoceptor 5 (ATP receptor) (P2X5)	0	0	0/4	1	1	1/4	Bs only	0.999996
Q9ERK9	P2Y purinoceptor 6 (P2Y6)	0	0	0/4	1	1	1/4	Bs only	0.999996
Q86VZ1	P2Y purinoceptor 8 (P2Y8)	1	5	3/4	1	3	3/4	-0.91143	1.000000
P61286	Polyadenylate-binding protein 1 (Poly(A)-binding protein 1)	0	0	0/4	1	1	1/4	Bs only	0.999996
Q28017	Platelet-activating factor acetylhydrolase precursor	1	1	1/4	1	1	1/4	-0.17447	1.000000
Q8NDF8	PAP associated domain-containing protein 5	0	0	0/4	1	1	1/4	Bs only	0.999996
Q13219	Pappalysin-1 precursor (EC 3.4.24.79)	1	1	1/4	0	0	0/4	Ns only	0.999960
Q8IWT3	p53-associated parkin-like cytoplasmic protein	1	1	1/4	1	1	1/4	-0.17447	1.000000
Q86U86	Protein polybromo-1 (hPB1) (Polybromo-1D)	0	0	0/4	1	1	1/4	Bs only	0.999996
P40424	Pre-B-cell leukemia transcription factor 1	0	0	0/4	1	1	1/4	Bs only	0.999996
Q96JQ0	Protocadherin 16 precursor (Dachsous 1)	1	2	1/4	0	0	0/4	Ns only	0.970245
Q8TAB3	Protocadherin 19 precursor	1	1	1/4	0	0	0/4	Ns only	0.999960
Q5DRF2	Protocadherin alpha 12 precursor (PCDH-alpha12)	1	1	1/4	0	0	0/4	Ns only	0.999960

TABLE 4 (continued). COMMON PROTEINS IDENTIFIED IN THE FIVE-YEAR-OLD NORMAL (N) AND BUPHTHALMIC (B) RABBITS

ACCESSION	DESCRIPTION	N PEPTIDES	N SCANS	N FREQUENCY /TOTAL*	B PEPTIDES	B SCANS	B FREQUENCY /TOTAL*	NORMALIZED LOG RATIO†	ADJUSTED *P* VALUE
Q9Y5G1	Protocadherin gamma B3 precursor	1	9	5/4	1	5	4/4	-1.02246	0.999849
O95613	Pericentrin (Pericentrin B) (Kendrin)	0	0	0/4	1	1	1/4	Bs only	0.999996
Q8VI59	Pecanex-like protein 3	0	0	0/4	1	1	1/4	Bs only	0.999996
P23439	Rod cGMP-specific 3',5'-cyclic phosphodiesterase beta-subunit precursor	1	1	1/4	0	0	0/4	Ns only	0.999960
Q5RCF7	PDZ domain-containing protein 1 (Na(+)/H(+) exchanger regulatory)	0	0	0/4	1	1	1/4	Bs only	0.999996
O75521	Peroxisomal 3,2-trans-enoyl-CoA isomerase	0	0	0/4	1	1	1/4	Bs only	0.999996
Q95121	Pigment epithelium–derived factor precursor (PEDF)	1	5	4/4	1	5	4/4	-0.17447	1.000000
P36955	Pigment epithelium–derived factor precursor (PEDF)	0	0	0/4	1	1	1/4	Bs only	0.999996
Q9D7R7	Gastricsin precursor (EC 3.4.23.3) (Pepsinogen C)	0	0	0/4	1	5	4/4	Bs only	0.384586
P56645	Period circadian protein 3 (hPER3)	1	1	1/4	0	0	0/4	Ns only	0.999960
P98160	Basement membrane–specific heparan sulfate proteoglycan core protein precursor	1	1	1/4	0	0	0/4	Ns only	0.999960
O97554	Prostaglandin G/H synthase 1 precursor	1	2	2/4	1	1	1/4	-1.17447	1.000000
O46377	Biglycan (Bone/cartilage proteoglycan I) (PG-S1)	0	0	0/4	1	1	1/4	Bs only	0.999996
Q28888	Decorin precursor (Bone proteoglycan II) (PG-S2)	1	1	1/4	0	0	0/4	Ns only	0.999960
Q96QT6	PHD finger protein 12 (PHD factor	1	1	1/4	0	0	0/4	Ns only	0.999960
Q9Y5J5	Pleckstrin homology-like domain family A member 3	1	1	1/4	0	0	0/4	Ns only	0.999960
P80109	Phosphatidylinositol-glycan-specific phospholipase D precursor	1	1	1/4	1	1	1/4	-0.17447	1.000000
Q9WTR8	PH domain leucine-rich repeat protein phosphatase	0	0	0/4	1	1	1/4	Bs only	0.999996
Q99453	Paired mesoderm homeobox protein 2B	0	0	0/4	1	1	1/4	Bs only	0.999996
Q8BTI9	Phosphatidylinositol-4,5-bisphosphate 3-kinase catalytic subunit beta isoform	1	1	1/4	0	0	0/4	Ns only	0.999960
P98161	Polycystin-1 precursor	0	0	0/4	1	1	1/4	Bs only	0.999996
Q13563	Polycystin-2	0	0	0/4	1	1	1/4	Bs only	0.999996
Q9NUQ2	1-acyl-sn-glycerol-3-phosphate	0	0	0/4	1	1	1/4	Bs only	0.999996
P80009	Plasminogen (EC 3.4.21.7)	0	0	0/4	1	1	1/4	Bs only	0.999996
P20918	Plasminogen precursor (EC 3.4.21.7)	1	16	6/4	1	12	6/4	-0.5895	0.999999
P55065	Phospholipid transfer protein precursor	1	2	1/4	0	0	0/4	Ns only	0.970245
Q9Y4D7	Plexin-D1 precursor	0	0	0/4	1	1	1/4	Bs only	0.999996
P29590	Probable transcription factor PML	1	1	1/4	0	0	0/4	Ns only	0.999960
P10400	Retrovirus-related Pol polyprotein	1	13	6/4	1	11	6/4	-0.41547	1.000000
Q9UNA4	DNA polymerase iota (EC 2.7.7.7)	0	0	0/4	1	1	1/4	Bs only	0.999996
P27169	Serum paraoxonase/arylesterase 1	0	0	0/4	1	3	2/4	Bs only	0.883260

TABLE 4 (continued). COMMON PROTEINS IDENTIFIED IN THE FIVE-YEAR-OLD NORMAL (N) AND BUPHTHALMIC (B) RABBITS

ACCESSION	DESCRIPTION	N PEPTIDES	N SCANS	N FREQUENCY /TOTAL*	B PEPTIDES	B SCANS	B FREQUENCY /TOTAL*	NORMALIZED LOG RATIO†	ADJUSTED *P* VALUE
P54832	Serum paraoxonase/arylesterase 2	0	0	0/4	1	1	1/4	Bs only	0.999996
P20611	Lysosomal acid phosphatase precursor	1	3	2/4	1	4	3/4	0.240572	1.000000
O14829	Serine/threonine-protein phosphatase with EF-hands 1	1	1	1/4	0	0	0/4	Ns only	0.999960
O43447	Peptidyl-prolyl cis-trans isomerase H	0	0	0/4	1	1	1/4	Bs only	0.999996
Q63425	Periaxin	0	0	0/4	1	2	2/4	Bs only	0.992014
Q13029	PR-domain zinc finger protein 2	1	1	1/4	0	0	0/4	Ns only	0.999960
Q9BGI1	Peroxiredoxin-5, mitochondrial precursor	1	14	3/4	1	12	3/4	-0.39686	1.000000
Q92954	Proteoglycan-4 precursor (Lubricin)	1	1	1/4	0	0	0/4	Ns only	0.999960
P40244	Major prion protein precursor (PrP) (PrP27-30)	1	1	1/4	0	0	0/4	Ns only	0.999960
P78527	DNA-dependent protein kinase catalytic subunit	1	6	2/4	0	0	0/4	Ns only	0.101428
Q9WU79	Proline oxidase, mitochondrial precursor	0	0	0/4	1	1	1/4	Bs only	0.999996
P81264	Prolactin-releasing peptide precursor (PrRP)	1	1	1/4	0	0	0/4	Ns only	0.999960
P60900	Proteasome subunit alpha type 6	0	0	0/4	1	1	1/4	Bs only	0.999996
P55786	Puromycin-sensitive aminopeptidase	1	1	1/4	0	0	0/4	Ns only	0.999960
Q99460	26S proteasome non-ATPase regulatory subunit 1	0	0	0/4	1	1	1/4	Bs only	0.999996
Q9TTY5	Platelet-activating factor receptor	1	2	2/4	1	1	1/4	-1.17447	1.000000
Q13635	Protein patched homolog 1 (PTC1)	1	1	1/4	0	0	0/4	Ns only	0.999960
O02853	Prostaglandin-H2 D-isomerase precursor	1	4	2/4	1	2	2/4	-1.17447	1.000000
O02695	Receptor-type tyrosine-protein phosphatase N2 precursor	1	1	1/4	0	0	0/4	Ns only	0.999960
P49446	Receptor-type tyrosine-protein phosphatase epsilon precursor	1	1	1/4	1	2	2/4	0.825535	1.000000
Q60673	Receptor-type tyrosine-protein phosphatase-like N precursor	1	1	1/4	0	0	0/4	Ns only	0.999960
Q8HXY5	Adenylosuccinate lyase	1	1	1/4	0	0	0/4	Ns only	0.999960
P54822	Adenylosuccinate lyase (EC 4.3.2.2)	0	0	0/4	1	1	1/4	Bs only	0.999996
P46664	Adenylosuccinate synthetase, non-muscle isozyme	0	0	0/4	1	1	1/4	Bs only	0.999996
P27708	CAD protein	0	0	0/4	1	1	1/4	Bs only	0.999996
Q16769	Glutaminyl-peptide cyclotransferase precursor	1	2	1/4	1	1	1/4	-1.17447	1.000000
Q9H0T7	Ras-related protein Rab-17	0	0	0/4	1	1	1/4	Bs only	0.999996
Q9H0U4	Ras-related protein Rab-1B	1	1	1/4	0	0	0/4	Ns only	0.999960
P70388	DNA repair protein RAD50 (EC 3.6.-.-)	0	0	0/4	1	1	1/4	Bs only	0.999996
Q5U651	Ras-interacting protein 1 (Rain)	0	0	0/4	1	1	1/4	Bs only	0.999996
Q9BXY0	MAK16-like protein (RBM13)	1	3	3/4	1	2	2/4	-0.75943	1.000000
P48820	Ran-binding protein 2 (RanBP2)	0	0	0/4	1	1	1/4	Bs only	0.999996

TABLE 4 (continued). COMMON PROTEINS IDENTIFIED IN THE FIVE-YEAR-OLD NORMAL (N) AND BUPHTHALMIC (B) RABBITS

ACCESSION	DESCRIPTION	N PEPTIDES	N SCANS	N FREQUENCY /TOTAL*	B PEPTIDES	B SCANS	B FREQUENCY /TOTAL*	NORMALIZED LOG RATIO†	ADJUSTED *P* VALUE
P78509	Reelin precursor (EC 3.4.21.-)	1	1	1/4	0	0	0/4	Ns only	0.999960
Q60841	Reelin precursor (EC 3.4.21.-)	1	1	1/4	0	0	0/4	Ns only	0.999960
Q5R563	Renin receptor precursor	1	2	2/4	0	0	0/4	Ns only	0.970245
P35601	Activator 1 140 kDa subunit	0	0	0/4	1	2	2/4	Bs only	0.992014
Q6WKZ4	Rab11 family-interacting protein 1	0	0	0/4	1	2	2/4	Bs only	0.992014
Q9NZL6	Ral guanine nucleotide dissociation	1	1	1/4	0	0	0/4	Ns only	0.999960
O08774	Regulator of G-protein signaling 12 (RGS12)	0	0	0/4	1	1	1/4	Bs only	0.999996
O94844	Rho-related BTB domain-containing protein 1	1	1	1/4	0	0	0/4	Ns only	0.999960
Q9BE31	Rho-GTPase-activating protein 12	1	1	1/4	0	0	0/4	Ns only	0.999960
O95153	Peripheral-type benzodiazepine receptor-associated protein 1	1	1	1/4	0	0	0/4	Ns only	0.999960
Q80U40	RIM-binding protein 2 (RIM-BP2)	1	1	1/4	0	0	0/4	Ns only	0.999960
Q91VI7	Ribonuclease inhibitor	1	1	1/4	0	0	0/4	Ns only	0.999960
Q60561	Ribonucleoside-diphosphate reductase M2 subunit	0	0	0/4	1	1	1/4	Bs only	0.999996
P28327	Rhodopsin kinase precursor (EC 2.7.1.125) (RK)	0	0	0/4	1	1	1/4	Bs only	0.999996
Q8HXB8	60S ribosomal protein L29	1	1	1/4	0	0	0/4	Ns only	0.999960
Q29375	60S ribosomal protein L7a (Fragment)	1	1	1/4	0	0	0/4	Ns only	0.999960
Q99L28	Probable ribosome biogenesis protein RLP24	0	0	0/4	1	1	1/4	Bs only	0.999996
Q9Y3B7	39S ribosomal protein L11, mitochondrial precursor	1	1	1/4	1	1	1/4	-0.17447	1.000000
Q05921	2-5A-dependent ribonuclease	0	0	0/4	1	1	1/4	Bs only	0.999996
Q9WUV4	Ribonuclease pancreatic precursor	1	1	1/4	0	0	0/4	Ns only	0.999960
Q9NRR4	Ribonuclease III (EC 3.1.26.3) (RNase III)	1	1	1/4	0	0	0/4	Ns only	0.999960
Q9NV58	RING finger protein 19 (Dorfin)	0	0	0/4	1	1	1/4	Bs only	0.999996
Q9H0F5	RING finger protein 38	0	0	0/4	1	1	1/4	Bs only	0.999996
P24928	DNA-directed RNA polymerase II largest subunit	1	1	1/4	0	0	0/4	Ns only	0.999960
Q8BKF1	DNA-directed RNA polymerase, mitochondrial precursor	1	1	1/4	0	0	0/4	Ns only	0.999960
Q9Y2L1	Exosome complex exonuclease RRP44	1	2	1/4	0	0	0/4	Ns only	0.970245
Q15050	Ribosome biogenesis regulatory	1	1	1/4	0	0	0/4	Ns only	0.999960
P61270	40S ribosomal protein S11	1	2	2/4	1	1	1/4	-1.17447	1.000000
P62844	40S ribosomal protein S15 (RIG protein)	1	1	1/4	0	0	0/4	Ns only	0.999960
P62276	40S ribosomal protein S29	0	0	0/4	1	2	2/4	Bs only	0.992014
P79183	40S ribosomal protein S4, Y isoform 1	1	1	1/4	0	0	0/4	Ns only	0.999960
Q99N87	Mitochondrial 28S ribosomal protein S5	0	0	0/4	1	1	1/4	Bs only	0.999996

TABLE 4 (continued). COMMON PROTEINS IDENTIFIED IN THE FIVE-YEAR-OLD NORMAL (N) AND BUPHTHALMIC (B) RABBITS

ACCESSION	DESCRIPTION	N PEPTIDES	N SCANS	N FREQUENCY /TOTAL*	B PEPTIDES	B SCANS	B FREQUENCY /TOTAL*	NORMALIZED LOG RATIO†	ADJUSTED *P* VALUE
Q92665	28S ribosomal protein S31, mitochondrial precursor	1	1	1/4	0	0	0/4	Ns only	0.999960
O75298	Reticulon-2 (Neuroendocrine-specific protein-like 1)	1	1	1/4	1	1	1/4	-0.17447	1.000000
Q01196	Runt-related transcription factor 1	1	1	1/4	0	0	0/4	Ns only	0.999960
Q9Y230	RuvB-like 2 (EC 3.6.1.-)	0	0	0/4	1	1	1/4	Bs only	0.999996
Q5U5Q9	Retinoid X receptor-interacting protein 110	1	1	1/4	1	1	1/4	-0.17447	1.000000
P16960	Ryanodine receptor 1	0	0	0/4	1	1	1/4	Bs only	0.999996
Q15413	Ryanodine receptor 3	1	1	1/4	0	0	0/4	Ns only	0.999960
P55015	Solute carrier family 12 member 1	1	1	1/4	0	0	0/4	Ns only	0.999960
Q9UHW9	Solute carrier family 12 member 6	1	1	1/4	0	0	0/4	Ns only	0.999960
P70545	Solute carrier family 13 member 2	0	0	0/4	1	1	1/4	Bs only	0.999996
Q92503	SEC14-like protein 1	0	0	0/4	1	1	1/4	Bs only	0.999996
Q6NZC7	SEC23-interacting protein	0	0	0/4	1	3	3/4	Bs only	0.883260
Q9UMX9	Membrane-associated transporter protein	0	0	0/4	1	1	1/4	Bs only	0.999996
Q9NZJ4	Sacsin	1	1	1/4	0	0	0/4	Ns only	0.999960
Q9Y467	Sal-like protein 2 (Zinc finger protein SALL2)	1	2	2/4	0	0	0/4	Ns only	0.970245
O46669	Sodium channel protein type X alpha subunit	1	1	1/4	0	0	0/4	Ns only	0.999960
O55192	Sodium-dependent noradrenaline transporter	1	3	2/4	0	0	0/4	Ns only	0.750080
P23389	Secretogranin-1 precursor	0	0	0/4	1	4	2/4	Bs only	0.634632
Q7M729	Sodium channel beta-4 subunit precursor	1	1	1/4	0	0	0/4	Ns only	0.999960
Q5R7F5	Semaphorin-6D precursor	1	1	1/4	0	0	0/4	Ns only	0.999960
P23246	Splicing factor, proline- and glutamine-rich	1	1	1/4	0	0	0/4	Ns only	0.999960
Q99963	SH3-containing GRB2-like protein 3	1	1	1/4	0	0	0/4	Ns only	0.999960
P15196	Sex hormone-binding globulin precursor (SHBG)	1	1	1/4	0	0	0/4	Ns only	0.999960
P70126	Alpha-2,8-sialyltransferase 8E	1	1	1/4	0	0	0/4	Ns only	0.999960
Q62141	Paired amphipathic helix protein Sin3b	0	0	0/4	1	1	1/4	Bs only	0.999996
Q60665	Ski-like protein (Ski-related protein)	1	1	1/4	0	0	0/4	Ns only	0.999960
Q15477	Helicase SKI2W (EC 3.6.1.-)	0	0	0/4	1	1	1/4	Bs only	0.999996
O88280	Slit homolog 3 protein precursor (Slit-3)	0	0	0/4	1	1	1/4	Bs only	0.999996
O43541	Mothers against decapentaplegic homolog 6	0	0	0/4	1	1	1/4	Bs only	0.999996
Q92922	SWI/SNF-related matrix-associated actin-dependent regulator of chromatin subfamily C member 1	0	0	0/4	1	1	1/4	Bs only	0.999996
Q8K0S9	snRNA-activating protein complex subunit 1 (SNAPc subunit 1)	1	28	6/4	1	24	6/4	-0.39686	1.000000

TABLE 4 (continued). COMMON PROTEINS IDENTIFIED IN THE FIVE-YEAR-OLD NORMAL (N) AND BUPHTHALMIC (B) RABBITS

ACCESSION	DESCRIPTION	N PEPTIDES	N SCANS	N FREQUENCY /TOTAL*	B PEPTIDES	B SCANS	B FREQUENCY /TOTAL*	NORMALIZED LOG RATIO†	ADJUSTED *P* VALUE
Q9Y5W8	Sorting nexin-13(RGS-PX1)	1	3	3/4	1	7	4/4	1.047927	0.999998
Q9H3E2	Sorting nexin-25	1	3	3/4	1	3	3/4	-0.17447	1.000000
Q9EP96	Solute carrier organic anion transporter family member 1A4	0	0	0/4	1	1	1/4	Bs only	0.999996
Q9JJL3	Solute carrier organic anion transporter family member 1B2	0	0	0/4	1	1	1/4	Bs only	0.999996
Q9NPD5	Solute carrier organic anion transporter family member 1B3	0	0	0/4	1	1	1/4	Bs only	0.999996
Q99N01	Solute carrier organic anion 4A1	0	0	0/4	1	1	1/4	Bs only	0.999996
O77760	Sterol O-acyltransferase 1	1	1	1/4	0	0	0/4	Ns only	0.999960
O14544	Suppressor of cytokine signaling 6 (SOCS-6)	1	1	1/4	0	0	0/4	Ns only	0.999960
Q95209	Sortilin-related receptor precursor	1	1	1/4	0	0	0/4	Ns only	0.999960
Q9N1Q7	Nuclear autoantigen Sp-100	1	1	1/4	0	0	0/4	Ns only	0.999960
Q13813	Spectrin alpha chain, brain	1	1	1/4	0	0	0/4	Ns only	0.999960
Q62270	Tyrosine-protein kinase Srms	1	1	1/4	0	0	0/4	Ns only	0.999960
Q5R5Q2	Serine/arginine repetitive matrix protein 1	1	1	1/4	1	1	1/4	-0.17447	1.000000
Q8WYL5	Protein phosphatase Slingshot homolog 1	0	0	0/4	1	1	1/4	Bs only	0.999996
P30938	Somatostatin receptor type 5 (SS5R)	1	1	1/4	0	0	0/4	Ns only	0.999960
Q8CFM6	Stabilin-2 precursor (Hyaluronan receptor for endocytosis)	0	0	0/4	1	1	1/4	Bs only	0.999996
Q92502	StAR-related lipid transfer protein 8 (StARD8)	0	0	0/4	1	1	1/4	Bs only	0.999996
Q14765	Signal transducer and activator of transcription 4	1	1	1/4	1	2	1/4	0.825535	1.000000
Q8CJ67	Double-stranded RNA-binding protein Staufen homolog 2	0	0	0/4	1	1	1/4	Bs only	0.999996
Q04752	Steroidogenic factor 1 (STF-1) (SF-1)	1	2	2/4	0	0	0/4	Ns only	0.970245
Q13277	Syntaxin-3	0	0	0/4	1	1	1/4	Bs only	0.999996
Q9Y2Z0	Suppressor of G2 allele of SKP1 homolog (Sgt1)	0	0	0/4	1	1	1/4	Bs only	0.999996
P47897	Glutaminyl-tRNA synthetase	1	1	1/4	1	2	2/4	0.825535	1.000000
Q9N0F3	Seryl-tRNA synthetase, mitochondrial precursor	1	1	1/4	0	0	0/4	Ns only	0.999960
Q9D0R2	Threonyl-tRNA synthetase, cytoplasmic	0	0	0/4	1	1	1/4	Bs only	0.999996
P23381	Tryptophanyl-tRNA synthetase	1	1	1/4	1	1	1/4	-0.17447	1.000000
Q8BYL4	Probable tyrosyl-tRNA synthetase,	0	0	0/4	1	1	1/4	Bs only	0.999996
P54797	Ser/Thr-rich protein T10 in DGCR region	1	1	1/4	0	0	0/4	Ns only	0.999960
Q62311	Transcription initiation factor TFIID subunit 6	0	0	0/4	1	1	1/4	Bs only	0.999996
Q9H175	TGF-beta-induced apoptosis protein 12 (TAIP-12)	0	0	0/4	1	1	1/4	Bs only	0.999996
O60343	TBC1 domain family member 4	1	1	1/4	0	0	0/4	Ns only	0.999960
Q92609	TBC1 domain family member 5	0	0	0/4	1	4	3/4	Bs only	0.634632

TABLE 4 (continued). COMMON PROTEINS IDENTIFIED IN THE FIVE-YEAR-OLD NORMAL (N) AND BUPHTHALMIC (B) RABBITS

ACCESSION	DESCRIPTION	N PEPTIDES	N SCANS	N FREQUENCY /TOTAL*	B PEPTIDES	B SCANS	B FREQUENCY /TOTAL*	NORMALIZED LOG RATIO†	ADJUSTED *P* VALUE
O60765	Zinc finger protein 354A (Transcription factor 17)	1	1	1/4	0	0	0/4	Ns only	0.999960
P09838	DNA nucleotidylexotransferase	1	1	1/4	0	0	0/4	Ns only	0.999960
Q10587	Thyrotroph embryonic factor	1	1	1/4	0	0	0/4	Ns only	0.999960
Q15554	Telomeric repeat binding factor 2	0	0	0/4	1	1	1/4	Bs only	0.999996
P05452	Tetranectin precursor (TN)	1	1	1/4	0	0	0/4	Ns only	0.999960
Q8K284	General transcription factor 3C polypeptide 1	0	0	0/4	1	1	1/4	Bs only	0.999996
Q8BL74	General transcription factor 3C polypeptide 2	1	1	1/4	0	0	0/4	Ns only	0.999960
Q9GLD3	Transferrin receptor protein 1 (TfR1) (TR) (TfR) (Trfr)	0	0	0/4	1	1	1/4	Bs only	0.999996
Q9UP52	Transferrin receptor protein 2 (TfR2)	1	6	2/4	1	2	2/4	-1.75943	0.990101
P61811	Transforming growth factor beta-2 precursor (TGF-beta-2)	1	1	1/4	0	0	0/4	Ns only	0.999960
P22735	Protein-glutamine gamma-glutamyltransferase K	1	1	1/4	0	0	0/4	Ns only	0.999960
Q8NI27	THO complex subunit 2 (Tho2)	0	0	0/4	1	1	1/4	Bs only	0.999996
P00735	Prothrombin precursor	1	1	1/4	1	1	1/4	-0.17447	1.000000
Q9CZB3	THUMP domain-containing protein 2	0	0	0/4	1	1	1/4	Bs only	0.999996
Q5REP2	TIM21-like protein, mitochondrial precursor	0	0	0/4	1	1	1/4	Bs only	0.999996
Q13009	T-lymphoma invasion and metastasis-inducing protein 1 (TIAM-1 protein)	1	1	1/4	0	0	0/4	Ns only	0.999960
Q6B855	Transketolase (EC 2.2.1.1) (TK)	0	0	0/4	1	2	1/4	Bs only	0.992014
O43897	Tolloid-like protein 1 precursor	1	2	1/4	0	0	0/4	Ns only	0.970245
Q6R5N8	Toll-like receptor 13 precursor	1	1	1/4	0	0	0/4	Ns only	0.999960
Q95LA9	Toll-like receptor 2 precursor (CD282 antigen)	0	0	0/4	1	1	1/4	Bs only	0.999996
Q689D1	Toll-like receptor 2 precursor (CD282 antigen)	0	0	0/4	1	1	1/4	Bs only	0.999996
O95807	Transmembrane protein 50A (Small membrane protein 1)	1	1	1/4	0	0	0/4	Ns only	0.999960
Q7TNJ0	Transmembrane 7 superfamily member 4 (Dendritic cell-specific transmembrane protein) (DC-STAMP)	1	1	1/4	0	0	0/4	Ns only	0.999960
Q6ZNR0	Transmembrane protein 91	1	1	1/4	1	4	2/4	1.825535	0.999931
Q8MKG8	Tumor necrosis factor precursor (TNF-alpha)	1	1	1/4	0	0	0/4	Ns only	0.999960
O35305	Tumor necrosis factor receptor superfamily member 11A precursor	0	0	0/4	1	1	1/4	Bs only	0.999996
Q8NDV7	Trinucleotide repeat-containing gene 6A protein (CAG repeat protein 26)	1	12	3/4	1	14	3/4	0.047927	1.000000
Q13472	DNA topoisomerase III alpha (EC 5.99.1.2)	1	1	1/4	0	0	0/4	Ns only	0.999960
O70157	DNA topoisomerase III alpha (EC 5.99.1.2)	1	1	1/4	0	0	0/4	Ns only	0.999960

TABLE 4 (continued). COMMON PROTEINS IDENTIFIED IN THE FIVE-YEAR-OLD NORMAL (N) AND BUPHTHALMIC (B) RABBITS

ACCESSION	DESCRIPTION	N PEPTIDES	N SCANS	N FREQUENCY /TOTAL*	B PEPTIDES	B SCANS	B FREQUENCY /TOTAL*	NORMALIZED LOG RATIO†	ADJUSTED *P* VALUE
P02787	Serotransferrin precursor (Transferrin)	1	2	2/4	0	0	0/4	Ns only	0.970245
Q921I1	Serotransferrin precursor (Transferrin)	1	3	2/4	1	2	2/4	-0.75943	1.000000
O77698	Lactotransferrin precursor (EC 3.4.21.-) (Lactoferrin)	1	1	1/4	0	0	0/4	Ns only	0.999960
Q07283	Trichohyalin	1	3	2/4	1	1	1/4	-1.75943	0.999994
P37709	Trichohyalin	1	1	1/4	1	3	3/4	1.410497	1.000000
Q9HCM9	Tripartite motif protein 39 (RING finger protein 23)	0	0	0/4	1	1	1/4	Bs only	0.999996
Q9C040	Tripartite motif protein 2 (RING finger protein 86)	1	1	1/4	0	0	0/4	Ns only	0.999960
Q9Y4A5	Transformation/transcription domain-associated protein	0	0	0/4	1	1	1/4	Bs only	0.999996
P06871	Cationic trypsin precursor (EC 3.4.21.4)	1	196	6/4	1	257	6/4	0.216449	0.992532
P00762	Anionic trypsin I precursor (EC 3.4.21.4)	1	6	4/4	1	7	4/4	0.047927	1.000000
P07146	Anionic trypsin II precursor (EC 3.4.21.4)	1	1	1/4	1	2	2/4	0.825535	1.000000
P35030	Trypsin-3 precursor (EC 3.4.21.4) (Trypsin III)	1	1	1/4	1	2	2/4	0.825535	1.000000
P08426	Cationic trypsin III precursor (EC 3.4.21.4)	0	0	0/4	1	1	1/4	Bs only	0.999996
Q9Z0R7	Taste receptor type 1 member 2 precursor (G-protein coupled receptor 71)	0	0	0/4	1	1	1/4	Bs only	0.999996
P49815	Tuberin (Tuberous sclerosis 2 protein)	1	1	1/4	0	0	0/4	Ns only	0.999960
P35443	Thrombospondin-4 precursor	1	1	1/4	0	0	0/4	Ns only	0.999960
Q6SA08	Testis-specific serine/threonine-protein kinase 4	1	1	1/4	1	2	2/4	0.825535	1.000000
P53804	Tetratricopeptide repeat protein 3	1	1	1/4	0	0	0/4	Ns only	0.999960
P53781	Tristetraproline (TTP) (Zinc finger protein 36 homolog)	1	3	3/4	1	1	1/4	-1.75943	0.999994
O08970	Tuftelin	0	0	0/4	1	1	1/4	Bs only	0.999996
Q9D883	Splicing factor U2AF 35 kDa	0	0	0/4	1	1	1/4	Bs only	0.999996
Q9CQA9	Probable UPF0334 kinase-like protein C1orf57 homolog	1	1	1/4	1	1	1/4	-0.17447	1.000000
O75643	U5 small nuclear ribonucleoprotein 200 kDa helicase	1	2	2/4	0	0	0/4	Ns only	0.970245
Q9Y5T5	Ubiquitin carboxyl-terminal hydrolase 16 (EC 3.1.2.15)	0	0	0/4	1	1	1/4	Bs only	0.999996
Q9UPT9	Ubiquitin carboxyl-terminal hydrolase 22 (EC 3.1.2.15)	1	1	1/4	0	0	0/4	Ns only	0.999960
Q96RU2	Ubiquitin carboxyl-terminal hydrolase 28 (EC 3.1.2.15)	0	0	0/4	1	3	2/4	Bs only	0.883260
Q8NFA0	Ubiquitin carboxyl-terminal hydrolase 32 (EC 3.1.2.15)	0	0	0/4	1	1	1/4	Bs only	0.999996
P35125	Ubiquitin carboxyl-terminal hydrolase 6 (EC 3.1.2.15)	1	1	1/4	0	0	0/4	Ns only	0.999960
P40818	Ubiquitin carboxyl-terminal hydrolase 8 (EC 3.1.2.15)	1	1	1/4	1	1	1/4	-0.17447	1.000000
Q8IWV7	Ubiquitin-protein ligase E3 component N-recognin-1	0	0	0/4	1	1	1/4	Bs only	0.999996
Q8BG34	UBX domain-containing protein 3	1	1	1/4	0	0	0/4	Ns only	0.999960

TABLE 4 (continued). COMMON PROTEINS IDENTIFIED IN THE FIVE-YEAR-OLD NORMAL (N) AND BUPHTHALMIC (B) RABBITS

ACCESSION	DESCRIPTION	N PEPTIDES	N SCANS	N FREQUENCY /TOTAL*	B PEPTIDES	B SCANS	B FREQUENCY /TOTAL*	NORMALIZED LOG RATIO†	ADJUSTED *P* VALUE
Q9N2J1	Mitochondrial uncoupling protein 2 (UCP 2)	0	0	0/4	1	1	1/4	Bs only	0.999996
Q9NYU1	UDP-glucose:glycoprotein glucosyltransferase 2 precursor	0	0	0/4	1	1	1/4	Bs only	0.999996
P29598	Urokinase-type plasminogen activator precursor	1	1	1/4	0	0	0/4	Ns only	0.999960
Q8K1B8	Unc-112-related protein 2 (Kindlin-3)	1	2	2/4	1	4	4/4	0.825535	1.000000
Q15849	Urea transporter, kidney	0	0	0/4	1	1	1/4	Bs only	0.999996
Q96LB4	Vacuolar ATP synthase subunit G 3	1	2	2/4	0	0	0/4	Ns only	0.970245
P26234	Vinculin (Metavinculin)	1	1	1/4	1	1	1/4	-0.17447	1.000000
Q01827	Synaptic vesicular amine transporter-Monoamine transporter	0	0	0/4	1	1	1/4	Bs only	0.999996
Q9TSX8	Pantetheinase precursor (EC 3.5.1.92) (Pantetheine hydrolase)	1	1	1/4	0	0	0/4	Ns only	0.999960
Q9D2N9	Vacuolar protein sorting 33A	0	0	0/4	1	1	1/4	Bs only	0.999996
P04275	Von Willebrand factor precursor (vWF)	1	4	2/4	1	2	1/4	-1.17447	1.000000
Q96I51	Williams-Beuren syndrome chromosome region 16 protein	0	0	0/4	1	1	1/4	Bs only	0.999996
Q9NNW5	WD-repeat protein 6	0	0	0/4	1	1	1/4	Bs only	0.999996
Q80ZK9	WD and tetratricopeptide repeats protein 1	0	0	0/4	1	1	1/4	Bs only	0.999996
P47810	Wee1-like protein kinase (EC 2.7.1.112)	0	0	0/4	1	1	1/4	Bs only	0.999996
Q5U2Y0	WD-repeat domain phosphoinositide-interacting protein 4	0	0	0/4	1	1	1/4	Bs only	0.999996
Q9H4A3	Serine/threonine-protein kinase WNK1 (EC 2.7.1.37)	1	2	1/4	0	0	0/4	Ns only	0.970245
Q8IWR0	Zinc finger CCCH-type domain-containing protein 7A	1	1	1/4	0	0	0/4	Ns only	0.999960
Q64726	Zinc-alpha-2-glycoprotein precursor (Zn-alpha-2-glycoprotein)	0	0	0/4	1	1	1/4	Bs only	0.999996
O88799	Zonadhesin precursor	1	2	2/4	1	1	1/4	-1.17447	1.000000
Q8IXZ2	Zinc finger CCCH-type domain-containing protein 3	0	0	0/4	1	1	1/4	Bs only	0.999996
Q8K3Y6	Zinc finger CCCH type antiviral protein 1 (rZAP)	1	8	5/4	1	4	2/4	-1.17447	0.999509
Q5TAX3	Zinc finger CCHC domain-containing protein 11	1	7	5/4	1	5	4/4	-0.65989	1.000000
Q61967	Zinc finger protein 90 (Zfp-90) (Zinc finger protein NK10)	0	0	0/4	1	1	1/4	Bs only	0.999996
Q96K21	Zinc finger FYVE domain-containing protein 19	1	1	1/4	1	2	2/4	0.825535	1.000000
Q9HBF4	Zinc finger FYVE domain-containing protein 1	0	0	0/4	1	1	1/4	Bs only	0.999996
Q14119	Zinc finger protein 161 (Putative transcription factor DB1)	0	0	0/4	1	1	1/4	Bs only	0.999996
Q9UL58	Zinc finger protein 215 (BWSCR2 associated zinc-finger protein 2)	0	0	0/4	1	1	1/4	Bs only	0.999996
Q9UDV7	Zinc finger protein 282 (HTLV-I U5RE binding protein 1)	1	1	1/4	0	0	0/4	Ns only	0.999960
O60281	Zinc finger protein 292	0	0	0/4	1	1	1/4	Bs only	0.999996
O75467	Zinc finger protein 324 (Zinc finger protein ZF5128)	0	0	0/4	1	1	1/4	Bs only	0.999996
Q9NW07	Zinc finger protein 358	0	0	0/4	1	1	1/4	Bs only	0.999996

TABLE 4 (continued). COMMON PROTEINS IDENTIFIED IN THE FIVE-YEAR-OLD NORMAL (N) AND BUPHTHALMIC (B) RABBITS

ACCESSION	DESCRIPTION	N PEPTIDES	N SCANS	N FREQUENCY /TOTAL*	B PEPTIDES	B SCANS	B FREQUENCY /TOTAL*	NORMALIZED LOG RATIO†	ADJUSTED *P* VALUE
Q9P243	Zinc finger protein 406 (Protein ZFAT)	1	1	1/4	0	0	0/4	Ns only	0.999960
Q96K75	Zinc finger protein 514	1	1	1/4	0	0	0/4	Ns only	0.999960
Q5R5S6	Zinc finger protein 540	1	1	1/4	0	0	0/4	Ns only	0.999960
Q9H582	Zinc finger protein 644 (Zinc finger motif enhancer binding protein 2)	0	0	0/4	1	1	1/4	Bs only	0.999996
Q05481	Zinc finger protein 91 (Zinc finger protein HTF10)	1	1	1/4	1	2	2/4	0.825535	1.000000
Q9BH11	Zona pellucida sperm-binding protein 4 precursor	1	1	1/4	0	0	0/4	Ns only	0.999960
Q62975	Protein Z-dependent protease inhibitor precursor	0	0	0/4	1	1	1/4	Bs only	0.999996

*Number of animals in which protein was detected/Total number of animals used (N=4, B=4).
†Calculated from the ratio of the scans (B/N) adjusted to the ratio of the total scans for all proteins detected in the sample.

TABLE 5. DIFFERENTIALLY EXPRESSED PROTEINS IN THE AQUEOUS HUMOR OF THE TWO-YEAR-OLD BUPHTHALMIC RABBITS

ACCESSION	PROTEIN	N PEPTIDES	N SCANS	N FREQUENCY /TOTAL*	B PEPTIDES	B SCANS	B FREQUENCY/ TOTAL*	NORMALIZED LOG RATIO†	ADJUSTED *P* VALUE
Q28640	Histidine-rich glycoprotein precursor (histidine-proline-rich glycoprotein) (HPRG)	21	216	6/6	20	160	6/6	-0.60742	0.043749

*****Number of animals in which protein was detected/Total number of animals used (N=4, B=6).
†Calculated from the ratio of the scans (B/N) adjusted to the ratio of the total scans for all proteins detected in the sample.

TABLE 6. DIFFERENTIALLY EXPRESSED PROTEINS IN THE AQUEOUS HUMOR OF THE FIVE-YEAR-OLD BUPHTHALMIC RABBITS

ACCESSION	PROTEIN	N PEPTIDES	N SCANS	N FREQUENCY/ TOTAL*	B PEPTIDES	B SCANS	B FREQUENCY/ TOTAL*	NORMALIZED LOG RATIO†	ADJUSTED *P* VALUE
P18287	Apolipoprotein E (Apo-E)	8	442	4/4	9	165	4/4	-1.76107	0.000000
P49065	Serum albumin	38	4328	4/4	49	7068	4/4	0.368113	0.000000
P07489	Transthyretin (prealbumin)	11	268	4/4	14	180	4/4	-0.91372	0.000000
P19007	Haptoglobin	7	62	4/4	4	19	4/4	-2.04576	0.000000
P20058	Hemopexin	10	80	4/4	6	38	4/4	-1.41349	0.000006
Q9XSC5	Clusterin (apolipoprotein J) (Apo-J)	7	47	4/4	13	115	4/4	0.951412	0.001422
Q28372	Gelsolin (actin-depolymerizing factor)	9	91	4/4	8	62	4/4	-0.89309	0.002137

TABLE 6 (continued). DIFFERENTIALLY EXPRESSED PROTEINS IN THE AQUEOUS HUMOR OF THE FIVE-YEAR-OLD BUPHTHALMIC RABBITS

ACCESSION	PROTEIN	N PEPTIDES	N SCANS	N FREQUENCY/ TOTAL*	B PEPTIDES	B SCANS	B FREQUENCY/ TOTAL*	NORMALIZED LOG RATIO†	ADJUSTED *P* VALUE
P01885	Beta-2-microglobulin	2	18	4/4	2	53	4/4	1.218507	0.007178
P80191	Alpha-2-HS-glycoprotein (fetuin-A)	4	39	4/4	5	21	4/4	-1.23257	0.006957

*****Number of animals in which protein was detected/Total number of animals used (N=4, B=4).

†Calculated from the ratio of the scans (B/N) adjusted to the ratio of the total scans for all proteins detected in the sample.

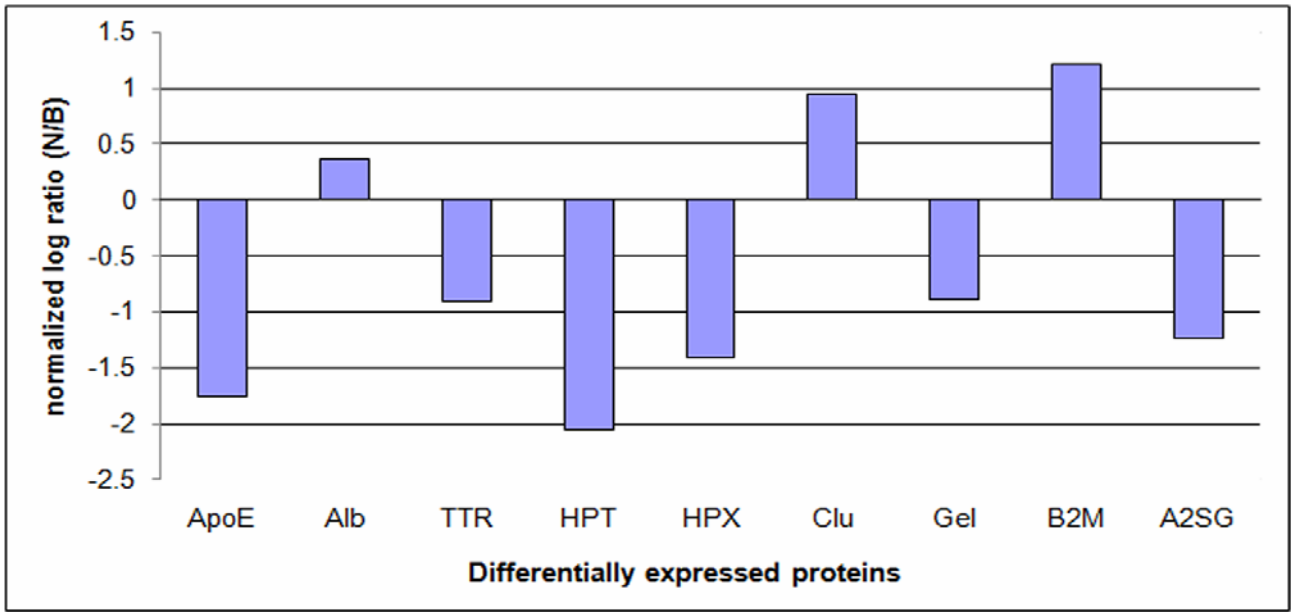

FIGURE 17

Bar graphs showing the log ratio (normal/buphthalmic) of the differentially expressed proteins in the 5-year-old buphthalmic rabbits. ApoE (apolipoprotein E), Alb (albumin), TTR (transthyretin), HPT (haptoglobin), HPX (hemopexin), Clu (clusterin), Gel (gelsolin), B2M (beta-2 microglobulin), A2SG (alpha-2-HS-glycoprotein).

TABLE 7. IMMUNOHISTOCHEMISTRY RESULTS FOR THE TWO-YEAR-OLD NORMAL (N) AND BUPHTHALMIC (B) RABBITS*

PROTEIN	ANIMAL	DESCEMET'S MEMBRANE	ENDOTHELIUM	CILIARY EPITHELIUM	TRABECULAR MESHWORK/ ENDOTHELIUM	LENS CAPSULE	LENS EPITHELIUM
Histidine-rich glycoprotein	N	0	2+	2+	Trace to 1+	0	1+
	B	0	3+	1 +	Trace to 1+	0	0
Clusterin	N	0	3	3	2	0	3
	B	0	3	3	2	0	3
Apolipoprotein E	N	0	2+	2+	1+	0	2
	B	0	2+	2+	1+	0	2+

TABLE 7(continued). IMMUNOHISTOCHEMISTRY RESULTS FOR THE TWO-YEAR-OLD NORMAL (N) AND BUPHTHALMIC (B) RABBITS*

PROTEIN	ANIMAL	DESCEMET'S MEMBRANE	ENDOTHELIUM	CILIARY EPITHELIUM	TRABECULAR MESHWORK/ ENDOTHELIUM	LENS CAPSULE	LENS EPITHELIUM
Cochlin	N	0	1	1	0	0	0
	B	0	1	2	3+	0	1
Inter-photoreceptor retinoid-binding protein	N	0	1+	3+	1+	0	1+
	B	0	2+	3+	1+	0	1+
Transthyretin	N	0	3+	1+	1+	0	1+
	B	0	3 +	1+	2+	0	1+
Gelsolin	N	0	1+	2	1+	0	0
	B	0	1+	2	1+	0	0
Haptoglobin	N	0	1	1+	1+	0	1+
	B	0	1	1+	2+	0	1+

*Fluorescence intensity was given scores from 0 to 4+ with 0 being no fluorescence and 4+ being intense fluorescence.

TABLE 8. IMMUNOHISTOCHEMISTRY RESULTS FOR THE FIVE-YEAR-OLD NORMAL (N) AND BUPHTHALMIC (B) RABBITS*

PROTEIN		DESCEMET'S MEMBRANE	CORNEAL ENDOTHELIUM	CILIARY EPITHELIUM	TRABECULAR MESHWORK/ ENDOTHELIUM	LENS CAPSULE	LENS EPITHELIUM
Histidine-rich glycoprotein	N	0	2 +	3 +	2 +	0	1 +
	B	0	2 +	1 +	1 +	0	0
Alpha-2-HS-glycoprotein	N	0	2 +	3 +	1 +	0	3 +
	B	0	2 +	3 +	1 +	0	0
Clusterin	N	0	2 +	1 +	2 +	0	2 +
	B	0	0	3 +	1 +	0	1 +
Apolipoprotein E	N	0	3+	2 +	3 +	0	1 +
	B	0	2 +	1 +	1 +	0	2 +
Cochlin	N	0	2 +	1 +	Trace	0	1 +
	B		2 +	2 +	2 +	0	1 +
Inter-photoreceptor retinoid-binding protein	N	0	1 +	1 +	1 +	0	1 +
	B	0	1-2+	0	0	0	0
Transthyretin	N	0	1 +	3 +	2 +	0	1 +
	B	0	1 +	0	1 +	0	1 +
Gelsolin	N	0	3 +	3 +	3 +	0	2 +
	B	0	0	1 +	1 +	0	0
Haptoglobin	N	0	3 +	2 +	3 +	0	2 +
	B	0	1 +	1 +	1 +	0	0.5
Hemopexin	N	0	1 +	2 +	1 +	0	2 +
	B	0	1	1 +	0	0	0

*Fluorescence intensity was given scores from 0 to 4+ with 0 being no fluorescence and 4+ being intense fluorescence.

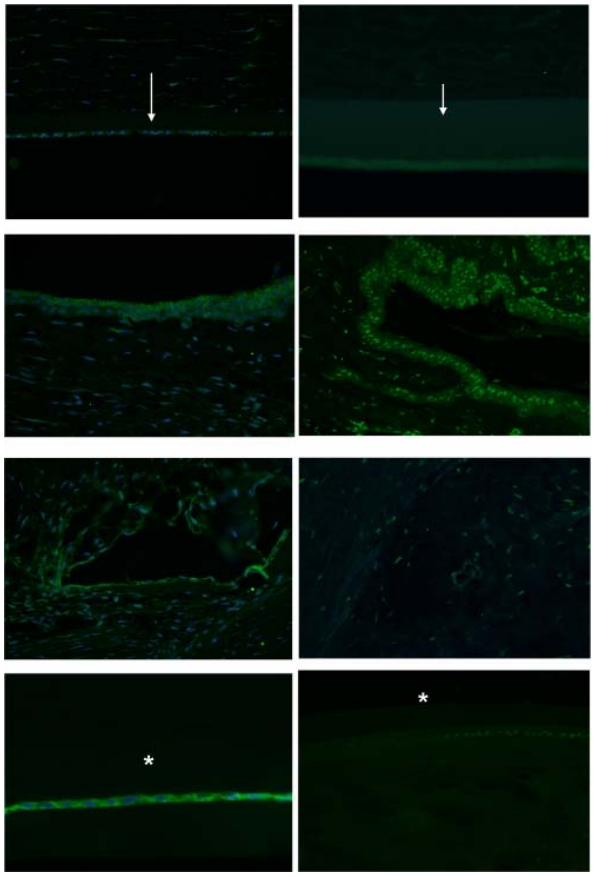

FIGURE 18

Clusterin immunofluorescence in the 5-year-old normal (left panel) and buphthalmic (right panel) rabbits in cornea (top panel), ciliary epithelium (second panel from top), angle (third panel from top), and lens epithelium (bottom panel). Note the reduced staining in the buphthalmic tissues except the ciliary epithelium, where it is increased, and its absence in Descemet's membrane (arrow) and lens capsule (*) (original magnification ×20, Alexa Fluor 488; DAPI nuclear stain).

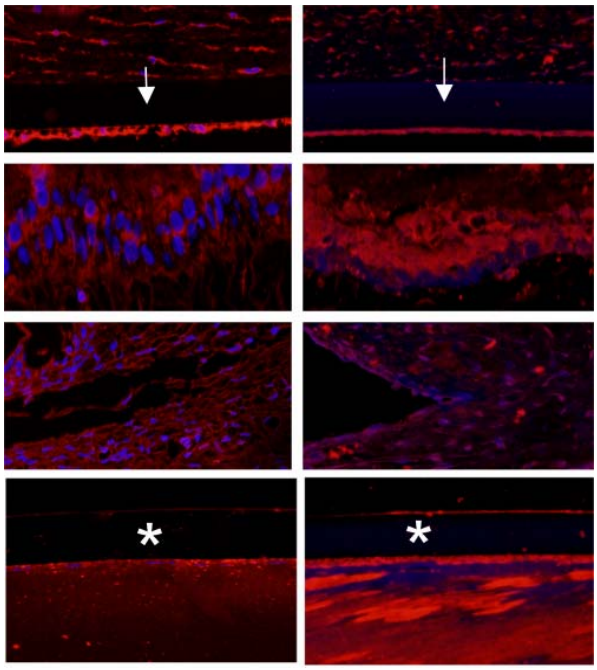

FIGURE 19

ApoE immunofluorescence in the 5-year-old normal (left panel) and buphthalmic (right panel) rabbits in cornea (top panel), ciliary epithelium (second panel from top), angle (third panel from top), and lens epithelium (bottom panel). Note the reduced staining in some of the buphthalmic tissues and its absence in Descemet's membrane (arrow) and lens capsule (*). Increased ApoE staining is seen in the ciliary body and anterior lens epithelium in the buphthalmic rabbit (original magnification ×20, Texas Red; DAPI nuclear stain).

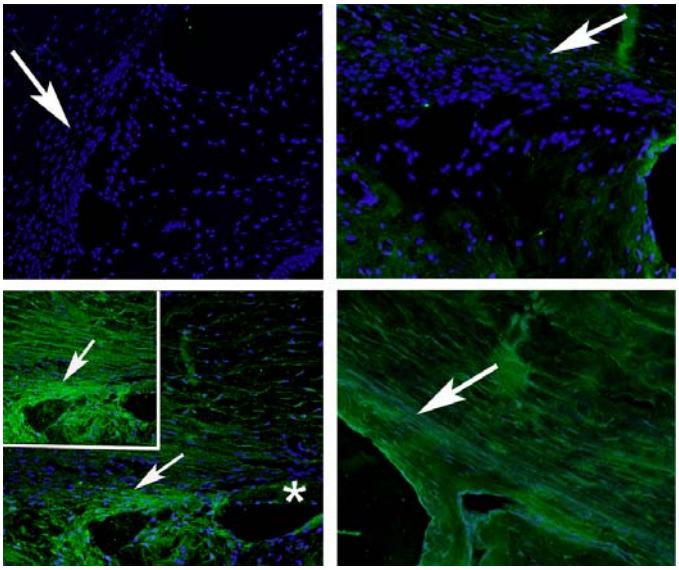

FIGURE 20

Cochlin immunoreactivity (IR) in the anterior chamber angle in the negative control (upper left), normal 2-year-old (upper right), 2-year-old buphthalmic (lower left), and 5-year-old buphthalmic (lower right) rabbits. Note the lack of IR in upper panels. In the 2-year-old buphthalmic (lower left), an intense IR localized to the trabecular beams and peripheral anterior iris is observed. Note cytoplasmic labeling in peripheral deep keratocytes. In the 5-year-old buphthalmic, nonuniform staining of lower intensity is noted in the fibrotic angular meshwork with some background labeling. Inset, lower left, shows cochlin IR of meshwork at higher magnification. There is cochlin labeling in the deep sclera (original magnification ×10; inset, original magnification ×20, Alexa Fluor 488; DAPI nuclear stain) (arrows point to angular meshwork and * to Descemet's membrane).

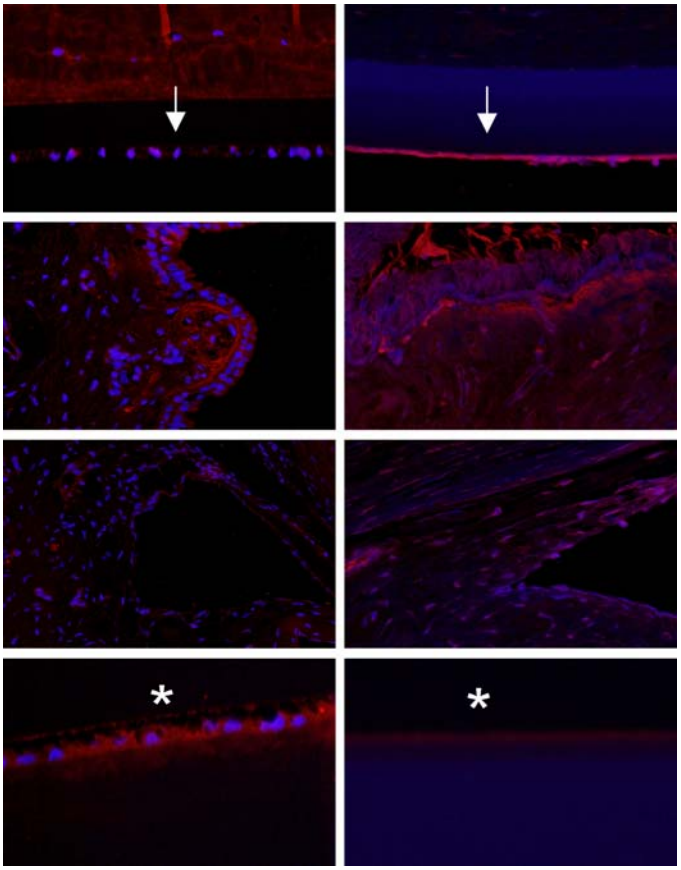

FIGURE 21

IRBP immunofluorescence in the 5-year-old normal (left panel) and buphthalmic (right panel) rabbit in cornea (top row), ciliary epithelium (second row), angle (third row), and lens epithelium (bottom row). Note the reduced staining in most buphthalmic tissues and its absence in Descemet's membrane (arrows) and lens capsule (*). There is slight increase in staining of corneal endothelium (original magnification ×20, Texas Red; DAPI nuclear stain).

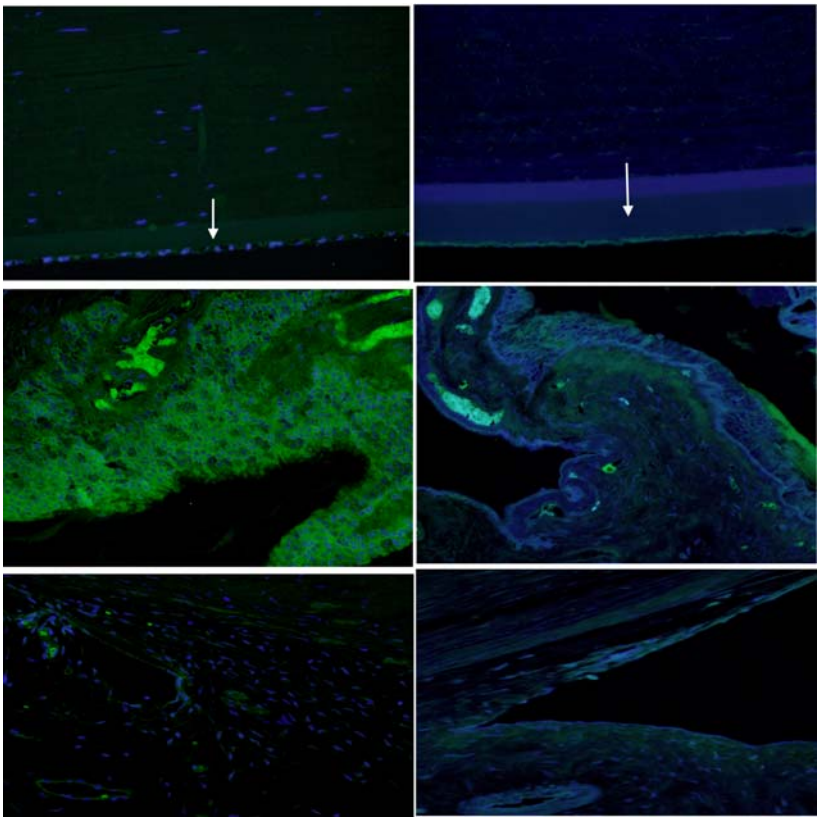

FIGURE 22

TTR immunofluorescence in the 5-year-old normal (left panel) and buphthalmic (right panel) rabbit in cornea (top row), ciliary epithelium (second row), and angle (third row). Note the reduced staining in the buphthalmic tissues and its absence in Descemet's membrane (arrows) (original magnification ×20, Alexa Fluor 488; DAPI nuclear stain).

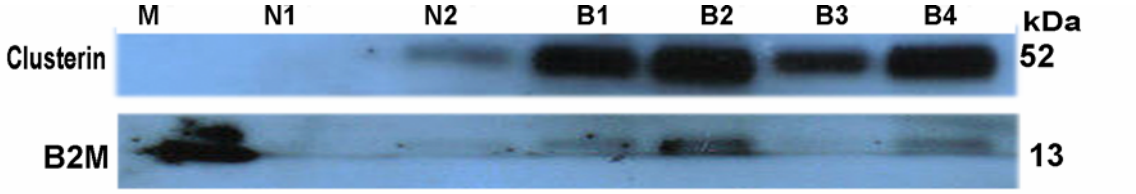

FIGURE 23

Western blot analysis of 5-year-old normal and buphthalmic aqueous humor using antibodies against clusterin (top) and B2M (bottom). M lane 1: protein marker; N1: control 1; N2: control 2; B1: buphthalmic 1; B2: buphthalmic 2; B3: buphthalmic 3; B4: buphthalmic 4. Note prominent bands for both proteins in buphthalmic animals.

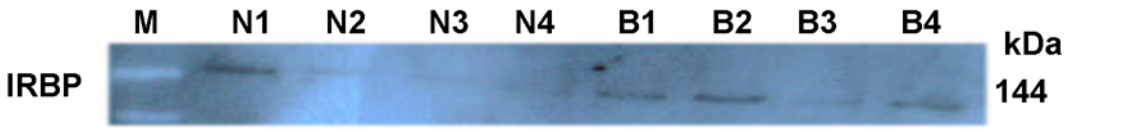

FIGURE 24

Western blot analysis of 2-year-old normal (lanes 1,2,3,4) and buphthalmic (5,6,7,8) AH against IRBP. M (lane 1): protein marker; N1 (lane 2): control 1; N2 (lane 3): control 2; N3 (lane 4): control 3; N4 (lane 5): control 4; B1 (lane 6): buphthalmic 1; B2 (lane 7): buphthalmic 2; B3 (lane 8): buphthalmic 3; B4 (lane 9): buphthalmic 4. Note faint bands in controls and also in buphthalmic animals.

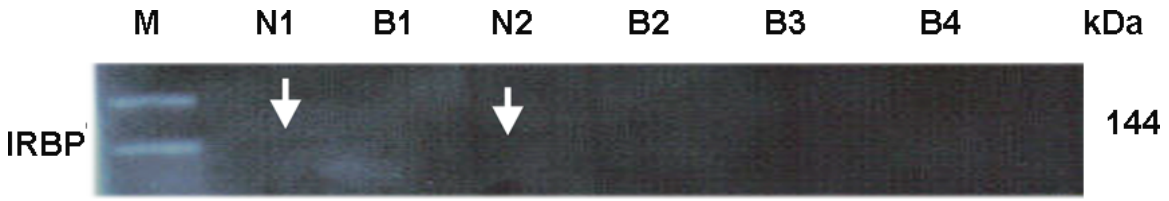

FIGURE 25

Western blot analysis of 5-year-old normal and buphthalmic aqueous humor using antibodies against IRBP. M (lane 1): protein marker; N1: control 1; N2: control 2; B1: buphthalmic 1; B2: buphthalmic 2; B3: buphthalmic 3.

DISCUSSION

In this study we described unique histologic alterations in the anterior segment of the buphthalmic rabbit and used comparative proteomic profiling to establish a correlation between the proteomic data and the phenotype. The clinical and histologic data were obtained using standard techniques. Proteomic profiling was carried out using liquid chromatography followed by tandem mass spectrometry (LC-MS/MS) and validated using Western blot or immunohistochemistry. LC-MS/MS–based shotgun proteomics is a highly sensitive technique for detecting alterations in the proteome of diseased tissues or body fluids. Label-free LC-MS/MS has been used in quantitation of proteins, assuming that increased abundance of a specific protein will lead to increased spectral counts of its tryptic peptides. The resultant observable indices include chromatographic ion peak intensity, sequence coverage, peptide number, and spectral count.[70] We used the spectral counting approach to determine the relative quantification of proteins in the AH. Comparison of the total number of MS/MS spectra detected for a given protein (spectral counting) is a reliable and highly reproducible method for relative quantitation. It has been demonstrated that spectral count is the factor with strongest correlation (r^2=0.9997) to protein abundance.[71] To determine the significance of the differential expression of proteins, we used the *G* statistic and then applied a post hoc Holm-Sidak adjustment of the *P* value to correct for multiple testing as previously described. The *G*-test was found to be the most appropriate method of statistical analysis based upon our experimental design.[67,72] We also applied additional layers of stringency to increase confidence in the final protein list. For example, proteins must have appeared in 100% of samples and have had a ratio of at least 2.0 where increased abundance was detected. This was done to minimize the rate of false discovery. The compiled list of proteins included proteins that were significantly different between groups and also proteins that were missing in buphthalmic but present in all normal rabbits with significantly high scan counts.

Clinically, the affected animals showed typical signs of buphthalmos with enlarged globes and corneas and corneal clouding. Overall, the phenotype in these animals was mild with IOP levels closer to the normal range. The IOP in the affected animals was higher than that seen in the controls in the 2- and 5-year-old buphthalmic rabbits but not higher than those reported in younger animals.[8,22] In this mild phenotype the average IOP in the 5-year-old buphthalmic rabbits was higher than that in the 2-year-old buphthalmic rabbits and consistent with the progressive degenerative changes seen in the outflow pathway on histology. The IOP in the older buphthalmic rabbits may be elevated, but normalization has also been reported in aging animals.[34,73] Many theories have been suggested to explain IOP lowering, and one possibility is that the ciliary body atrophied secondary to elevated IOP.[8,14] We investigated the role of ciliary epithelium atrophy in IOP reduction in the older buphthalmic rabbit. Morphometric measurements revealed no statistically significant differences in the density of the nonpigmented ciliary epithelium in any of the age groups, suggesting that factors other than ciliary epithelial atrophy played a role in normalization of IOP in these animals.

The first unique observation upon histologic examination of the buphthalmic rabbit was thickening of the anterior lens capsule, which was significantly thicker than in the control. The posterior lens capsule thickness, however, was comparable to the control. The lens capsule or the lens basement membrane is an acellular and structurally complex ECM, consisting of a meshwork of various glycoproteins and proteoglycans, such as collagen type IV and fibronectin.[74] The capsular ECM of the lens is continually produced and remodeled anteriorly by the lens epithelial cells throughout life. On the other hand, the posterior capsule is secreted during development by the epithelial cells that line the lens vesicle. The cells on the posterior capsule eventually elongate to fill the interior lumen and become the primary fiber cells.[75] At this point, the thickness of the posterior capsule remains unchanged throughout life. Thickening of the anterior lens capsule has been previously described in humans in anterior subcapsular cataracts[76] and in secreted protein, acidic, cysteine-rich (SPARC) mutant mice, but this thickening is associated with cataract formation, whereas the lens in the buphthalmic rabbit was clear.[77,78] Though SPARC was detected in the AH of rabbits, the levels in the buphthalmic rabbit were not different from the controls.

The exaggerated thickening of the anterior lens capsule in the buphthalmic rabbit is an unusual event that has not been previously reported. At the light microscopic and ultrastructural level, the lens capsule, apart from its increased uniform thickness, did not demonstrate morphologic changes in the underlying lens epithelium. However, immunohistochemistry showed a significant increase in staining intensity with collagen type IV and fibronectin antibodies, both of which are major components of the lens capsule.[79] It is

possible that secretion of these and other components of the lens capsule by abnormally stimulated lens epithelial cells resulted in anterior capsular thickening. One might speculate that factors in the AH, which comes in direct contact with the anterior lens surface, might modulate the lens epithelium and thereby contribute to capsular thickening. It is unclear if these capsular changes are present or absent in younger buphthalmic rabbits, and it would be worthwhile to further investigate this observation in future studies.

The other basement membrane that showed significantly increased thickening was DM. It is the basement membrane of the corneal endothelium, and its thickness increases with age similar to the anterior lens capsule. Abnormal thickening of DM has been described in many corneal dystrophies, such as congenital hereditary endothelial dystrophy, posterior polymorphous corneal dystrophy, and Fuchs' endothelial corneal dystrophy (FECD), all of which are associated with abnormal endothelial cells.[61] Thickening of DM in the buphthalmic rabbit was described by Van Horn and colleagues[62] as either an increased thickness of the posterior nonbanded zone or a posterior collagenous layer in severe buphthalamia. In our study, DM thickening resulted mainly from diffuse thickening of the posterior nonbanded layer with a normal anterior banded layer being present in both control and affected animal groups, consistent with the mild phenotype of the buphthalmic animals in the Van Horn study. An unusual observation was the presence of long-spacing collagen in the posterior parts of DM in 2-year-old controls and its absence in the buphthalmic rabbits. A previous study suggested that the normal rabbit's DM lacks long-spacing collagen.[63] Long-spacing collagen typically increases with aging, and it is possible that the single animal used in the previous study was younger and lacked long-spacing collagen, in contrast to our 2-year-old normal rabbits. Long-spacing collagen, which is composed mainly of collagen type VIII,[80] is commonly deposited in the abnormal posterior collagenous layer of a thickened DM in a variety of conditions affecting corneal endothelial cells, including FECD.[81] Some of the similarities between AH protein changes in FECD and the corneal changes in the buphthalmic rabbit are discussed in the following paragraphs. Interestingly, collagen VIII mutant mice show thinning of DM and not thickening.[69] The reason for the absence of long-spacing collagen in the thickened abnormal DM in the buphthalmic rabbit is unclear. It is possible that factors from the AH or surrounding tissues influence collagen VIII deposition by endothelial cells. These may be altered in the buphthalmic rabbit and merit further investigation. The corneal endothelial cells in the buphthalmic rabbit were attenuated with dilated intercellular spaces as described previously.[62] We also observed in our study dilated intercellular spaces in the controls, suggesting that these changes may not be pathologic.

To further characterize the changes in the basement membrane in the buphthalmic rabbits, we investigated the expression of some of its components. Collagen IV and fibronectin proteins are major components of basement membranes, and the expression of both proteins appeared significantly greater in DM and the anterior lens capsule in the buphthalmic rabbits compared to their control littermates. Apart from thickening of the anterior lens capsule and DM, none of the other ocular basement membranes were thickened in the buphthalmic rabbit. This selective thickening at first suggests that the changes observed in both basement membranes could have resulted from either a common inherited or an acquired abnormality in the corneal endothelial or lens epithelial cells. However, this speculation is unlikely, since both cells are derived from progenitor cells of different lineage. A more likely explanation for this observation suggested above is the possibility that aberrant factors present in the AH bathe the anterior lens capsule, its epithelium, DM, and endothelium, stimulating the cells to produce excessive basement membrane. The regulation of basement membrane synthesis, including those in the eye, is complex and poorly understood.[74,82] Thickening of basement membranes is observed universally in diabetes, where elevated TGF beta-1 is the main molecule implicated in the process that influences basement membrane thickening. The influence of TGF beta-1 and its regulation of ECM turnover in the TM matrix have been previously studied.[83] In POAG, components of the ECM such as collagen type IV, laminin, and fibronectin are increased in the TM of eyes[79,84] in response to up-regulated TGF beta-2.[85] TGF beta-2 levels are higher in the AH of patients with POAG.[86] However, its role in PCG or in the buphthalmic rabbit is not known. In our study, many proteins that influence ECM deposition and regulation were differentially expressed in AH of the buphthalmic rabbit, but levels did not reach statistical significance.

PROTEOMIC ANALYSIS

Analysis of data obtained from LC-MS/MS revealed that the AH protein profile in the normal rabbits was similar to that described earlier in both rabbits and humans using mass spectrometry.[46,87] The majority of proteins in the normal rabbit AH were cellular and plasma-based with a wide range of various biologic functions. In addition, several differentially expressed AH proteins were identified in the buphthalmic rabbit. This finding confirmed our premise that the AH is altered in the buphthalmic rabbit. It was interesting to note that some of the differentially expressed proteins identified in this study are similar to those identified in AH from human PCG.[4] The common proteins included albumin, TTR, and IRBP, and their AH levels in the buphthalmic rabbit followed the same pattern as human PCG. Many of the differentially expressed proteins identified in this study were multifunctional and generally fell under three categories based on their biologic function: ECM remodeling/development, oxidative stress, and binding/transport proteins. In addition, an age-related difference in the AH proteome profile was demonstrated in the buphthalmic rabbit. This age-dependent change could be explained by the aging of the rabbits. It is also possible that the changes in AH protein profile may play a role in the increased severity of disease in the older buphthalmic rabbits in some instances or might be the result of progressive degeneration of tissues secreting the protein.

In the following paragraphs we discuss the relevance of the altered AH proteins in the buphthalmic rabbit and how the alterations of these proteins could potentially relate to the phenotypic changes in the buphthalmic anterior segment, specifically, changes in the basement membranes of the cornea and lens, as well as the role that some of these proteins may play in causing the glaucoma phenotype. These observations are consistent with our hypothesis. Though the discussion of differential protein expression focuses mainly on events that might affect corneal endothelial cells and changes in DM, some of these pathways that affect corneal endothelial

cell function and result in thickness of DM may be responsible for changes in the anterior lens capsule in the buphthalmic rabbit, since many of these differentially expressed proteins were also localized in the lens epithelium. In addition, other alterations in the proteome could be related to the progressive histopathologic changes in the angular meshwork of the buphthalmic rabbit.

Basement Membrane Changes

The four proteins differentially expressed in the AH of the buphthalmic rabbit discussed in the following paragraphs may be involved in the basement membrane thickening observed in the buphthalmic animals.

Histidine-rich glycoprotein. HRG was the only protein that was significantly decreased in the AH of the 2-year-old buphthalmic rabbits. The differences could not be confirmed by Western blot owing to difficulty in acquiring an antibody that cross-reacts with rabbit proteins in Western blot. However, immunohistochemistry showed a decrease of HRG in the anterior chamber tissues of the buphthalmic rabbits compared to control, except for the corneal endothelium (Table 7). HRG immunoreactivity was detected in the normal ciliary epithelium, lens capsule, corneal endothelium, and trabecular endothelial cells (Figure 19). The labeling was cytoplasmic and was not detected in DM or the lens capsule. HRG is a plasma protein with potent anti-angiogenic properties[88] and is one of the proteins in a subgroup (denoted type 3) within the cystatin superfamily of cysteine protease inhibitors. HRG has been previously detected in the AH of normal healthy rabbits and humans.[46,87] Using a proteomic approach similar to that used in this study, Richardson and colleagues[56] detected a significant decrease in HRG in the AH of patients with end-stage FECD similar to that seen in the buphthalmic rabbit. It was suggested that HRG might be involved in protective processes, such as clearance of apoptotic cells described by Gorgani and Theofilopoulos.[89] Such a decrease in protective effect could contribute to disease progression in FECD patients. In the buphthalmic rabbit, expression of HRG was noted in the corneal endothelial cells. We suggest that alterations in HRG may result from changes in a common pathway that causes endothelial cells to be affected in both FECD and the buphthalmic rabbit with consequent thickening of DM.

Alpha-2-HS-glycoprotein. Similar to HRG, A2SG, also known as fetuin A, belongs to the cystatin superfamily. A2GS was significantly decreased (P=.006) but only in the AH of the 5-year-old buphthalmic rabbits. Though we were unable to show a direct relationship between A2SG levels and basement membrane thickening in the buphthalmic rabbit, A2SG is listed in this section, since it belongs to the same family as HRG and has known effects on the ECM. A decrease in A2SG immunoreactivity was noted in the buphthalmic angular meshwork and lens epithelium of the 5-year-old buphthalmic rabbit, but moderate labeling was observed in the corneal endothelium and the ciliary epithelium that was comparable to that seen in the controls. Interestingly, the choroid plexus responsible for cerebrospinal fluid (CSF) production was shown to express A2SG and so did the ciliary epithelium, which is responsible for AH production. A2SG interacts with many other proteins that affect the ECM. For example, it is known to be a significant inhibitor of TGF beta-2, a protein that shows increased expression in the TM in open-angle glaucoma causing ECM deposition in the human TM.[90] A2SG also inhibits bone morphogenetic proteins that are altered in the TM in open-angle glaucoma.[91] The literature suggests potential interactions of A2SG with many proteins that are significantly altered in open-angle glaucoma. However, the mechanistic pathways that regulate A2SG are not well understood, and it is therefore difficult to assign a specific relationship between the change in A2SG levels in the AH with the histologic alterations in the buphthalmic rabbit.

Clusterin (apolipoprotein J, CLU). Clusterin levels were elevated in the AH of the 5-year-old buphthalmic rabbit. This observation was validated by Western blot. Immunohistochemistry showed reduced labeling in the corneal endothelial cells and the angular meshwork of the buphthalmic rabbits, and increased labeling in the ciliary epithelium. Clusterin has been localized to the corneal endothelial cells and has also been identified in normal human iris, the ciliary body, lens capsule, optic nerve, and AH.[92] It is locally synthesized in ocular structures.[93] Elevated levels of clusterin seen in the AH of the buphthalmic rabbit could be due to increased secretion of the protein from the cells in the anterior segment. Increased clusterin expression was noted in the endothelial cells in FECD and in retinal pigment epithelium and drusen in age-related macular degeneration.[94] In FECD, it is suggested that the up-regulation was a compensatory response to cell loss from apoptotic endothelial cells, but the increased secreted protein is sequestered by albumin, preventing the intended protective effect. In age-related macular degeneration, it was suggested that clusterin accumulates in response to injury.[94] This interpretation was based on reports that the protein plays a role in maintaining cells at tissue-fluid interfaces, inhibition of complement-mediated cell lysis, and protection from apoptosis, as well as reducing oxidative stress–induced apoptosis in human corneal endothelial cells in culture.[95] We suggest that clusterin plays a similar role in the buphthalmic rabbit, where its activity may reflect the changes seen in the corneal endothelial cell and subsequent thickening of DM. Clusterin has also been localized in the lens capsular epithelium, in normal AH, and as a component of exfoliation material in pseudo-exfoliation.[96] The physiologic function of clusterin in the lens epithelium is unclear, but it could play a similar role as has been suggested for its interaction with corneal endothelium in FECD and in the buphthalmic rabbit, resulting in increased lens capsular thickness. Because clusterin binds to albumin,[97] an increase in albumin may lead to an increase in clusterin in the AH. Richardson and associates[56] found increased levels of clusterin in the AH of FECD in the non-albumin-depleted fraction, but when albumin was depleted, no changes in clusterin levels were noted. In our study, the increase in AH clusterin in the 5-year-old buphthalmic rabbit was accompanied by an increase in AH albumin, suggesting that elevated clusterin levels in the 5-year-old buphthalmic rabbit may be due to increased AH albumin levels, possibly accompanied by increased synthesis and secretion by the ciliary epithelial cells as suggested by the immunohistochemical observations. The effect of increased clusterin may therefore mimic what was described in FECD and described above.

Apolipoprotein E. ApoE levels were significantly decreased in the 5-year-old buphthalmic AH compared to the 5-year-old control AH. ApoE immunoreactivity of the anterior chamber tissues in the 5-year-old buphthalmic rabbits was consistently decreased when compared to the 5-year-old control rabbits. ApoE has multiple biologic properties aside from its physiologic role in cholesterol

transport. In the eye, ApoE is locally synthesized by the retinal pigment epithelium.[98] Furthermore, ApoE has been recently found to be a component of pseudoexfoliation material,[99] suggesting that ApoE is likely derived from the circulating AH or cells lining the anterior segment structures. In this study, immunolocalization of ApoE in the cytoplasm of the ciliary epithelium, lens epithelium, and corneal endothelium of normal and buphthalmic rabbits suggested that this carrier protein is secreted into the AH from multiple structures in the anterior segment. The decrease in AH ApoE may also play a role in influencing basement membrane thickness. In ApoE-deficient mice, Bruch's membrane showed thickening with membranous deposits.[100] Also, ApoE polymorphisms have been associated with POAG, but this finding and its relationship to POAG have been somewhat controversial.[101] ApoE also has antioxidant properties in body fluids,[102] and its deficiency promotes oxidative stress.[103] Many studies have suggested that increased oxidative stress in the TM leads to degeneration of the trabecular endothelial cells in POAG.[104] It is therefore possible that decreased ApoE levels in the AH and in the angular meshwork as demonstrated in this study may contribute to the more advanced changes seen in the angular meshwork of the 5-year-old buphthalmic rabbits.

Summary. The similarities in differential protein profile in the AH and corneal endothelium between FECD and the buphthalmic rabbit, and consequent alterations in DM, are remarkable. The findings suggest that convergent common pathways downstream are likely affected in the corneal endothelial cells in both disorders. The protein changes are likely secondary to other inciting events upstream and need to be identified in future studies. The thickening of the lens capsule in the buphthalmic rabbit is more difficult to explain, since the lens capsule changes have not been observed with Fuchs' dystrophy. However, since most of the differentially expressed proteins in the AH are also expressed in the lens epithelium, one can speculate that the changes in the AH proteins may also lead to changes in expression of proteins in the capsular epithelium and eventually thickening of the anterior lens capsule.

Changes in the Anterior Chamber Angle

The histologic anterior chamber angle anomalies seen in both the 2- and 5-year-old buphthalmic rabbits were similar to those previously described in younger animals.[14] These include absence of iris pillars, compressed and disorganized angular meshwork, and deposition of abnormal cellular ECM in the angle. The angle changes in the 5-year-old animals appeared more severe with increased fibrosis in the angular meshwork area, suggesting that there are progressive changes in the angular meshwork, though the reasons behind normalization of IOP with age remains unclear.[8,14,23] Though the anterior chamber angle and outflow pathway in the rabbit has a different anatomic structure than that of the human, the degenerative changes in the trabecular/angular meshwork and deposition of ECM in this region were common histologic changes between the buphthalmic rabbit and human developmental glaucoma.[105] Additional histologic findings included thinning of the corneal stroma in the 5-year-old animals, which was likely due to stretching of the cornea and enlargement of the globe. Unfortunately, we did not have axial measurements on gross examination for the 5-year-old specimens, but the globes appeared larger on histologic sections. Globe enlargement is often a sensitive sign of uncontrolled IOP in congenital glaucoma.[106] It is possible that the rabbits had intermittent elevation of IOP or other mechanisms of globe enlargement based on certain proteins involved in myopia being overexpressed in these animals, as discussed below.

ECM Remodeling/Development

The data from this study suggested that the four proteins that were altered in the AH of the buphthalmic rabbit may also have influenced the angle abnormalities. The proteomic alterations that show potential relationships with damage to the angle structures include those functionally involved in ECM remodeling, tissue differentiation/development, or oxidative stress.

Cochlin. Cochlin levels in the AH were similar in the 2-year-old normal and buphthalmic rabbits. Immunohistochemistry showed increased cochlin immunoreactivity in the 2-year-old buphthalmic angular meshwork when compared to the control. In contrast, in the 5-year-old buphthalmic animals, cochlin was missing in the AH and present with a significantly high scan count number in normal AH. Immunohistochemistry showed enhanced cochlin labeling in the angular meshwork of the 5-year-old buphthalmic rabbit, albeit at a lower intensity than that seen in the 2-year-old buphthalmic rabbits.

Cochlin is a noncollagenous ECM protein that is expressed in the TM. Similar to what was observed in this study, cochlin expression was increased in the TM in POAG and in the DBA/2J mouse, a model for pigmentary glaucoma.[107,108] It was suggested that elevated expression of cochlin in the TM in POAG was likely due to the relative abundance of transcription factors.[109]At least two studies have shown that cochlin played an important role in regulating trabecular outflow. Cochlin gene delivery in a monkey organ culture perfusion model resulted in increased expression of cochlin, a decrease in outflow, and increased pressure in the organ culture system.[53] Injection of *si RNA* targeting cochlin in New Zealand white rabbits decreased IOP by approximately 25% for 78 hours, suggesting that changes in cochlin expression can influence IOP (Peral A, ARVO meeting, 2007, Abstract). These findings suggest that cochlin may be partly responsible for the altered outflow facility described in the buphthalmic rabbit. Though we believe that cochlin likely plays a role in lowering the outflow facility, it remains to be investigated whether similar proteomic and immunohistochemical changes are seen in younger buphthalmic rabbits, where the IOP is often higher. A study in younger mice demonstrated elevated cochlin levels prior to IOP elevation.[110] It is possible that a similar relationship may be seen in affected younger rabbits. The increased expression of cochlin in the buphthalmic rabbit, in DBA/2J mice with glaucoma, and in human POAG suggests that the alteration in cochlin expression is likely a downstream event and that other molecular events are likely to trigger the change in cochlin expression. The factors that regulate cochlin expression in the TM are not currently well understood. It is reported that alterations in transcriptional factor expression could result in increased cochlin expression in the TM.[109] In the buphthalmic rabbit, changes in transcriptional factor expression during development could lead to changes in cochlin expression seen in this study. The increased expression of cochlin in the 2-year-old buphthalmic rabbit with comparable aqueous levels in controls and affected animals suggested that there is a secreted component of cochlin and that there might be an aberrant secretion of the protein from the angular

meshwork into the AH, leading to the increased immunolabeling of the angular meshwork observed in this study. In contrast, in the 5-year-old buphthalmic animals, presence of cochlin in the angular meshwork was also increased when compared to the controls but decreased when compared with the 2-year-old buphthalmic rabbit, and cochlin was absent in the AH. This finding suggest that cochlin is still being synthesized but accumulating in the degenerating angular meshwork and that levels of the secretory component of the protein are not detectable in the AH owing to a paucity of cells resulting in secretion of a smaller quantity of protein.

Interphotoreceptor retinoid-binding protein. When analyzed with proteomics, IRBP was detected at comparable levels in the 2-year-old normal and buphthalmic rabbits, whereas in the 5-year-old rabbits, IRBP was undetectable in the buphthalmic rabbits and present with a high scan count number in the normal rabbits. These results were confirmed by Western blot (Figures 24 and 25). By immunohistochemistry, IRBP localization showed a corresponding decrease in labeling in the anterior segment structures of the 5-year-old buphthalmic rabbits. IRBP is a 145 kDa glycoprotein that is expressed by the photoreceptor cells and is secreted into the surrounding matrix. It plays a role in retinoid transport in the retina.[111] In the anterior segment, IRBP is expressed in the ciliary epithelium in the adult[112] and in the human fetal eye by 7 weeks of gestation (Chomyk A, ARVO meeting, 2010, Abstract). The exact role of IRBP in the anterior segment of the developing and adult eye is unclear. It could potentially act as a transporter for retinoids to the anterior segment structures. Interestingly, a recent study showed that IRBP was significantly reduced in the AH of patients with PCG.[4] It was suggested that this reduction and that of other retinoid-binding proteins may play a role in the impaired development of the angle structures in the human condition. In the buphthalmic rabbit, this temporal relationship was less clear, since there appeared to be a decrease in IRBP AH with time. IRBP immunolabeling of the anterior segment structures showed a progressive decrease in intensity, but the labeling was not absent in the buphthalmic animals. This observation suggests that the reduction in AH IRBP results from decreased synthesis accompanied by a possible defect in IRBP secretion from the cells in the anterior segment structures, or increased degradation of the protein in the AH. In humans with Behçet's disease and Vogt-Koynagi syndrome, IRBP levels are decreased in the AH with increased inflammation and elevated matrix metalloproteinases.[113] The investigators suggested that the decrease in IRBP in the AH resulted from degradation of the protein by MMPs. We did not see evidence of anterior segment inflammation on histology, nor were proteases significantly increased in the AH of the buphthalmic rabbits in this study. Such a temporal decrease of IRBP in the aging animals makes IRBP an unlikely candidate to play a major role in the initial defects causing changes in the anterior segment structures. One could suggest that a decrease in IRBP in the buphthalmic rabbit AH may influence the availability of retinoids in later stages of the disease, which contributes to progressive alterations in the angular meshwork and/or other anterior segment structures.

Transthyretin. Like IRBP, TTR in the AH did not show significant differences in the 2-year-old buphthalmic rabbits but showed a significant decrease in the AH of the 5-year-old buphthalmic rabbits compared to their control littermates. TTR is a plasma protein mostly known for being a promiscuous protein that binds to a number of other plasma proteins. It is notably known as an important transporter of thyroxine and retinol. In the brain, TTR is secreted by the choroidal plexus into the CSF.[114] In the normal rabbit, immunolabeling was detected in the ciliary epithelium, which produces AH. It is likely that TTR detected in the AH is secreted by the ciliary epithelium, demonstrating interesting similarities between CSF and AH content and secretory patterns of TTR. In the buphthalmic rabbit, the ciliary epithelium labeling was markedly reduced, which indicated that the reduced AH content resulted from reduced synthesis. Mutations in the *TTR* gene are associated with familial amyloid polyneuropathy.[115] Amyloid deposition has not been observed in the buphthalmic rabbit, and the decrease in TTR in the AH at 5 years of age is unlikely to be secondary to a mutation in the *TTR* gene. Additionally, *TTR* knockout mice do not exhibit any developmental anomalies[116] but exhibit only a minor disruption of retinol transport, resulting in 20% lower vitamin A in eyecup preparations.[117] Lower TTR levels in the CSF have been associated with a number of neuropathologic states, including Alzheimer's disease,[118] but mechanistic insights are lacking. TTR in the AH, like the CSF, could serve as a binding protein for retinol and potentially other proteins that may contribute to anterior segment changes in the later stages of buphthalmos.

Gelsolin. GSN is an actin depolymerizing protein that was reduced in the AH of 5-year-old buphthalmic animals but not in the 2-year-old animals in this study. In both the 2- and 5-year-old animals, the normal anterior segment structures showed increased GSN labeling, but in the buphthalmic animal, the immunolabeling was reduced in most tissues, except for the ciliary epithelium. GSN is known as a secretory component of AH and is reported to be elevated in the AH in POAG (Lalane RA, ARVO meeting 2010, Abstract). GSN may play a similar role in influencing axial length in these animals. GSN was recently determined to be a myopia marker protein in a fish model of myopia where the protein was down-regulated.[119] One can suggest that the decrease in GSN in the buphthalmic rabbit AH may contribute to the increase in the globe size/axial length in this animal.

Oxidative Stress–Related Proteins

The role of oxidative stress in damaging the trabecular endothelial cells and affecting the outflow pathway in POAG has been studied extensively. Evidence in the literature suggests that reactive oxygen species may play a key pathogenic role by reducing local antioxidant activities and inducing outflow resistance in glaucoma through various mechanisms.[120] Changes in AH proteins that play a role in oxidative stress include HRG, A2SG, HPT, and HPX. These proteins protect tissues from oxidative stress, and hence a decrease in the AH levels of these proteins suggests that this pathway may contribute to further damage to structures in the anterior segment, particularly the angular meshwork, resulting in the pathologic changes noted in later stages of the disease.

Haptoglobin. HPT, which was detected at lower levels in the 5-year-old buphthalmic rabbits compared to control, is a multifunctional protein, and its presence in the AH has been previously described.[121] HP binds ApoE, which is also reduced in the AH of the buphthalmic rabbits as discussed above. This binding protects ApoE against hydroxyl radicals, thus preventing loss of ApoE function in enzyme stimulation.[122] Immunohistochemistry showed reduced HP labeling in all tissues in the anterior chamber of the 5-

year-old buphthalmic rabbits when compared to normal rabbits.

Hemopexin. HPX was significantly decreased in the 5-year-old buphthalmic AH. Immunohistochemistry also showed a decrease in HPX labeling in the anterior chamber tissues. HPX immunoreactivity appeared decreased in the corneal endothelium and the ciliary epithelium of the buphthalmic rabbit compared to the control and was absent in both the angular meshwork and lens epithelium of these rabbits, suggesting a decrease in HPX synthesis by anterior segment structures. HPX has significant antioxidant properties, which it exerts by binding to the heme molecule.[123] The decreased expression of HPX at 5 years in the buphthalmic rabbit may contribute to oxidative damage to the angle in the later stages of the disease. A lower HPX level was detected in the CSF in Alzheimer's disease and is considered to be significant among an important panel of biomarkers for that disease; however, its functional significance remains unclear.[124]

Additional Proteins

Beta-2 microglobulin. B2M was detected at significantly higher levels in the AH of the 5-year-old buphthalmic rabbits. B2M was previously detected in normal and POAG AH at comparable levels. The detection technique used an older, less sensitive mass spectroscopic method.[125] Unfortunately, immunohistochemistry for B2M was performed for this study with multiple antibodies but was not successful. Increased levels of B2M in the AH of the 5-year-old buphthalmic rabbits was confirmed by Western blot (Figure 23). B2M has been identified as the light chain of the class I major histocompatibility (HLA) antigens. As a result of degradation of HLA, B2M is dissociated from the heavy chain and appears in its free form in extracellular fluid. At least 95% of B2M in plasma or urine is present as a free monomer.[126] It can serve as a nonspecific but relatively sensitive marker of various neoplastic, inflammatory, and infectious conditions, especially in the context of renal diseases, where its secretion is believed to be a sensitive marker for kidney injury.[127] Interestingly, patients with tubulointerstitial nephritis and uveitis (TINU) syndrome, which is characterized by acute anterior uveitis, show elevated levels of B2M in the urine as a marker for renal tubular damage. The anterior border layer of the iris, the nonpigmented and pigmented epithelium of the ciliary body, the external basement membrane of the ciliary body, and the vascular endothelium in the uvea showed positive staining for class I antigens.[128] It is likely that the B2M detected in the AH of buphthalmic rabbits is derived from one or more of these anterior segment tissues. The stimulus for the elevated B2M in the AH and its functional significance in alterations in the buphthalmic rabbit remains unknown. We suggest that elevated B2M levels in the AH may represent a nonspecific marker of tissue damage in the anterior segment of the buphthalmic rabbit and possibly reflect increased leakiness of the protein at the tight junctions of the blood-aqueous barrier.

Albumin. Albumin, which was the most prominent protein in our samples, was detected at significantly higher levels in the 5-year-old buphthalmic AH. Albumin is the major protein component of the normal human AH,[129] and it is thought to be required for proper growth and differentiation of epithelial cells in ocular tissues because of its ability to transport fatty acids, vitamins, hormones, metal ions, and retinoids.[130,131] Albumin is also a major component of plasma as well as CSF and has been implicated in Alzheimer's disease because of its ability to transport amyloid β. It has multiple functions, which include maintenance of colloid osmotic pressure of plasma, antioxidant activity, and regulation of normal microvascular permeability, fatty acids, and hormone transport.[132] Increased levels of albumin have been described in the CSF of patients with Alzheimer's disease, in the retina of glaucomatous monkeys, and in the AH of human PCG.[4,133,134] Increased albumin in the retina of the glaucomatous monkeys was thought to be due to the oxidative damage caused by the induction of glaucoma. Increased levels of albumin in the buphthalmic rabbit AH could be a secondary response to oxidative stress caused by elevated IOP, increased leakiness at the blood-aqueous barrier,[135] or as a function of aging, since it was not elevated in the 2-year-old rabbits. It has been reported that albumin and TTR change in AH during aging, as determined by increased AH levels in cataract patients.[136]

THE AH PROTEOME IN PCG AND THE BUPHTHALMIC RABBIT

A recent study[4] described differential expression of a group of proteins in the AH of human PCG. The proteins included albumin, ANT3, ApoA-IV, TTR, IRBP, PTGDS, and opticin. Differential expression of some proteins, namely, albumin, TTR, and IRBP, was common to human PCG and the buphthalmic rabbit. However, changes in the AH proteome in POAG involve a different set of proteins that include caspases, cadherins, optineurin, superoxide dismutase, and many others that were not significantly altered in the buphthalmic rabbit or in human PCG.[137] This observation demonstrating a distinct difference between the AH profile of adult-onset POAG and developmental glaucomas in the human and rabbit strengthens our assertion that the rabbit model could potentially be used to investigate mechanistic pathways that involve alterations in the AH proteome and changes in the anterior segment in developmental glaucoma.

PROTEIN EXPRESSION AND ALTERATIONS IN THE CSF IN NEURODEGENERATIVE DISEASES AND THE ALTERATIONS IN THE AH PROTEOME OF THE BUPHTHALMIC RABBIT

It was interesting to note the similarities between proteomic AH profile changes in the buphthalmic rabbit and those in the CSF in neurodegenerative diseases. The AH and CSF are both secreted fluids and share many common protein components. In recent literature, many proteins, such as ApoE, GSN, HP, HPX, A2SG, B2M, and Clu, were reportedly altered in neurodegenerative diseases such as Alzheimer's disease.[124] The role of these biomarkers in the pathophysiology of neurodegenerative disorders has not yet been completely elucidated, and the significance of these similarities in body fluid proteomics such as AH in the pathophysiology of a developmental disease in the rabbit needs to be further investigated. A common theme appears to be alterations in proteins involved in oxidative stress, which may suggest that loss of proteins that protect tissues from oxidative stress may contribute to tissue damage in both organ systems under pathologic conditions.

AGE-DEPENDENT CHANGES IN AH PROTEOME AND ITS RELATIONSHIP TO ALTERATIONS NOTED IN THE ANTERIOR SEGMENT STRUCTURES

Changes in DM and the anterior lens capsule appeared to be progressive with an increase in thickness in both basement membranes with age. Also, the angular meshwork showed progressive damage with fibrotic changes seen in the 5-year-old buphthalmic rabbits. Protein concentrations in body fluids decrease with age, but in this study the data was normalized to eliminate the possibility that changes were secondary to altered protein concentrations.[138] However, the AH proteomic profile in the normal rabbits did not appear to change with age, suggesting that the age-related changes in the buphthalmic rabbit were pathologic.

The changes in the AH proteome and immunohistochemical analysis appeared to reflect some of the changes seen by histology, but the observations also suggested that there were different mechanisms by which protein levels might be altered in the AH. In some instances, low levels of AH proteins corresponded with decreased expression in the anterior segment structures (eg, IRBP in the 5-year-old buphthalmic rabbit), suggesting decreased protein synthesis or its degradation in the AH. For other proteins, a decrease in AH levels was accompanied by increased tissue immunoreactivity (eg, cochlin), suggesting impaired secretion of the protein from the cells. Table 9 illustrates the effect of four such altered AH proteins on target tissues in the anterior segment.

TABLE 9. EFFECT OF CHANGE IN AQUEOUS HUMOR PROFILE OF FOUR PROTEINS AND THE RESULTANT PATHOLOGIC CHANGES IN THE BUPHTHALMIC RABBIT

PROTEIN	CHANGE IN AH	IHC	POSSIBLE MOLECULAR EVENT	HISTOLOGIC CORRELATE IN BUPHTHALMIC RABBIT	POSSIBLE FUNCTIONAL GROUP
Cochlin	Absent in 5-year-old BR	Increased TM IR	Impaired protein secretion	TM degeneration	Unknown mechanism causing elevated IOP
Interphotoreceptor retinoid-binding protein	Absent in 5-year-old BR	Generalized reduction in IR	Decreased synthesis or possible degradation by AH MMPs	TM degeneration	Retinoid deprivation
Haptoglobin	Reduced in 5-year-old BR	Reduction in IR at 5 years	Decreased synthesis	TM damage	Oxidative stress
Histidine-rich glycoprotein	Reduced at 2-year-old BR	Reduction in IR	Decreased synthesis	Increased DM thickness	Endothelial cell degeneration through apoptosis

AH, aqueous humor; BR, buphthalmic rabbit; DM, Descemet's membrane; IHC, immunohistochemistry; IOP, intraocular pressure; IR, immunoreactivity; TM, trabecular meshwork; MMPs, matrix metalloproteinases.

STUDY LIMITATIONS

This unique study has a few limitations, some of which have been pointed out in previous paragraphs. The lack of a known mutation in the buphthalmic gene limits the ability to further investigate the relationships between some of these alterations in the AH proteome, which appear to be downstream, yet may have a direct or indirect effect that results in tissue alteration or damage. As a result of this knowledge gap, rabbit gene sequences of some of the proteins described in this study were not known. Recently, the Broad Institute has completed a deep coverage of the rabbit genome, and this new effort will help assist researchers to look for genetic mutations in the buphthalmic rabbit (http://www.broadinstitute.org/science/projects/mammals-models/rabbit/rabbit-genome-sequencing-project; accessed Dec 2010). Other limitations, including lack of a broad range of commercially available antibodies to some of the altered AH proteins that react with rabbit tissues, and the paucity of AH samples, made validation of the LC-MS/MS data challenging. Despite these relative limitations, a number of distinctive observations and potential pathways that result in anterior segment pathology were unraveled.

CONCLUSION

In summary, this study described progressive alterations in the anterior chamber angle and specific basement membranes in the ocular anterior segment of the buphthalmic rabbit. In addition, a differential AH protein profile is reported, which may explain some of the histologic observations. Protein alterations in the AH of the buphthalmic rabbit belong to a wide range of biologic functional groups, such as modulation of the ECM, regulation of apoptosis, mitigating oxidative stress, or protein transport. Some of these functional

processes that were potentially affected by an altered protein profile appeared to be common to other forms of glaucoma (eg, human PCG) and corneal diseases. The findings suggest that changes in AH proteins could result from decreased synthesis, abnormal secretion, or increased degradation of proteins. The alterations in AH proteins may directly or indirectly contribute to tissue damage or represent tissue responses to damaging signals. Additional studies in younger animals, especially in the prodromal stages of glaucoma, as well as in vitro testing of potential pathways that have been suggested by these experiments, may provide further insight into the specific factors involved in its pathogenesis.

ACKNOWLEDGMENTS

Funding/Support: This work is funded in part by the Summa Foundation, Akron, Ohio.

Financial Disclosures: Dr Edward has received financial support from Alcon Inc (research support), Pfizer Inc (research support), Allergan (speakers bureau), and the Department of Defense (research grant support).

Author Contributions: Design and conduct of the study (D.E., R.B.)*;* Collection, management, analysis, and interpretation of the data (D.E., R.B.); Preparation, review (D.E., R.B.), and approval of the manuscript (D.E.).

Conformity With Author Information: Experimental procedures using laboratory animals in this study were approved by the local Institutional Animal Care and Use Committee at the Northeastern Ohio Universities Colleges of Medicine and Pharmacy.

REFERENCES

1. Francois J. Congenital glaucoma and its inheritance. *Ophthalmologica* 1980;181:61-73.
2. Bejjani BA, Lewis RA, Tomey KF, et al. Mutations in CYP1B1, the gene for cytochrome P4501B1, are the predominant cause of primary congenital glaucoma in Saudi Arabia. *Am J Hum Genet* 1998;62:325-333.
3. Doshi M, Marcus C, Bejjani BA, Edward DP. Immunolocalization of CYP1B1 in normal, human, fetal and adult eyes. *Exp Eye Res* 2006;82:24-32.
4. Bouhenni RA, Al Shahwan S, Morales J, et al. Identification of differentially expressed proteins in the aqueous humor of primary congenital glaucoma. *Exp Eye Res* 2011;92:67-75.
5. Libby RT, Smith RS, Savinova OV, et al. Modification of ocular defects in mouse developmental glaucoma models by tyrosinase. *Science* 2003;299:1578-1581.
6. Young C, Festing MF, Barnett KC. Buphthalmos (congenital glaucoma) in the rat. *Lab Anim* 1974;8:21-31.
7. Gelatt KN, Peiffer RL Jr, Gwin RM, Gum GG, Williams LW. Clinical manifestations of inherited glaucoma in the beagle. *Invest Ophthalmol Vis Sci* 1977;16:1135-1142.
8. Hanna BL, Sawin PB, Sheppard LB. Recessive buphthalmos in the rabbit. *Genetics* 1962;47:519-529.
9. Gelatt KN. Animal models for glaucoma. *Invest Ophthalmol Vis Sci* 1977;16:592-596.
10. Gelatt KN, Brooks DE, Samuelson DA. Comparative glaucomatology. II: The experimental glaucomas. *J Glaucoma* 1998;7:282-294.
11. Schloesser CV. Acutes Secundar-Glaucom beim Kaninchen. *Z Vergleich Augenheilkd 1886;6*:79-88.
12. Pichler A. Spontanes Glaukom beim Kaninchen. *Arch Vergleigh Ophthalmol 1910;*1:175-179.
13. Vogt A. Vererbter Hydrophthalmus beim Kaninchen. *Z Vergleigh Augenheilkd* 1919;63:233.
14. Rochon-Duvigneaud A. Un cas de buphthalmie chez le lapin: etude anatomique et physiologique. *Ann Oculist (Paris)* 1921;108:293-297.
15. Beckh W. A case of spontaneous glaucoma in a rabbit. *Am J Ophthalmol* 1935;18:1144-1145.
16. Greaves DP, Perkins ES. Buphthalmos in the rabbit. *Br J Ophthalmol* 1951;35:232-233.
17. Franceschetti A. Die Vererbung von Augenleiden. In: Schieck and Bruckner, eds. *Kurzes Handbuch Ophthalmol* Berlin: Springer; 1930:631-855.
18. Nachtsheim H. Erbpathologie des Kaninchens. *Erbartz 1937;*4:30,50-55.
19. Geri G. Considerazioni e ricerche sull'eridita dell 'idoftalmia nel coniglio. *Ricerca Sci* 1954;24:2299-2315.
20. Geri G. Richerche sull'eridia dell' idroftalmia nell coniglio. *Riv Zootec* 1955;28:37-42.
21. Fox RR, Crary DD, Babino EJ Jr, Sheppard LB. Buphthalmia in the rabbit. Pleiotropic effects of the (bu) gene and a possible explanation of mode of gene action. *J Hered* 1969;60:206-212.
22. Kolker AE, Moses RA, Constant MA, Becker B. The development of glaucoma in rabbits. *Invest Ophthalmol* 1963;2:316-321.
23. Knepper PA, McLone DG, Goossens W, Vanden Hoek T, Higbee RG. Ultrastructural alterations in the aqueous outflow pathway of adult buphthalmic rabbits. *Exp Eye Res* 1991;52:525-533.
24. Beit-Yannai E, Trembovler V, Solomon AS. Decrease in reducing power of aqueous humor originating from glaucomatous rabbits. *Eye (Lond)* 2007;21:658-664.
25. Babino EJ Jr, Fox RR. Buphthalmia in the rabbit: effect of age and repeated testing on the cornified cell count diagnostic technique. *Proc Soc Exp Biol Med* 1967;126:216-217.
26. Fox RR, Babino EJ Jr. Buphthalmia in the rabbit: a test for early diagnosis. *Proc Soc Exp Biol Med* 1965;119:229-233.
27. Sheppard LB, Shanklin WM. Corneal epithelium changes in rabbit congenital glaucoma. *Am J Ophthalmol* 1968;65:406-413.
28. McMaster PR, Macri FJ. The rate of aqueous humor formation in buphthalmic rabbit eyes. *Invest Ophthalmol 1967;*6:84-87.
29. Becker B. The decline in aqueous secretion and outflow facility with age. *Am J Ophthalmol* 1958;46:731-736.

30. Becker B, Constant MA. Species variation in facility of aqueous outflow. *Am J Ophthalmol* 1956;42:189-194.
31. Becker B, Constant MA. The facility of aqueous outflow: a comparison of tonography and perfusion measurements in vivo and in vitro. *Arch Ophthalmol* 1956;55:305-312.
32. Lee P. Gonioscopic study of hereditary buphthalmia in rabbits. *Arch Ophthalmol 1968;*79:775-778.
33. Tesluk GC, Peiffer RL, Brown D. A clinical and pathological study of inherited glaucoma in New Zealand white rabbits. *Lab Anim* 1982;16:234-239.
34. Bunt-Milam AH, Dennis MB Jr, Bensinger RE. Hereditary glaucoma and buphthalmia in the rabbit. *Prog Clin Biol Res* 1987;247:397-406.
35. Fox RR, Eaton HD, Crary DD. Vitamin A, beta carotene, and hereditary buphthalmus in the rabbit. *J Hered* 1982;73:370-374.
36. Zhan GL, Toris CB, Camras CB, Wang YL, Yablonski ME. Bunazosin reduces intraocular pressure in rabbits by increasing uveoscleral outflow. *J Ocul Pharmacol Ther* 1998;14:217-228.
37. Vareilles P, Coquet P, Lotti VJ. Intraocular pressure responses to antiglaucoma agents in spontaneous buphthalmic rabbits. *Ophthalmic Res* 1980;12:296-302.
38. Ueno A, Tawara A, Kubota T, Ohnishi Y, Inomata H, Solomon AS. Histopathological changes in iridocorneal angle of inherited glaucoma in rabbits. *Graefes Arch Clin Exp Ophthalmol* 1999;237:654-660.
39. Fox RR, Lam KW, Coco JF. Effect of ascorbic acid on intraocular pressure of normal and buphthalmic rabbits. *J Hered* 1977;68:179-183.
40. Constant MA. The chemistry of the rabbit aqueous humor. Older offspring of glaucomatous animals. *Am J Ophthalmol* 1968;65:78-80.
41. Fox RR, Lam KW, Lewen R, Lee P. Ascorbate concentration in tissues from normal and buphthalmic rabbits. *J Hered* 1982;73:109-111.
42. Harris TM, Nance CS, Sheppard LB, Fox RR. Evidence for an hereditary defect in taurine transport in the ciliary epithelium of an inbred strain of rabbits. *J Inherit Metab Dis* 1983;6:163-166.
43. Lam KW, Mansour AM, Fox RR, Lee P, Smith R. Fibrinogen concentration in the aqueous humor of buphthalmic rabbits. *Curr Eye Res* 1982;2:153-157.
44. Lam KW, Tabor G, Fox R, Lee P-F. Immunohistochemical evidence indicating the obstruction of aqueous humor drainage by fibrin in hereditary buphthalmic rabbits. *Glaucoma* 1989;11:139.
45. Ozcan AA, Ozdemir N, Canataroglu A. The aqueous levels of TGF-beta2 in patients with glaucoma. *Int Ophthalmol* 2004;25:19-22.
46. Stastna M, Behrens A, Noguera G, Herretes S, McDonnell P, Van Eyk JE. Proteomics of the aqueous humor in healthy New Zealand rabbits. *Proteomics* 2007;7:4358-4375.
47. Coca-Prados M, Escribano J. New perspectives in aqueous humor secretion and in glaucoma: the ciliary body as a multifunctional neuroendocrine gland. *Prog Retin Eye Res* 2007;26:239-262.
48. To CH, Kong CW, Chan CY, Shahidullah M, Do CW. The mechanism of aqueous humour formation. *Clin Exp Optom* 2002;85:335-349.
49. McLaughlin CW, Peart D, Purves RD, Carre DA, Macknight AD, Civan MM. Effects of HCO3- on cell composition of rabbit ciliary epithelium: a new model for aqueous humor secretion. *Invest Ophthalmol Vis Sci* 1998;39:1631-1641.
50. Janciauskiene S, Brandt L, Wallmark A, Westin U, Krakau T. Secreted leukocyte protease inhibitor is present in aqueous humours from cataracts and other eye pathologies. *Exp Eye Res* 2006;82:505-511.
51. Sakamoto T, Ito S, Yoshikawa H, et al. Tissue factor increases in the aqueous humor of proliferative diabetic retinopathy. *Graefes Arch Clin Exp Ophthalmol* 2001;239:865-871.
52. Tong JP, Chan WM, Liu DT, et al. Aqueous humor levels of vascular endothelial growth factor and pigment epithelium-derived factor in polypoidal choroidal vasculopathy and choroidal neovascularization. *Am J Ophthalmol* 2006;141:456-462.
53. Fleenor DL, Shepard AR, Hellberg PE, Jacobson N, Pang IH, Clark AF. TGFbeta2-induced changes in human trabecular meshwork: implications for intraocular pressure. *Invest Ophthalmol Vis Sci 2*006;47:226-234.
54. Maatta M, Tervahartiala T, Harju M, Airaksinen J, Autio-Harmainen H, Sorsa T. Matrix metalloproteinases and their tissue inhibitors in aqueous humor of patients with primary open-angle glaucoma, exfoliation syndrome, and exfoliation glaucoma. *J Glaucoma* 2005;14:64-69.
55. Duan X, Lu Q, Xue P, et al. Proteomic analysis of aqueous humor from patients with myopia. *Mol Vis* 2008;14:370-377.
56. Richardson MR, Segu ZM, Price MO, et al. Alterations in the aqueous humor proteome in patients with Fuchs endothelial corneal dystrophy. *Mol Vis* 2010;16:2376-2383.
57. Choi J, Miller AM, Nolan MJ, et al. Soluble CD44 is cytotoxic to trabecular meshwork and retinal ganglion cells in vitro. *Invest Ophthalmol Vis Sci 2005;*46:214-222.
58. Ho SL, Dogar GF, Wang J, et al. Elevated aqueous humour tissue inhibitor of matrix metalloproteinase-1 and connective tissue growth factor in pseudoexfoliation syndrome. *Br J Ophthalmol 2005;*89:169-173.
59. Koh SW, Rutzen A, Coll T, Hemady R, Higginbotham E. VIP immunoreactivity in human aqueous humor. *Curr Eye Res* 2005;30:189-194.
60. Tezel G, Yang X, Luo C, et al. Oxidative stress and the regulation of complement activation in human glaucoma. *Invest Ophthalmol Vis Sci* 2010;51:5071-5082.

61. Klintworth GK. Corneal dystrophies. *Orphanet J Rare Dis* 2009;4:7.
62. Van Horn DL, Hyndiuk RA, Edelhauser HF, McDonald TO, De Santis LM. Ultrastructural alterations associated with loss of transparency in the cornea of buphthalmic rabbits. *Exp Eye Res* 1977;25:171-182.
63. Hayashi S, Osawa T, Tohyama K. Comparative observations on corneas, with special reference to Bowman's layer and Descemet's membrane in mammals and amphibians. *J Morphol* 2002;254:247-258.
64. Yu H, Wakim B, Li M, Halligan B, Tint GS, Patel SB. Quantifying raft proteins in neonatal mouse brain by 'tube-gel' protein digestion label-free shotgun proteomics. *Proteome Sci* 2007;5:17.
65. Old WM, Meyer-Arendt K, Aveline-Wolf L, et al. Comparison of label-free methods for quantifying human proteins by shotgun proteomics. *Mol Cell Proteomics* 2005;4:1487-1502.
66. Bantscheff M, Schirle M, Sweetman G, Rick J, Kuster B. Quantitative mass spectrometry in proteomics: a critical review. *Anal Bioanal Chem* 2007;389:1017-1031.
67. Hendrickson EL, Xia Q, Wang T, Leigh JA, Hackett M. Comparison of spectral counting and metabolic stable isotope labeling for use with quantitative microbial proteomics. *Analyst* 2006;131:1335-1341.
68. Mesrobian HG, Mitchell ME, See WA, et al. Candidate urinary biomarker discovery in ureteropelvic junction obstruction: a proteomic approach. *J Urol* 2010;184:709-714.
69. Puk O, Dalke C, Calzada-Wack J, et al. Reduced corneal thickness and enlarged anterior chamber in a novel ColVIIIa2G257D mutant mouse. *Invest Ophthalmol Vis Sci* 2009;50:5653-5661.
70. Washburn MP, Wolters D, Yates JR 3rd. Large-scale analysis of the yeast proteome by multidimensional protein identification technology. *Nat Biotechnol* 2001;19:242-247.
71. Liu H, Sadygov RG, Yates JR 3rd. A model for random sampling and estimation of relative protein abundance in shotgun proteomics. *Anal Chem* 2004;76:4193-4201.
72. Zhang B, VerBerkmoes NC, Langston MA, Uberbacher E, Hettich RL, Samatova NF. Detecting differential and correlated protein expression in label-free shotgun proteomics. *J Proteome Res* 2006;5:2909-2918.
73. Bunt-Milam AH, Dennis MB Jr, Bensinger RE. Optic nerve head axonal transport in rabbits with hereditary glaucoma. *Exp Eye Res* 1987;44:537-551.
74. Danysh BP, Duncan MK. The lens capsule. *Exp Eye Res* 2009;88:151-164.
75. Yan Q, Liu JP, Li DW. Apoptosis in lens development and pathology. *Differentiation* 2006;74:195-211.
76. Pau H, Novotny GE. Ultrastructural investigations on anterior capsular cataract. Cellular elements and their relationship to basement membrane and collagen synthesis. *Graefes Arch Clin Exp Ophthalmol* 1985;223:41-46.
77. Norose K, Lo WK, Clark JI, Sage EH, Howe CC. Lenses of SPARC-null mice exhibit an abnormal cell surface-basement membrane interface. *Exp Eye Res* 2000;71:295-307.
78. Yan Q, Clark JI, Wight TN, Sage EH. Alterations in the lens capsule contribute to cataractogenesis in SPARC-null mice. *J Cell Sci* 2002;115:2747-2756.
79. Rodrigues MM, Katz SI, Foidart JM, Spaeth GL. Collagen, factor VIII antigen, and immunoglobulins in the human aqueous drainage channels. *Ophthalmology* 1980;87:337-345.
80. Akimoto Y, Sawada H, Ohara-Imaizumi M, Nagamatsu S, Kawakami H. Change in long-spacing collagen in Descemet's membrane of diabetic Goto-Kakizaki rats and its suppression by antidiabetic agents. *Exp Diabetes Res* 2008;2008:818341.
81. Zhang C, Bell WR, Sundin OH, et al. Immunohistochemistry and electron microscopy of early-onset Fuchs corneal dystrophy in three cases with the same L450W COL8A2 mutation. *Trans Am Ophthalmol Soc* 2006;104:85-97.
82. Khoshnoodi J, Pedchenko V, Hudson BG. Mammalian collagen IV. *Microsc Res Tech* 2008;71:357-370.
83. Tamm ER. The trabecular meshwork outflow pathways: structural and functional aspects. *Exp Eye Res* 2009;88:648-655.
84. Babizhayev MA, Brodskaya MW. Fibronectin detection in drainage outflow system of human eyes in ageing and progression of open-angle glaucoma. *Mech Ageing Dev* 1989;47:145-157.
85. Fuchshofer R, Yu AH, Welge-Lussen U, Tamm ER. Bone morphogenetic protein-7 is an antagonist of transforming growth factor-beta2 in human trabecular meshwork cells. *Invest Ophthalmol Vis Sci* 2007;48:715-726.
86. Tripathi RC, Li J, Chan WF, Tripathi BJ. Aqueous humor in glaucomatous eyes contains an increased level of TGF-beta 2. *Exp Eye Res* 1994;59:723-727.
87. Richardson MR, Price MO, Price FW, et al. Proteomic analysis of human aqueous humor using multidimensional protein identification technology. *Mol Vis* 2009;15:2740-2750.
88. Simantov R, Febbraio M, Crombie R, Asch AS, Nachman RL, Silverstein RL. Histidine-rich glycoprotein inhibits the antiangiogenic effect of thrombospondin-1. *J Clin Invest* 2001;107:45-52.
89. Gorgani NN, Theofilopoulos AN. Contribution of histidine-rich glycoprotein in clearance of immune complexes and apoptotic cells: implications for ameliorating autoimmune diseases. *Autoimmunity* 2007;40:260-266.
90. Wordinger RJ, Fleenor DL, Hellberg PE, et al. Effects of TGF-beta2, BMP-4, and gremlin in the trabecular meshwork: implications for glaucoma. *Invest Ophthalmol Vis Sci* 2007;48:1191-1200.
91. Umulis D, O'Connor MB, Blair SS. The extracellular regulation of bone morphogenetic protein signaling. *Development* 2009;136:3715-3728.
92. Burdon KP, Sharma S, Hewitt AW, et al. Genetic analysis of the clusterin gene in pseudoexfoliation syndrome. *Mol Vis* 2008;14:1727-1736.

93. Reeder DJ, Stuart WD, Witte DP, Brown TL, Harmony JA. Local synthesis of apolipoprotein J in the eye. *Exp Eye Res* 1995;60:495-504.
94. Sakaguchi H, Miyagi M, Shadrach KG, Rayborn ME, Crabb JW, Hollyfield JG. Clusterin is present in drusen in age-related macular degeneration. *Exp Eye Res* 2002;74:547-549.
95. Rosenberg ME, Silkensen J. Clusterin: physiologic and pathophysiologic considerations. *Int J Biochem Cell Biol* 1995;27:633-645.
96. Creasey R, Sharma S, Craig JE, et al. Detecting protein aggregates on untreated human tissue samples by atomic force microscopy recognition imaging. *Biophys J* 2010;99:1660-1667.
97. Gundry RL, Fu Q, Jelinek CA, Van Eyk JE, Cotter RJ. Investigation of an albumin-enriched fraction of human serum and its albuminome. *Proteomics Clin Appl* 2007;1:73-88.
98. Ishida BY, Bailey KR, Duncan KG, et al. Regulated expression of apolipoprotein E by human retinal pigment epithelial cells. *J Lipid Res* 2004;45:263-271.
99. Sharma S, Chataway T, Burdon KP, et al. Identification of LOXL1 protein and Apolipoprotein E as components of surgically isolated pseudoexfoliation material by direct mass spectrometry. *Exp Eye Res* 2009;89:479-485.
100. Dithmar S, Curcio CA, Le NA, Brown S, Grossniklaus HE. Ultrastructural changes in Bruch's membrane of apolipoprotein E-deficient mice. *Invest Ophthalmol Vis Sci* 2000;41:2035-2042.
101. Zetterberg M, Tasa G, Palmer MS, et al. Apolipoprotein E polymorphisms in patients with primary open-angle glaucoma. *Am J Ophthalmol* 2007;143:1059-1060.
102. Tarnus E, Wassef H, Carmel JF, et al. Apolipoprotein E limits oxidative stress-induced cell dysfunctions in human adipocytes. *FEBS Lett* 2009;583:2042-2048.
103. Shea TB, Rogers E, Ashline D, Ortiz D, Sheu MS. Apolipoprotein E deficiency promotes increased oxidative stress and compensatory increases in antioxidants in brain tissue. *Free Radic Biol Med* 2002;33:1115-1120.
104. Zhou L, Li Y, Yue BY. Oxidative stress affects cytoskeletal structure and cell-matrix interactions in cells from an ocular tissue: the trabecular meshwork. *J Cell Physiol* 1999;180:182-189.
105. Hollander DA, Sarfarazi M, Stoilov I, Wood IS, Fredrick DR, Alvarado JA. Genotype and phenotype correlations in congenital glaucoma. *Trans Am Ophthalmol Soc* 2006;104:183-195.
106. Gupta V, Jha R, Srinivasan G, Dada T, Sihota R. Ultrasound biomicroscopic characteristics of the anterior segment in primary congenital glaucoma. *J AAPOS* 2007;11:546-550.
107. Bhattacharya SK, Rockwood EJ, Smith SD, et al. Proteomics reveal cochlin deposits associated with glaucomatous trabecular meshwork. *J Biol Chem* 2005;280:6080-6084.
108. John SW, Smith RS, Savinova OV, et al. Essential iris atrophy, pigment dispersion, and glaucoma in DBA/2J mice. *Invest Ophthalmol Vis Sci* 1998;39:951-962.
109. Picciani RG, Diaz A, Lee RK, Bhattacharya SK. Potential for transcriptional upregulation of cochlin in glaucomatous trabecular meshwork: a combinatorial bioinformatic and biochemical analytical approach. *Invest Ophthalmol Vis Sci* 2009;50:3106-3111.
110. Bhattacharya SK, Peachey NS, Crabb JW. Cochlin and glaucoma: a mini-review. *Vis Neurosci* 2005;22:605-613.
111. Porrello K, Bhat SP, Bok D. Detection of interphotoreceptor retinoid binding protein (IRBP) mRNA in human and cone-dominant squirrel retinas by in situ hybridization. *J Histochem Cytochem* 1991;39:171-176.
112. Salvador-Silva M, Ghosh S, Bertazolli-Filho R, et al. Retinoid processing proteins in the ocular ciliary epithelium. *Mol Vis* 2005;11:356-365.
113. Descamps FJ, Kangave D, Cauwe B, et al. Interphotoreceptor retinoid-binding protein as biomarker in systemic autoimmunity with eye inflictions. *J Cell Mol Med* 2008;12:2449-2456.
114. Aleshire SL, Bradley CA, Richardson LD, Parl FF. Localization of human prealbumin in choroid plexus epithelium. *J Histochem Cytochem* 1983;31:608-612.
115. Saraiva MJ. Transthyretin mutations in hyperthyroxinemia and amyloid diseases. *Hum Mutat* 2001;17:493-503.
116. Episkopou V, Maeda S, Nishiguchi S, et al. Disruption of the transthyretin gene results in mice with depressed levels of plasma retinol and thyroid hormone. *Proc Natl Acad Sci U S A* 1993;90:2375-2379.
117. Wei S, Episkopou V, Piantedosi R, et al. Studies on the metabolism of retinol and retinol-binding protein in transthyretin-deficient mice produced by homologous recombination. *J Biol Chem* 1995;270:866-870.
118. Fleming CE, Nunes AF, Sousa MM. Transthyretin: more than meets the eye. *Prog Neurobiol* 2009;89:266-276.
119. Jostrup R, Shen W, Burrows JT, Sivak JG, McConkey BJ, Singer TD. Identification of myopia-related marker proteins in tilapia retinal, RPE, and choroidal tissue following induced form deprivation. *Curr Eye Res* 2009;34:966-975.
120. Sacca SC, Izzotti A, Rossi P, Traverso C. Glaucomatous outflow pathway and oxidative stress. *Exp Eye Res* 2007;84:389-399.
121. Yu TC, Okamura R. Comparative study of native proteins in aqueous humor and serum—detection of characteristic aqueous humor proteins. *Jpn J Ophthalmol* 1987;31:235-248.
122. Salvatore A, Cigliano L, Carlucci A, Bucci EM, Abrescia P. Haptoglobin binds apolipoprotein E and influences cholesterol esterification in the cerebrospinal fluid. *J Neurochem* 2009;110:255-263.
123. Li RC, Saleem S, Zhen G, et al. Heme-hemopexin complex attenuates neuronal cell death and stroke damage. *J Cereb Blood Flow Metab* 2009;29:953-964.

124. Roher AE, Maarouf CL, Sue LI, Hu Y, Wilson J, Beach TG. Proteomics-derived cerebrospinal fluid markers of autopsy-confirmed Alzheimer's disease. *Biomarkers* 2009;14:493-501.
125. Rohde E, Tomlinson AJ, Johnson DH, Naylor S. Comparison of protein mixtures in aqueous humor by membrane preconcentration–capillary electrophoresis–mass spectrometry. *Electrophoresis* 1998;19:2361-2370.
126. Schardijn GH, Statius van Eps LW. Beta 2-microglobulin: its significance in the evaluation of renal function. *Kidney Int* 1987;32:635-641.
127. Metzger J, Kirsch T, Schiffer E, et al. Urinary excretion of twenty peptides forms an early and accurate diagnostic pattern of acute kidney injury. *Kidney Int* 2010;78:1252-1262.
128. Bakker M, Kijlstra A. The expression of HLA-antigens in the human anterior uvea. *Curr Eye Res* 1985;4:599-604.
129. Tripathi RC, Millard CB, Tripathi BJ. Protein composition of human aqueous humor: SDS-PAGE analysis of surgical and post-mortem samples. *Exp Eye Res* 1989;48:117-130.
130. McAvoy JW. Cell division, cell elongation and distribution of alpha-, beta- and gamma-crystallins in the rat lens. *J Embryol Exp Morphol* 1978;44:149-165.
131. Wakabayashi Y, Kawahara J, Iwasaki T, Usui M. Retinoic acid transport to lens epithelium in human aqueous humor. *Jpn J Ophthalmol* 1994;38:400-406.
132. Quinlan GJ, Martin GS, Evans TW. Albumin: biochemical properties and therapeutic potential. *Hepatology* 2005;41:1211-1219.
133. Carter-Dawson L, Zhang Y, Harwerth RS, et al. Elevated albumin in retinas of monkeys with experimental glaucoma. *Invest Ophthalmol Vis Sci* 2010;51:952-959.
134. Carter-Dawson L, Zhang Y, Harwerth RS, et al. Elevated albumin in retinas of monkeys with experimental glaucoma. *Invest Ophthalmol Vis Sci* 2010;51:952-959.
135. Sacca SC, Izzotti A. Oxidative stress and glaucoma: injury in the anterior segment of the eye. *Prog Brain Res* 2008;173:385-407.
136. Inada K, Murata T, Baba H, Murata Y, Ozaki M. Increase of aqueous humor proteins with aging. *Jpn J Ophthalmol* 1988;32:126-131.
137. Izzotti A, Longobardi M, Cartiglia C, Sacca SC. Proteome alterations in primary open angle glaucoma aqueous humor. *J Proteome Res* 2010;9:4831-4838.
138. Zhang J, Goodlett DR, Peskind ER, et al. Quantitative proteomic analysis of age-related changes in human cerebrospinal fluid. *Neurobiol Aging* 2005;26:207-227.